MIRELA SIMONA VLAD-CRISTEA

PRODUCTION OF BIOACTIVE LACTOBIONIC ACID USING A NOVEL CATALYTIC METHOD

Mémoire présenté
à la Faculté des études supérieures de l'Université Laval
dans le cadre du programme de maîtrise en génie chimique
pour l'obtention du grade de maître ès sciences (M.Sc.)

DÉPARTEMENT DE GÉNIE CHIMIQUE
FACULTÉ DES SCIENCES ET DE GÉNIE
UNIVERSITÉ LAVAL
QUÉBEC

2007

RÉSUMÉ

La faisabilité de l'oxydation du lactose vers l'acide lactobionique en milieu alcalin en présence d'un catalyseur bimétallique hétérogène Bi-Pd supporté sur la silice mesostructurée, SBA-15, a été étudiée dans un réacteur discontinu agité.

Les objectifs étaient : (i) la formulation du catalyseur bimétallique avec la charge optimale des métaux sur le support, (ii) l'optimisation des conditions de réaction: la température, le débit d'air, le rapport métal/lactose, le pH; (iii) l'évaluation de la stabilité du catalyseur et de sa performance dans des études à plus grande échelle.

Les réactions ont été effectuées à des températures comprises entre 38 et 80°C et le pH situé entre 7 et 9. Le catalyseur 1.02% Pd 0.64% Bi/SBA-15 avec un rapport molaire de Bi:Pd=0.3 a montré une activité et une sélectivité envers l'acide lactobionique les plus élevées. Les conditions optimales du procédé ont été déterminés à 65°C et à un pH de 9 avec un contrôle strict de l'oxygène dissous (<1% à la concentration d'équilibre de l'oxygène à la température de la réaction). Après 3 heures de réaction, le nouveau catalyseur a montré une très bonne stabilité à la lixiviation des métaux. L'activité et la sélectivité du nouveau catalyseur sont reliés à l'alliage $Bi_{1.75}Pd$ trouvé.

ABSTRACT

The feasibity of microaerial oxidation of lactose to lactobionic acid (LBA) in alkaline medium over heterogeneous bimetallic Bi-Pd catalyst supported on mesostructured silica material, SBA-15 in an agitated batch reactor was studied.

The objectives were: (i) formulation of the bimetallic catalyst with optimum metal loading on the support, (ii) optimization of reaction conditions, metal/lactose ratio, temperature, airflow, pH of the reaction and (iii) evaluation of catalyst stability and its performance in scale-up studies.

Reactions were carried out in a range of temperature (38 – 80°C) and pH (7-9). The 1.02%Pd 0.64%Bi/SBA-15 catalyst with Bi:Pd=0.3 molar ratio showed the highest activity and selectivity towards lactobionic acid. The optimal conditions were found at 65°C and pH 9 with a systematic control of dissolved oxygen (<1% of O_2 equilibrium concentration at reaction temperature). After 3 hours of reaction, the novel catalyst has shown to have a very good stability against metals leaching. The activity and selectivity of the novel catalyst appear to relate to $Bi_{1.75}Pd$ alloy.

RÉSUMÉ ÉTENDU

La faisabilité de l'oxydation du lactose vers l'acide lactobionique en milieu alcalin en présence d'un catalyseur bimétallique hétérogène Bi-Pd supporté sur la silice mesostructurée, SBA-15, a été étudiée dans un réacteur discontinu agité.

Les objectifs étaient : (i) la formulation du catalyseur bimétallique avec la charge optimale des métaux sur le support, (ii) l'optimisation des conditions de réaction: la température, le débit d'air, le rapport métal/lactose, le pH; (iii) l'évaluation de la stabilité du catalyseur et de sa performance dans des études à plus grande échelle.

Le catalyseur bimétallique Bi-Pd préparé par l'imprégnation successive de la SBA-15 a été testé dans la réaction d'oxydation du lactose. Les réactions ont été effectuées à des températures comprises entre 38 et 80°C et le pH situé entre 7 et 9. Le catalyseur 1.02% Pd 0.64% Bi/SBA-15 avec un rapport molaire de Bi:Pd=0.3 a montré une activité et une sélectivité envers l'acide lactobionique les plus élevées. Les analyses DRX, MET, chimisorption d'H_2 et BET ont confirmé la structure mésoporeuse du catalyseur et la disposition uniforme de particules de Pd et d'alliage Pd-Bi dans les pores de matériaux SBA-15. L'analyse ESCA a confirmé la présence d'un alliage $Bi_{1.75}Pd$ qui est responsable de l'activité et de la sélectivité du nouveau catalyseur.

Les conditions optimales du procédé ont été déterminés à 65°C et à un pH de 9 avec un contrôle strict de l'oxygène dissous (<1% à la concentration d'équilibre de l'oxygène à la température de la réaction), quand la conversion du lactose est maximale (96.14%). Les cinétiques de la réaction d'oxydation du lactose ont montré une forte dépendance de la conversion du lactose avec le pH et la température. Après 3 heures de réaction, le nouveau catalyseur a montré une très bonne stabilité à la lixiviation des métaux. Finalement, les études à plus grande échelle ont fournis des résultats prometteurs pour la production de l'acide lactobionique par la nouvelle méthode.

EXTENDED ABSTRACT

The feasibity of microaerial oxidation of lactose to lactobionic acid (LBA) in alkaline medium over heterogeneous bimetallic Bi-Pd catalyst supported on mesostructured silica material, SBA-15 in an agitated batch reactor was studied.

The objectives were: (i) formulation of the bimetallic catalyst with optimum metal loading on the support, (ii) optimization of reaction conditions, metal/lactose ratio, temperature, airflow, pH of the reaction and (iii) evaluation of catalyst stability and its performance in scale-up studies.

The bimetallic Bi-Pd catalysts prepared by successive impregnation of SBA-15 material were tested in oxidation reaction of lactose. Reactions were carried out in a range of temperature (38-80°C) and pH (7-9). 1.02%Pd 0.64%Bi/SBA-15 catalyst with Bi:Pd=0.3 molar ratio showed the highest activity and selectivity towards lactobionic acid.

XRD, TEM, H_2-chemisorption and BET analysis confirmed mesostructured structure of the catalyst, uniform dispersion of the Pd and bimetallic nanocrystallites in the SBA-15. The XPS revealed a Bi-Pd alloy with stoechiometric formula $Bi_{1.75}Pd$, which appears to confer to the catalyst a high activity and selectivity.

The optimal reaction conditions were found to be 65°C and pH 9, with a strict control of dissolved oxygen (<1% of O_2 equilibrium concentration at reaction temperature), where lactose conversion was maximum at 96.14%. The kinetics of the reaction of lactose oxidation exhibited a strong dependence of the lactose conversion with pH as well as temperature. After 3 hours of reaction, the novel catalyst proved to be stable against metal leaching. Finally, the scale-up studies showed promising results for the production of LBA by the novel method.

AVANT-PROPOS

First and foremost, I express my gratitude to my research Director, Professor Khaled Belkacemi and my co-director Professor Safia Hamoudi for their generous faith and superb guidance in this research project.

Dairy Farmers of Canada and Natural Sciences and Engineering Research Council of Canada are acknowledged for providing funds for this research.

Thank you to Professor Joseph Arul for his precious advice and for his acceptance to examine this memoire.

My gratitude to Alain Adnot, Serge Groleau and Richard Janvier for providing technical assistance in performing XPS, ICP and TEM analysis.

Special thanks are also due to Zahir Dehouche and Gaétan Desnoyers for their generous assistance during this project.

I also wish to thank my colleagues for their constant support and encouragement.

At last, but not the least, I thank my family, my husband, Calin and my son, Teo for their moral support and understanding.

TABLE OF CONTENTS

ACRONYMS

BET: Brunauer, Emmett and Teller

BJH: Barrett, Joyner and Halenda

ESCA: Electron Spectroscopy for Chemical Analysis

ICP-AES: Inductively Coupled Plasma - Atomic Emission Spectrometer

LBA: Lactobionic Acid

P123: Poly(ethylene glycol)-poly(propylene glycol)-poly(ethylene glycol) triblock copolymer

SBA-15: Family of mesoporous solids structured by triblock copolymers

TEM: Transmission Electron Microscopy

TEOS: Tetraethylorthosilicate

HPLC: High Performance Liquid Chromatography

XPS: X-Ray Photoelectron Spectroscopy

XRD: X-Ray Diffraction

LIST OF TABLES

LIST OF FIGURES

CHAPTER 1

INTRODUCTION

Lactose is on of the most abundant carbohydrates. The principal source of lactose is (sweet) whey or casein (acid) whey, the main by-products, in the cheese and casein production in the dairy industry. Lactose is widely used in the dairy and pharmaceutical industries. The most important transformations of lactose include acid and enzymatic hydrolysis, dehydratation, isomerization, hydrogenation and oxidation. The lactose derivatives with nutraceutical and pharmaceutical value are lactulose, lactitol, lactobionic acid, lactosyl-urea and lactose-based oligosaccharides. Despite existing transformations, lactose potential as an organic raw material for the elaboration of industrially useful chemical intermediates and products is far from being fully exploited.

A successful way to process lactose is to obtain value-added products such as lactobionic acid (LBA). LBA has many applications in the food and pharmaceutical industries, particularly in the medical field and cosmetology. Usually, LBA is produced by enzymatic oxidation of lactose. Catalytic oxidation of lactose to lactobionic acid presents the same advantages as the enzymatic oxidation, namely, a high selectivity and mild reaction conditions (oxidation with air at atmospheric pressure near room temperature). However, it presents other additional advantages. The catalytic oxidation is possible in a single reaction vessel, whereas the enzymatic route involves a multistep process with cumbersome installations and expensive enzymes. All the enzymatic processes are long, whereas the catalytic oxidation requires shorter reaction time. Otherwise, in the catalytic oxidation, the LBA yield is very high and the process is environmentally clean since it is conducted on recyclable catalysts and gives no noxious effluents or side products.

Compared to other chemical processes, the oxidation process is complex and difficult to control. For these reasons, the selective catalytic oxidation of lactose depends not only on the activity but also on the selectivity and stability of the involved catalyst.

Many studies on heterogeneous catalytic oxidation of lactose were developed with mono- or bimetallic catalyst supported on carbon or silica. Generally, the monometallic catalysts involve Pd, Pt and Au. The bimetallic catalyst involves the noble metal and promoters such as Bi, Sn, Tl and Co. It is clear that the catalyst performance required a high surface areas or high active phase dispersions as well as fast mass transfer of the reactants and products to and from the catalytic sites.

The use of mesoporous silica materials as a support for designing a novel catalyst, for lactose oxidation is the goal of the present work. The obtention of bimetallic nanoparticles with controlled particle size and the high dispersion of these on the support is very important for catalyst performance in this process. Hence, catalytic oxidation of lactose which involves a Bi-Pd supported on a mesostructured silica was studied in this work and a new catalytic method for lactose oxidation is proposed to the fine chemicals industry.

CHAPTER 2

REVIEW OF THE LITERATURE

2.1. Lactose production and transformation

2.1.1. Lactose – a by-product of the dairy industry

Lactose, 4-O-β-D-galactopyranosyl-α-D-glucopyranose, or milk sugar is among the most abundant carbohydrates. In nature, lactose is present in the milk of most mammals at concentrations varying from 0 to 9% (w/w) depending on the species [Jenness and Sloan, 1970]. The principal source of lactose is (sweet) whey or casein (acid) whey, the main by-product in cheese and casein production in the dairy industry [Kavanaugh, 1975; Hobman, 1984]. Due to the large volume of the dairy industry, only a limited part of the whey is processed for the production of lactose. The remaining whey is handled as a waste; therefore, it might create environmental problem. Despite that, worldwide lactose production is large, about 500 million pounds per year in the USA and 730 million pounds per year in Europe. The lactose surplus is estimated at about 1.2 million tons per year [FAO, 2004].

Much effort has been made to develop new products and processes based on lactose but only a small percentage of this amount is being currently processed.

2.1.2. Lactose – chemical structure and properties

Lactose is a disaccharide where the galactose and glucose units are joined by a beta-glycoside bond between C1 (anomeric carbon) of galactose and C4 of glucose, conventionally indicated by the notation β(1-4). Therefore, lactose exists in the forms α- and β- lactose.

Milk, at body temperature, contains an equilibrium mixture composed of approximately 40% α-lactose and 60% β-lactose. The α anomer may be selectively crystallized from the whey concentrate at temperature below 95°C. The mixture of these two anomeric forms has been obtained by spray drying [Roelfsema and Kuster, 2000].

Since the glucopyranose component of the disaccharide may undergo mutarotation (Fig. 1), the lactose is considered to be a reducing sugar.

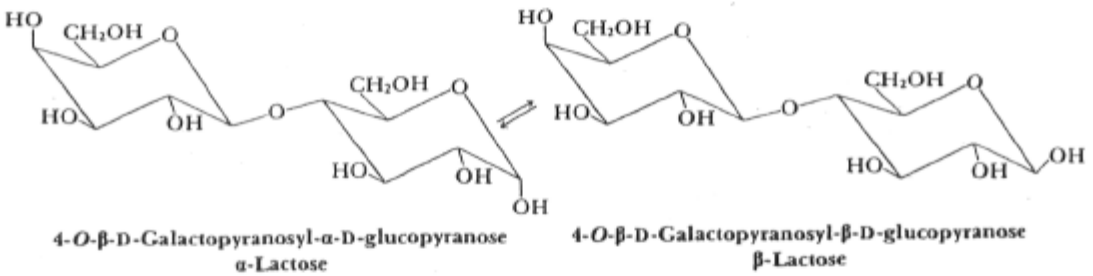

Fig. 1. The mutarotation of α-lactose into β-lactose

2.1.3. Lactose utilization

Lactose is widely used in the dairy and pharmaceutical industries. It is used in many foods as an additive for improving organoleptic quality, promoting browning reaction for color and flavor, or enhancing the emulsifying properties of shortenings [Webb and Whittier, 1970]. Also lactose is used in the manufacturing baby and infant foods. It is employed in the pharmaceutical industry for tablet making as filler, sweetener and binding substance [Booij, 1985, Nyqvist and Niklasson, 1985]. In the dairy industry, lactose is used as a substrate in fermentation media [Pritzwald-Stegmann, 1986].

2.1.4. Lactose processing and derivatives

The most important transformations of lactose include acid and enzymatic hydrolysis, dehydration, isomerization, hydrogenation and oxidation. The hydrolysis of lactose to glucose and galactose occurs in the presence of mineral acids [Mulherin et al., 1979] or in the presence of a β-galactosidases enzyme [Roger et al., 1977; Chiu and Kosikowski, 1985]. The dehydration of lactose was made possible by heating lactose under anhydrous conditions and consequently hydroxymethylfurfural, furfural alcohol, formic and acetic acids were produced [Jennes and Patton, 1959]. Lactulose was obtained in the isomerization reaction of α-lactose with calcium hydroxide [Okado et al. 1977; Hicks and Parrish, 1980]. Lactitol was obtained by the catalytic hydrogenation of lactose and is produced at industrial level [Saijonmaa et al. 1978; CCA Biochem B.V. 1981. European Patent # 039981]. The galarose was obtained by the lactose degradation with hydrogen peroxide and a borate catalyst [Ron van der Berg et al. 1995].

The oxidation of lactose for lactobionic acid production presents a great interest. Generally, enzymatic and electrochemical pathways produce lactobionic acid. The lactose derivatives with nutraceutical and pharmaceutical value are lactulose, lactitol, lactobionic acid, lactosyl urea and lactose-containing oligosaccharides [Zadow, 1984, 1986, Yang and Silva, 1995].

2.1.5. Lactobionic acid – a high value product from lactose

In the dairy industry, lactobionic acid is employed as an ingredient for foods and functional foods. According to FDA, lactobionic acid is a safe food and is employed as an additive in the form of calcium salt of lactobionic [FDA, 2003], as a firming agent and could be a food acidulant due to its sweet-sour and mildly acidic taste. The mineral salt complexes of LBA are added to beverages to fortify with minerals, and in foods as a prebiotic [Peterbauer et al., 2002].

In the production of cheese and yoghurt, LBA improves the gelation structure and the taste of sourness. As a preservative agent, it keeps flavours fresh and protects the partially hydrogenated vegetable fats against oxidation [Gerling, 1998].

In the pharmaceutical industry, LBA is used in the salt form for intravenously delivered erythromycin and in mineral supplementation component. LBA is valuable for its chelating proprieties due to its capability to form complex structures with Mn^{2+}, Cu^{2+}, Fe^{2+} and Ca^{2+} [Shepherd et al., 1993]. Therefore, LBA as iron chelator is a potent ingredient of a solution used to preserve organs prior to transplantation [Isaacson et al., 1989; Suminoto and Kamada, 1990; Shepherd et al., 1993]. LBA has the ability to suppress tissue damage caused by oxygen radicals during organ storage and subsequent reperfusion, allowing organs to be preserved outside of the body for up to two days [Southard et al., 1995]. LBA is a hygroscopic compound, which tenaciously binds the waters and provides beneficial effects to human skin. The antioxidant and humectant proprieties make LBA a potential ingredient of skin care products [Berardesca et al., 1997]. The Neostrata Company is a leader in the utilization of LBA and performs research in the optimization of skin care products.

Moreover, amine derivatives of sulphated bis-lactobionic acid exhibit anticoagulant and antithrombotic activities [Raake, 1989; Kloecking et al., 1991; Martin et al., 1999] and could replace the glycosaminoglycan heparin.

In the medical field, the latest research has demonstrated that LBA is a good acceptor for sialic acid and it may be used in the treatment of Changas disease because it acts as an inhibitor for *Trypanosoma cruzi trans-sialidase* activity [Agusti et al., 2004].

2.2. Production of lactobionic acid from lactose oxidation

The production of lactobionic acid (4-β-galactosido-D-gluconic acid) is performed by biochemical, chemical, electrochemical and catalytic oxidations of lactose.

2.2.1. Enzymatic production of LBA

A biochemical approach consists in the enzymatic oxidation of lactose using different microorganisms such as *Pseudomonas sp.*, *Bacterium pyocyaneum*, *Bacterium fluorescenns* [Stodola and Lockwood, 1946], *glucose dehydrogenase* [Satory et al., 1997], cellobiose dehydrogenase [Ludwig, 2003]. The *Pseudomonas sp.* LS13-1 has been isolated for LBA production from whey [Miyamoto et al., 2000] with a yield of more than 90% after 155 h.

The synergic effect of *cellobiose dehydrogenase* from *Sclerotium rolfsii* and *laccase* from *Trametes pubescens* MB 89 on a substrate containing lactose, monosaccharides and galacto-oligosaccharides was reported [Splechtna et al., 2001]. The conversion of lactose to LBA was 95% within 3h.

Mostly all these enzymatic processes are time consuming and require expensive enzymes and chemicals. The environmental impact of wastewater is also significant.

2.2.2. Electrochemical oxidation of lactose to LBA

Many electrochemical methods for the oxidation of lactose into lactobionic acid have already been reported. The electrolytic oxidation of lactose reported by Gupta et al. [1967] was performed using bromide in the presence of calcium carbonate, while Dutta and Sanat [1979] and Jankiewicz and Soloniewicz [1991] carried out the same reaction in the presence of $NaHCO_3$ and NaBr. The fact that lactose undergoes hydrolysis in acidic

medium and that its stability is low in alkaline solution (where interconversion occurs) explains that most of the previous work was carried out in solutions with pH values between 7 and 10 [Hendricks et al., 1990].

Similarly, the electrochemical oxidation of lactose to LBA was performed on lead-modified noble metal electrodes in Na_2CO_3 and $NaHCO_3$ buffered medium [Druliolle et al. 1994, Druliolle et al. 1995, Druliolle et al. 1997]. After 4 h, the conversion of lactose reached 95%, with 76% selectivity towards LBA in the case of Pb-Pt electrode. Unfortunately, the presence of toxic CO species and irreversible adsorption of product species caused the electrode fouling. A high conversion of lactose with a good selectivity close to 100% was obtained with a gold electrode [Druliolle et al, 1997]. Later, Casella et al. [2004] observed the formation of D-Galacturonic, D-Gluconic and D-Glucuronic acids on a polycrystalline structure of platinum and gold electrode modified with bismuth oxide adlayers.

Recently, the electrocatalytic oxidation of lactose was studied on a nanolength scale Au-colloids (5 nm) embedded in carbon felt as electrode (Au-NMC) [Kokoh and Alonso-Vante, 2006]. A production of lactobionic acid with a good yield of 91% was observed.

Despite the high yields in lactobionic acid, the electrochemical oxidation remains a method for laboratory scale. Its implementation to higher level, is expensive and complex to realize.

2.2.3. Chemical oxidation of lactose to LBA

The chemical oxidation of lactose using halogens in alkaline and acid media [Green, 1948] was reported. Also the oxidation by ferricyanide in alkaline medium [Srivastava et al., 1967], in ammoniacal solution [Gupta et al., 1981] and by alkaline hypoiodide [Ingels et al., 1948] was studied. It has also been reported that under certain conditions (pH about 9.2), the β-D-form is oxidized approximately 28 times faster than α-D anomer [Ingels et al., 1948]. Meanwhile, the oxidation process is difficult to stop and therefore lactose is oxidized to keto-sugar.

A number of intermediate products from lactose oxidation include mucic, tartaric, oxalic, gluconic or galactonic acids. Unfortunately, the chemical oxidation methods required expensive chemicals and undesired by-products.

2.2.4. Catalytic oxidation of lactose to LBA

Homogeneous catalytic oxidations of aldoses with several metal ions as catalysts and O_2, H_2O_2, halogens, or HNO_3 as oxidants, have been reported [Green, 1980].

Heterogeneous catalytic oxidation of simple aldoses to aldonic acid on supported noble metals such as platinum and palladium have been studied in detail, without mentioning lactose [Heyns et al., 1957, Heyns et al., 1962, Heyns et al., 1969, Okada et al., 1967, Dirkx and van der Baan, 1981]. Contrarily to the fact that the platinum is less sensitive to deactivation by overoxidation than palladium [Gomes et al., 2004], the selectivity towards aldonic acid is much greater for palladium-catalyzed reaction [Kiyoura et al., 1976, Nakayama et al., 1982].

Hendriks el al. [1990] have studied lactose oxidation with molecular oxygen. They have demonstrated that the presence of promoter, suppress the poisoning of the catalyst and that theoretical conversion was achieved with high selectivity toward sodium lactobionate (95%) within 1 h. 100% selectivity for sodium lactobionate was found in the pH range 7-10. At pH>10, alkaline degradation of lactose occurred, as reflected in the appearance of a yellow-brown color and a decrease of selectivity. An optimum ratio Bi: Pd in the range 0.50-0.67 for the oxidation of lactose was found. At a higher Bi:Pd ratio, the initial oxidations rate decreases to a level lower than that of the unpromoted Pd-C catalyzed oxidation. To prevent the catalyst poisoning by overoxydation, the dissolved oxygen was kept at a level <1% of the equilibrium concentration during reaction at the temperature preset.

Abbadi and van Bekkum, [1995a] have studied the catalytic oxidation reaction of lactose to sodium lactobionate and 1-carboxylactulose (Fig. 2). In order to prevent the deactivation of noble metal catalyst, they have investigated the effect of a promoting metal such as Bi and Pb in the bimetallic Pt-Bi and Pt-Pb catalysts supported on carbon.

The lactose conversion to 1-carboxylactulose (2-keto-lactobionic acid) by oxidation with air on Bi-Pt/C catalyst was also reported [Abbadi et al., 1997]. Lactose was completely oxidized to lactobionic acid within 2 hours and to 1-carboxylactulose with a maximum conversion of 83% after 4.5 hours. High conversion and yield were obtained at pH 7.

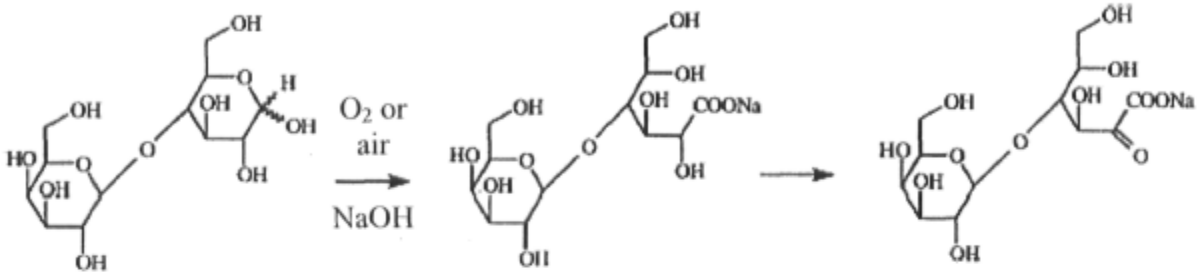

Lactose — Sodium lactobionate — 1-carboxy lactulose (2-keto-Na-lactobionate)

Fig. 2. Oxidation reaction of lactose

The influence of the addition of thallium to the catalytic properties of palladium catalysts supported on SiO_2 in the reaction of aldoses (glucose and lactose) oxidation to aldonic acid was studied [Karski, 2005]. The maximum lactose conversion was 82% within 2 hours.

Recently, Karski et al. [2006] showed that the bimetallic catalysts Pd-Bi/SiO_2 with a small amount of bismuth (1-3 wt. %) are more effective in the oxidation of lactose.

A short review of catalytic oxidation of lactose is presented in the Table 1.

Table 1. Review of catalytic oxidation of lactose

Catalysts	Conversion, %	Selectivity, %	Comments	Authors
5%Bi-5%Pd/C	95 (after 1.1 h)	100 (LBA)	Strict control of dissolved O_2	Hendriks et al, 1990.
5%Bi-5%Pt/C, 5%Pb-5%Pt/C	83 (LBA) (after 2h) >95 (2-keto-aldonic acid)	– 50 (2-keto-aldonic acid)	2-keto-aldonic acid as by-product	Abbadi et al., 1995a, 1997.
5%Tl-5%Pd/SiO_2 (1-3)%Bi-5%Pd/SiO_2	82 (after 2h) 92 (after 2 h)	92 (LBA) 98 (LBA)	(6-10)% metal loading	Karski et al. 2005, 2006.

2.2.5. Mechanism of the catalytic oxidation of lactose

Tokarev et al. [2006] described the mechanism of oxidation reaction of lactose in alkaline media (fig. 3). They explained that the mutarotation takes place through lactose with the open glucose cycle, at the same time the open form has very low concentration being most probably on a short living mutarotation intermediate. Therefore, they supposed that lactose participates in the reaction not as an aldehyde, but as a semi-acetal (α- or β-lactose), which is oxidatively dehydrogenated on the metal surface giving lactobionic acid. Since the oxidation of lactose is more efficient in basic solutions, they focused on the study of the mechanism of oxidation reaction in alkaline media, where (*) stands for a surface site. The oxidation of lactose is retarded in acidic media, which is connected to catalyst deactivation by lactobionic acid strongly adsorbed on the metal surface. The mechanism is similarly to the case described in the alcohol oxidation involving adsorption and reduction of oxygen, dehydrogenation of alcohol (semiacetal in the case of lactose) and over-oxidation of metal surfaces.

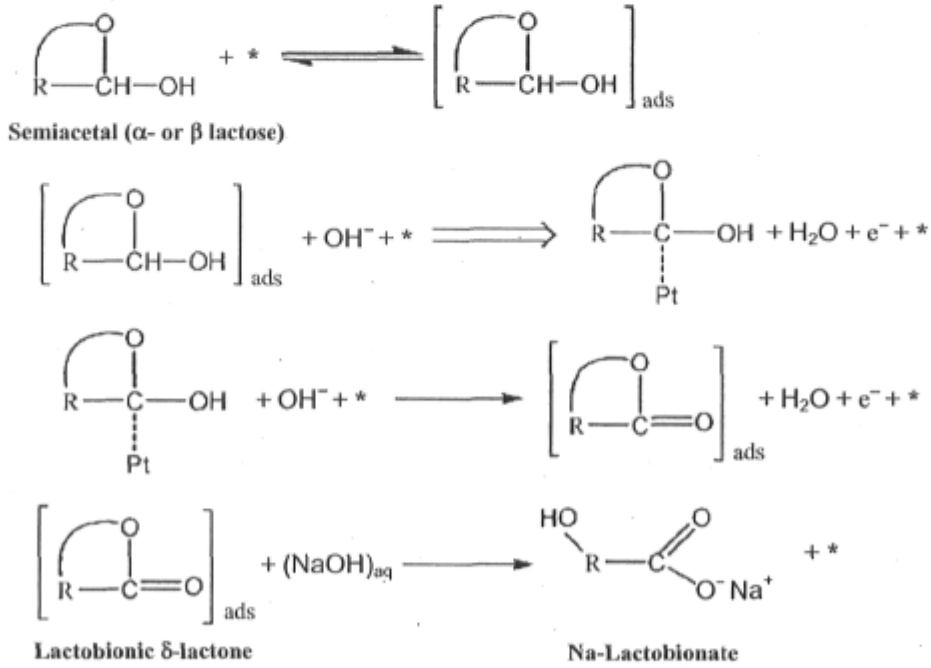

Fig. 3. The mechanism of lactose oxidation in alkaline media is proposed by Tokarev et al. [2006]

The sequence of steps in the oxidation of lactose should include molecular adsorption of oxygen, $O_2 + * \rightarrow O_2*$, as well as adsorption with dissociation $O_2 + 2* \rightarrow 2O*$. Reduction of oxygen in alkaline medium involves the participation of water and transfer of two $O* + H_2O + 2e^- \rightarrow 2OH^- + *$ or four electrons $O_2* + 2H_2O + 4e^- \rightarrow 4OH^- + *$ for atomic and molecular adsorption, respectively. Hydroxyl (OH^-) species can adsorb on the catalyst surface, leading to adsorbed hydroxyls ($OH^- + * \rightarrow OH^-*$). In alkaline medium, such adsorption can result in the formation of atomically adsorbed oxygen and H^+: $OH^- + * \rightarrow O* + H^+ + 2e^-$. Protonic ($H^+$) species can quickly recombine with OH^- giving water.

2.2.6. Catalytic oxidation of glucose

As the catalytic oxidation of lactose involves mainly the oxidation of gluconic part of the molecule to gluconic acid, an overview of the catalytic oxidation of glucose is necessary to understand the overall reaction occurred in lactose oxidation to LBA.

The catalytic oxidation of glucose with molecular oxygen on a Pd-Bi/C catalyst was previously studied [Mallat and Baiker, 1994; Wenkin et al., 2002]. The rate of glucose oxidation to gluconate was 20 times higher on the Pd-Bi/C catalyst than on Pd/C. Wenkin et al. [2002] presented interesting results connected with the role of bismuth as a promoter in the Pd–Bi catalysts for the selective oxidation of glucose. They measured the promoting effect of bismuth with $0.33 <$ molar ratio Bi:Pd < 3.

The effect of pH in the range 2-9 was studied for the Pt-catalyzed oxidation reaction of glucose [Abbadi et al. 1995b]. Poisoning of the catalyst by the reaction products in a neutral and acidic medium was observed and the degree of the inhibition of the catalytic activity was pH-dependent. They concluded that D-gluconic acid in its free form is considered to be the main inhibiting species of the platinum catalyst during the oxidation of glucose in acidic medium.

Catalytic properties of bimetallic Pd–Bi, Pd–Tl, Pd–Sn, and Pd–Co catalysts supported on C (from plum stones) and SiO_2 were studied in the reaction of glucose oxidation to gluconic acid [Karski et al., 2003]. 5% Pd–5% Bi/C and 5%Pd–5% Bi/SiO_2

catalytic systems were compared with the results for a commercial catalyst containing 1% Pt–4% Pd–5% Bi supported on active carbon. Catalysts modified with Bi showed the best selectivity and activity [Karski and Witonska, 2003].

Önal et al. [2004] have studied the oxidation of D-glucose to D-gluconic acid over Au/C catalyst. The activity of Au/C catalyst exhibited significant dependence on the pH value, thereby increasing the pH value of the reaction mixture from 7.0 to 9.5 (T=50°C) the initial reaction rate of D-gluconic acid could be accelerated by a factor of 3.2.

Besson et al. [1995] have employed, as a catalyst for the oxidation of glucose, a BiPd/C catalyst with 4.7% Pd and an atomic ratio Bi/Pd=0.1. No bismuth leakage was detected in the gluconate solution.

A short review of catalytic oxidation of glucose is presented in Table 2.

Table 2. Review of catalytic oxidation of glucose

Catalysts	Conversion, %	Selectivity, %	Comments	Authors
~5%Pd/C, 5%Bi-5%Pd/C	99 (after 4 h)	99.8 (gluconate)	(5-10)% metal loading; very good conversion and selectivity	Besson et al., 1994, Besson et Gallezot, 2000.
5%Pt/C	60 (2-keto-gluconic) 100 (gluconate) (after 2h)	– 70 (2-keto-gluconic)	2-keto-gluconic as by-product	Abaddi et van Bekkum, 1995a
5%Bi-5%Pd/C	~100 (after 4h)	~100 (gluconate)	(5-10)% metal loading; maximum of conversion and selectivity	Wenkin et al., 1996, 2002
1 % Au/C (specific surface of the support=1635 m^2/g)	80 (after 1.6 h)	95 (gluconate)	High dispersion of Au particles on the support; Au leaching	Önal et al., 2004
(5-8)%M 5%Pd/SiO_2 M=Bi, Tl, Sn, Co	82 – 98 (after 2h)	98 (gluconate)	(10-13)% metal loading	Karski et al. 2002, 2003, 2005

2.2.7. Mechanism of catalytic oxidation of glucose

The mechanism of oxidation of glucose on a Bi-Pd catalyst was explained as an oxidative dehydrogenation mechanism [Besson et al., 1995; Besson and Gallezot, 2000].

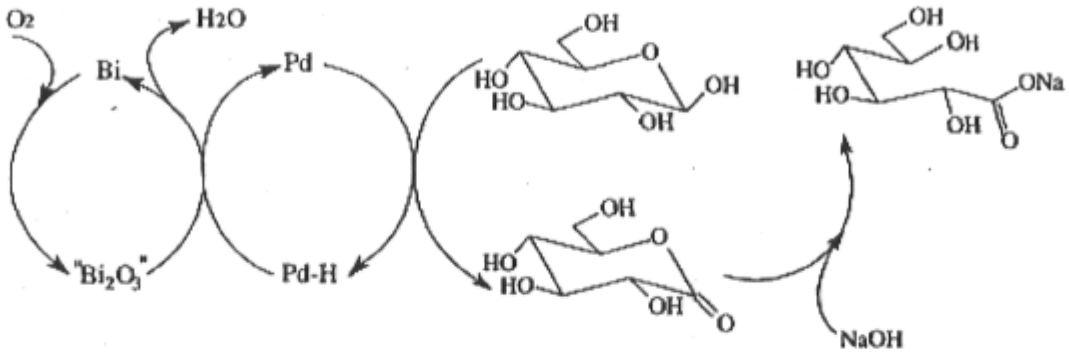

Fig. 4. Mechanism of the catalytic oxidation of glucose on Pd-Bi catalyst

The mechanism of the catalytic oxidation of glucose involves the sugar dehydrogenation and hydride transfer on the catalyst surface with the chemisorption of hydrogen. The hydride bound to the catalyst with oxygen to form water and the lactone is finally desorbed and transformed to sodium gluconate in alkaline medium. The bismuth is preferentially oxidized; therefore it extracts the hydrogen from palladium hydrides, avoiding chemisorption of O_2 on palladium surface.

2.3. Catalyst synthesis

2.3.1. Mesoporous silica molecular sieves as catalytic support

Mesoporous molecular sieves possess a large surface area and uniform mesoporous channels; these are advantageous characteristics of a catalytic support.

SBA-15 is a new type of mesoporous silica molecular sieve with uniform hexagonal channels ranging from 5 to 30 nm, thick walls (3.1–6.4 nm), and a high hydrothermal stability.

The ordered nanostructured silica has a number of advantages over conventional catalyst supports:

- The surface area is two to three times higher than that of traditional supports, like silica gels and activated alumina. This greater surface area gives a higher concentration of active sites on a weight basis, controlling the sintering dispersion at proportionally higher metal loadings.
- Limitations on particle growth inside the ordered nanostructured silica channels with controlled diameters maintain a high dispersion of the metal at loadings beyond those dictated by the requirements for a surface diffusion mechanism for metal sintering.
- It is possible to control the locations of the metal in the ordered nanostructured silica matrix. The metal may be inside the mesopores (as nanoparticles or as a thin layer), inside the micro pores that arise within the pore walls after removal of single polymer chains belonging to the corona of co-polymer surfactant micelles, or at the external surface of the nanostructured silica micro crystals [Landau et al., 2005].

The synthesis of SBA-15 comprises the solvent, the template (triblock copolymer) and the Si precursor (Fig. 5).

The triblock copolymers of poly(ethyleneoxide) and poly(propylene oxide) in water forms micelles in which the core and shell are composed of poly(propylene oxide) (PPO) blocks and poly(ethylene oxide) (PEO) blocks, respectively [Alexandridis and Hatton,

1995]. At low pH, protonated PEO chains are associated with cationic silica species through weak electrostatic interactions mediated by the negatively charged chloride ions. Below the aqueous isoelectric point of silica in acidic media, cationic silica species will be presented as precursors, and the assembly might be expected to proceed through an intermediate form of $(S^0H^+)(X^-I^+)$ (Fig. 6). Block copolymers have the advantage that they provide sacrificial templates whose microstructures can be tuned by adjusting solvent composition, molecular weight, or copolymer architecture [Zhao et al., 1998].

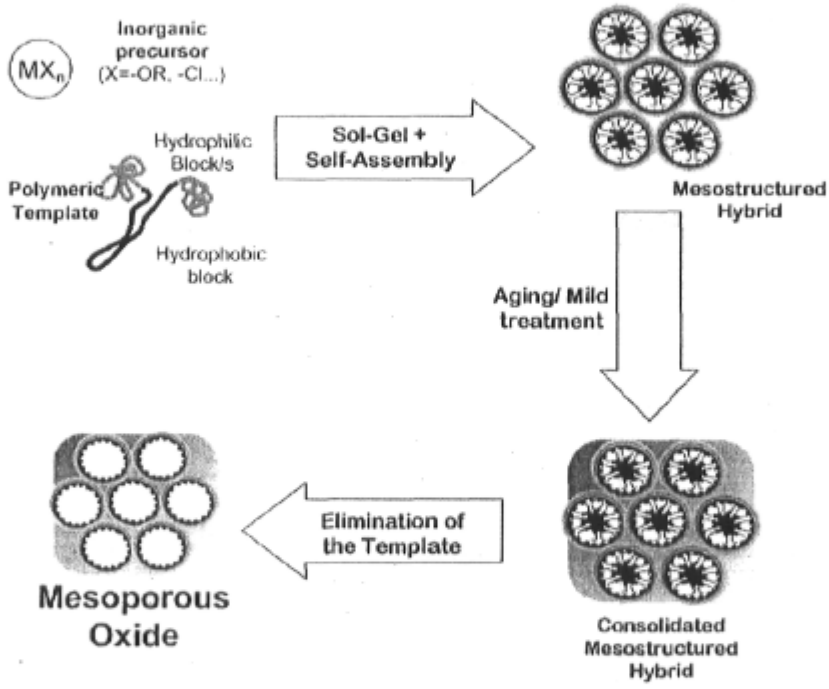

Fig. 5. Schematic view of the steps leading from a solution to a mesoporous oxide network. [Galo et al. 2003]

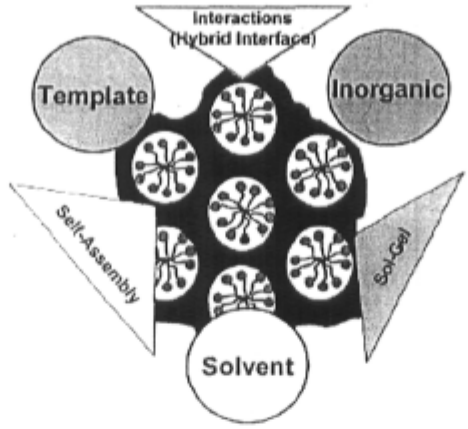

Fig. 6. Scheme of the main relationships between the solvent, the template and the inorganic center. [Galo et al. 2003]

2.3.2. Pd supported on SBA-15 material

For the preparation of Pd supported catalysts, the ion-exchange of silanol groups with precursor cations is the common technique used for the metal deposition on the internal wall surface of the mesopores. This technique involves contacting the mesoporous SBA-15 with an aqueous solution of Pd precursor. Only when a sufficiently high interaction between the two exists, can a high dispersion of the active component be achieved.

The syntheses of size-controlled noble metal nanoparticles within the channels of mesoporous molecular sieves were described [Fukuoka et. al., 2001; Magnoux et al., 2000; Mehnert et al., 1998; Koh et al., 1997; Bronstein et. al., 2001]. For example, Yuranov et al. [2002] have synthesized Pd nanoparticles with controlled size (d_{Pd} = 1–3.6 nm) by the ion-exchange technique.

Okitsu et al. [1996] have reported the formation of noble metal particles by ultrasonic radiation. Chen et al. [2000] also have studied a sonochemical procedure at room temperature for the preparation of palladium Pd nanoparticles (5-6 nm in diameter) loaded within mesoporous silica. The chemical effect of ultrasound is attributed to cavitation: the

formation, growth and implosive collapse of bubbles, which lead to the decomposition of water molecules into hydrogen H and hydroxyl OH radicals owing to the production of high temperature and high pressure in collapsing cavities. Therefore, the Pd salt is reduced *in situ*.

Shortly, the goals of these syntheses are:

- the size control of Pd particles confined within the mesopores (Fig. 7 and Fig. 8);
- the incorporation of Pd at high loading and
- the resistance of the Pd/mesoporous silica structure against a collapse and sintering at elevated temperatures.

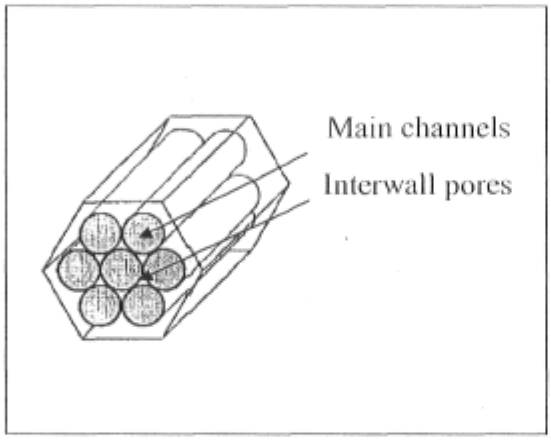

Fig. 7. Nanostructured silica representation.

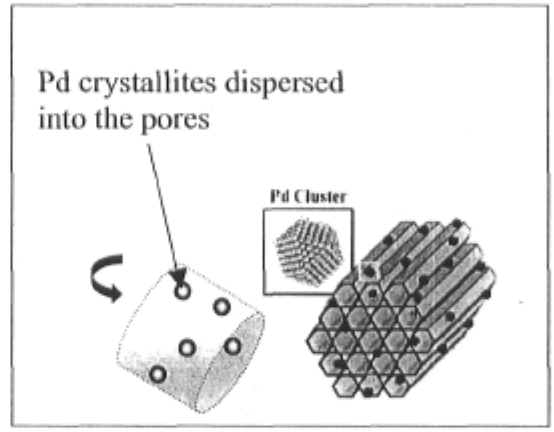

Fig. 8. Model for Palladium dispersion on nanostructured silica

2.3.3. Formulation of bimetallic catalyst Pd-Bi

The molar ratio Bi:Pd was studied and optimized for lactose and glucose reaction in order to improve the selectivity and the activity of the bimetallic supported catalyst. [Besson et al. 1995; Besson and Gallezot 2000; Karski et al. 2002]. The experiments performed with the pure intermetallics Bi_2Pd, BiPd and $BiPd_3$ showed that the intrinsic catalytic behaviour of these phases were very different; the most active phase, Bi_2Pd, is the one that loses the largest amount of Bi, whereas $BiPd_3$, the most stable phase during operation, remains totally inactive [Wenkin et al. 2002].

Recently, Karski [2006] studied the interactions between Pd and Bi in Pd–Bi/SiO_2 catalysts and their connection with activity and selectivity of those systems in the selective oxidation of glucose and lactose. In the case of the oxidation of lactose, better catalytic properties were found for Pd–Bi/SiO_2 systems with a small amount of bismuth, where mainly a binary alloy BiPd is formed.

2.4. Oxidation reaction in a three-phase slurry reactor

In fine-chemical production, three-phase reaction systems using the mechanically stirred batch reactors are common. A three-phase slurry reactor consists of a solid catalyst (usually a fine powder) suspended in a liquid by means of an agitator with gas diffusing through the system. In the oxidation reaction, oxygen from air bubbles and a solid catalyst oxidize the aqueous solution of the reactant. Due to the nature of the slurry reactor, where the three phases must meet on the catalyst surface in order for the reaction to occur, mass transfer plays a crucial role in the process. Five reaction steps describe the mass transfer of oxygen:

1. Absorption from the gas phase into the liquid phase at the bubble surface
2. Diffusion in the liquid phase from the bubble surface to the bulk liquid
3. Diffusion from the bulk liquid to the external surface of the solid catalyst
4. Internal diffusion of the reactant in the porous catalyst
5. Reaction within the porous catalyst.

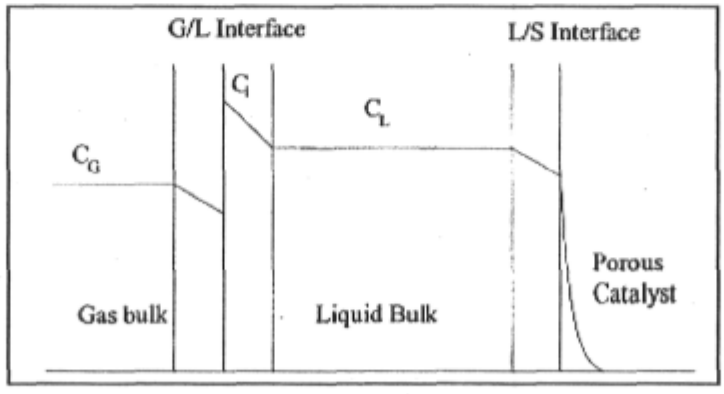

Fig. 9. Mass transfer and reaction in series for a porous catalyst. [Kluytmans et al., 2000]

Fig. 9 presents the concentration profile for a dissolving gas, transferred to the catalyst surface and reacting inside the catalyst, C_i being the interface, equilibrium concentration. For oxygen dissolving in water, C_G is not to scale. It represents about $50C_L$.

In order to carry out properly the kinetic aspects of the reaction, it is useful to discern two extreme regimes. The first one is the so-called *intrinsic kinetic regime*, i.e. the reaction rate is *only* determined by the chemistry at the catalytic site and not limited by mass transfer and diffusion effects, and the second one is the full *oxygen mass transfer limited regime*, i.e. the reaction rate *only* depends on oxygen mass transfer and diffusion.

Generally, the reactions using unpromoted platinum fall in the first category, whereas those using promoted platinum and palladium fall in the second category. Literature data from other authors [Mallat et al. 1994], always concern batchwise oxidations, where the mixing characteristics of the laboratory reactor used are rather unspecified. Generally these data fall in a mixed regime, where the reaction rate is partly limited by oxygen mass transfer at the start of the reaction with a fresh, active catalyst, and finally, when the reactivity of the mixture is diminished or the catalyst becomes partly deactivated, the system ends up in the kinetic regime. [Kluytmans et al., 2000].

Consequently, the most important choices in the design of batch reactors are:

- Reactor volume;
- Selection of the agitator;
- Speed of the agitator;
- Geometry of the tank;
- Heat exchange area (internal and external).

Therefore, it is useless to try and improve the reaction rate by using a more active catalyst or by increasing the catalyst load, when the overall rate of reaction is determined by mass transfer from the gas bubbles to the liquid phase, i.e. when the latter is slow compared with the intrinsic rate of reaction. Instead, one should try to increase the gas-to-liquid mass transfer rate, for example by improving mixing conditions [Moulijn et al., 2001].

2.5. Catalyst deactivation

A short overview on catalyst deactivation is presented, based on Mallat and Baiker's review [1994] and Vleeming et al. [1997], mainly referring to carbon supported catalysts.

a) Crystallite sintering

In a strongly reducing environment, noble metal crystallites become mobile on the carbon support, probably due to destruction of the anchoring sites. The result is agglomeration of metal crystallites and a reduction of available active surface.

b) Inhibition (poisoning, coking, product inhibition)

This type of deactivation may occur at any potential range, but is generally more pronounced in the lower potential range. Poisoning can be due to impurities in the reactor feed, to too much promoter metal [Hendriks et al., 1990], and to strongly adsorbing intermediates or side products, e.g. CO, which are especially formed in the low potential range. Carbonaceous compound formation (coking) from reactive intermediates results in pore filling and loss of activity. Finally, an adsorbing main product, e.g. carboxylic acids at low pH, will prevent the starting reactant from reaching the catalytic site. This can be avoided by working at pH > 7 [Abbadi et al., 1997] or by removing the product by e.g. ion-exchange or electrodialysis.

c) Over-oxidation

Working under kinetic control, the catalyst potential will be close to 1 V immediately after the starting of a reaction, and deactivation is caused by "over-oxidation i.e. an inactive oxidized corroded surface is slowly formed and catalyst activity drops typically by a factor 5 within 2 h [Vleeming et al., 1997]. This type of deactivation is reversible. It was found that promoted catalysts are more sensitive to over-oxidation, i.e. if there is no mass transfer limitation of oxygen, these catalysts show no activity at all from the start of reaction [Smits et al., 1986; Hendriks et al., 1990]. These catalysts probably work well only below the potential where the promoting metal is oxidized to a too-high oxidation state.

In their review, Mallat and Baiker [1994] suggest a causal sequence: chemical poisoning by over-oxidation corrosion. Therefore, also the causal sequence given by Gallezot [1997], that "promotion improves catalyst activity by preventing over-oxidation", better can be reverted to "promotion prevents over-oxidation by improving catalyst activity".

d) Crystallite growth, leaching

After prolonged over-oxidation, especially in the presence of chelating substances or high pH, metal crystallites inside the catalyst pores grow (Ostwald ripening) due to dissolution and redeposition, i.e. large crystallites are formed at the expense of the small ones. This generally results in permanent loss of catalyst activity [Schuurman et al., 1992; Vleeming et al., 1997]. If such conditions persist, the active metal may leaches from the catalyst and get lost. Obviously such conditions should be avoided.

e) Promoter leaching

As the promoters used, e.g. Pb, Sn, Bi, are less noble than Pt and Pd, they are most susceptible to leaching. In fact, it can be stated that the location of the promoter is a rather dynamical one, where it can be present on the noble metal crystallite, on the catalyst support [Smits et al., 1986; Smits et al., 1987] or in solution [Gallezot, 1997; Groenland et al., 1995]. Low promoter loadings generally result in insignificant leaching [Gallezot, 1997].

2.6. Problematical

The investigation of the heterogeneous catalytic oxidations of lactose and glucose highlights the following points:

- bismuth acting as a co-catalyst preventing the oxygen poisoning of palladium was found optimum in the range of Bi:Pd ratio 0.1-1;
- bimetallic compound such as BiPd and Bi_2Pd alloys were formed and they seem to be responsible for the catalyst performance;
- carbon and SiO_2 support catalysts were mostly employed for the oxidation reaction of aldose;
- dissolved oxygen during reaction is clearly responsible for catalyst poisoning by over- oxidation;
- operating temperature was optimum in the range 50-65^{0}C;
- oxidation process must be performed under reaction conditions (sufficient stirring and airflow rate) at which by external mass transfer at the phase boundaries does not limit the overall reaction rate [Önal et al., 2004];
- the rate of reaction of glucose oxidation increased by increasing the specific area of the support employed [Önal et al., 2004];
- reaction medium is kept at pH level in the range 7-10 in order to prevent the catalyst self-poisoning and also because the lactose undergoes hydrolysis in acidic medium and its stability is low in alkaline solution.

Despite the high yields in aldonic acids obtained by catalytic oxidation of aldoses many issues are observed, such as:

- Bi-Pd/C catalysts do not maintain the continuous dehydrogenation and the reaction stops when the catalyst surface is saturated with H_2 and aldonic acid;
- The loss of catalyst selectivity under weakly alkaline conditions is assumed to be due to non-selective gluconic interaction between the promoter and aldonic acid/ 2-keto-aldonic acids leading to C3 oxidation [Abbadi et al., 1995a];

- Carbon supports were found to be unstable at a moderately high temperature [Gerling, 1998];
- Catalyst deactivation can occur via geometric blocking of a fraction of active sites with the strongly adsorbed products or the agglomeration of metal crystallites with the reduction of available active surface and/or the leaching of Bi as Bi^{3+} with the formation of complex species.

2.7. Bibliography

1) Abbadi A., van Bekkum H. **1995a**. Highly selective oxidation to 2-keto-aldonic acids over Pt-Bi and Pt-Pb catalysts. Appl. Catal. A: General. 124: 105-115.
2) Abbadi A., van Bekkum H. **1995b**. Effect of pH in the Pt-catalyzed oxidation of D-glucose to D-gluconic acid. J. Mol. Catal. A: Chemical. 97: 111.
3) Abbadi A. Gotlied K.F., Meiberg J.B.M., van Bekkum H. **1997**. Selective Chemo-Catalytic Oxidation of Lactose and/of Lactobionic Acid towards 1-Carboxylactulose (2-keto-Lactobionic Acid). Appl. Catal. A: General. 156: 105.
4) Agusti R., Paris G., Ratier L., Frasch A. C. C., Lederkremer R. M. **2004**. Lactose derivates are inhibitors of *Trypanosoma cruzi trans-sialidase* activity toward conventional substrates in vitro and in vivo. Glycobiology. 14: 659.
5) Alexandridis P., Hatton T.A.. **1995**. Colloids Surface. A 96: 1.
6) Berardesca E., Distante F., Vignoli G. P., Oresajo C., Green B. **1997**. Alpha Hydroxyacids Modulate Stratum Corneum Barrier Function. British J Dermatol. 137: 934.
7) Besson M., Lahmer F., Gallezot P., Fuertes P., Fleche G. **1995**. Catalytic Oxidation of Glucose on Bismuth-Promoted Palladium. Catalysts. J Catal. 152: 116.
8) Besson M. and Gallezot P. **2000.** Selective oxidation of alcohols and aldehydes on metal catalysts. Catal. Today. 57: 127–141.
9) Booij C.J. **1985**. Use of Lactose in the Pharmaceutical and Chemical Industry. J Soc. Dairy Technol. 38: 105.
10) Bronstein L.M., Polarz S., Smarsly B., Antonieti M. **2001**. Adv. Mater. 13: 1333. Yuranov I., Moeckli P., Suvorova E., Buffat P., Minsker L.K., Renken A. 2003. Pd/SiO_2 catalysts: synthesis of Pd nanoparticles with the controlled size in mesoporous silicas. J. Mol. Catal. A: Chemical 192: 239.
11) Casella G. I., Gatta M., Contursi M. **2004**. Oxidation of Sugar Acids on Polycrystalline Platinum and Gold Modified with Adsorbed Bismuth Oxide Adlayers. J Electroanalytical. Chem. 561: 103.

12) Chen W., Cai W., Lei Y., Zhang L. **2001**. A sonochemical approach to the confined synthesis of palladium nanoparticles in mesoporous silica. Materials Lett. 40: 53.

13) Chiu C.P., Kosikowksi F.W. **1985**. Hydrolyzed Lactose Syrup from Concentrated Sweet Whey Permeates. J Dairy Sci. 68: 16.

14) Dirkx M. H. and Van der Baan H. S. **1981**. J. Catal. 67: l-13.

15) Druliolle H., Kokoh K.B., Beden B. **1994**. Electro-Oxidation of Lactose on Platinum and on Modified Platinum Electrodes in Alkaline Medium. Electrochemica Acta. 39: 2577.

16) Druliolle H., Kokoh K.B., Beden B. **1995**. Selective Oxidation of Lactose to Lactobiotic Acid on Lead-Adatoms Modified Platinum Electrodes in Na_2C0_3 + $NaHC0_3$ Buffered Medium. J Electroanalytical. Chem. 385: 77.

17) Druliolle H., Kokoh K.B., Hahn, F., Lamy C., Beden B. **1997**. On some Mecanistic Aspects of the Electrochemical Oxidation of Lactose at Platinum and Gold Electrodes in Alkaline Medium. J Electroanalytical. Chem. 426: 103.

18) Dutta S.K. and Sanat K., US Patent 4137397, 30 January **1979**. Chem. Abstr. 90: 174677z.

19) FAO, FAOSTAT Data, **2004**.

20) FDA. **2003**. Calcium lactobionate. Food Additives Permitted for Direct Addition to Food for Human Consumption: Part 172, Code of Federal Regulations, Title 21, Vol. 3.

21) Fukuoka A., Higashimoto N., Sakamoto Y., Sasaki M., Sugimoto N., Inagaki S., Fukushima Y., Ichikawa M. **2001**. Catal. Today. 66: 23.

22) Gallezot P. **1997**. Selective oxidation with air on metal catalysts. Catal. Today 37: 410.

23) Galo J. de A.A. Soler-Illia, Crepaldi E.L., Grosso D., Sanchez C. **2003**. Block copolymer-templated mesoporous oxides. Current Opinion in Colloid and Interface Science. 8: 113.

24) Gerling. K. G. **1998**. Large-Scale Production of Lactobionic Acid - Use and New Applications. In Whey, Proceedings of the Second International Whey Conference, Chicago, IL. 27-29 Oct. 1997. International Dairy Federation. Brussels. Belgium, pp. 251.

25) Gomes H.T., Orfao J. J. M., Figueiredo J. L., Faria J. L. **2004**. CW AO of Butyric Acid Solutions: Catalyst Deactivation Analysis. Ind. Eng. Chem. Res. 43: 1216.

26) Green J.W. **1948**. The halogen oxidation of simple carbohydrates. Advanced in Carbohydrate Chemistry. Vol.3. Acad. Press. New York.

27) Green J. W., in Pigman W. and Horton D. (Eds.). **1980**.The Carbohydrates, Chemistry and Biochemistry, Vol. lB, Academic Press , chapter 24.

28) Groenland W.P.T., van Zundert A.F.M., Kuster B.F.M., Marin G.B. January **1995**. Report to Glucons (AVEBE, AKZO), Veendam, the Netherlands.

29) Gupta M.L.S., Bhattacharya N. and Basu U.P. **1967**. Indian J. Technol. 5: 152.

30) Gupta K.C., Sharma A., Misra V.D. **1981**. Kinetics of oxidation of some disaccharides in amoniacal medium. Tetrahedron. 37: 2887.

31) Hendriks H. E.J., Kuster B. F.M., Marin G. B. **1990**. The Effect of Bismuth on the Selective Oxidation of Lactose on Supported Palladium Catalysts. Carbohydr. Res. 204:121.

32) Heyns K. and Paulsen H. **1957**. Angew. Chem., 69: 600-608.

33) Heyns K. and Paulsen H. **1962**. Adv. Carbohydr. Chem.. 17: 169-211.

34) Heyns K., Paulsen H., Ruediger G., and Weyer J., Fortschr. **1969**. Chem. Forsch., 11: 285-374.

35) Hicks K. B., Parrish F. W. **1980**. A New Method for Preparing Lactulose from Lactose. Carbohydr. Res. 82: 393.

36) Hobman P.G. **1984**. Review of Processing for Utilization of Lactose in Deproteinated Milk Serum. J Dairy Sci. 82: 2630.

37) Ingels O. G. and Israel E. C. **1948**. J. Chem. Soc. 810.

38) Isaacson Y., Salem O., Shepherd R E., van Thiel D. **1989**. Lactobionic Acid as an Iron Chelator: A Rationale for its Effectiveness as an Organ Preservant. Life Sciences. 45: 2373.

39) Jankiewicz B. and Soleniewicz R. **1991**. Acta Pol. Pharm.-Drug Res. 48 : **7.**

40) Jenness R. and Patton S. **1959**. Principles of dairy chemistry. New York: Wiley, pp 446.

41) Jenness R., Sloan R. E. **1970**. The Composition of Milks of Various Species: A Review. Dairy Sci. Abstr. 32: 599.

42) Karski S., Paryjczak T., Witonska I. **2003**. Selective Oxidation of Glucose to Gluconic Acid over Bimetallic Pd-Me Catalysts (Me= Bi, Tl, Sn, Co). Kinet. Catal. 44: 619.

43) Karski S. and Witonska I. **2003**. Bismuth as an Additive Modifying the Selectivity of Palladium Catalysts. J Molec. Catal. A: Chemical. 191: 87.

44) Karski S., Witonska I., Gołuchowska J. **2005**. Catalytic properties of Pd–Tl/SiO_2 systems in the reaction of liquid phase oxidation of aldoses. J Mol.Catal. A: Chemical 245: 225.

45) Karski S. **2006**. Activity and selectivity of Pd-Bi/SiO_2 catalysts in the light mutual interaction between Pd and Bi. J. Mol. Catal. A: Chemical 253: 147.

46) Kavanaugh J.A. **1975**. Production of Crude Lactose from Ultrafiltration Permeate. NZ. J Dairy Sci. Technol.10: 132.

47) Kiyoura T., Kimura T., and Sugiura T. **1976**. Japan. Kokai 76: 52,121; 85: 160,467r.

48) Kloecking, H.P., Hoffmann A., Fareed J. **1991**. Influence of Synthetic Sulfated bis-Lactobionic Acid Amides on Tissue Type Plasminogen Activator Release. Thromb. Res. 62: 227.

49) Kluytmans J.H.J., Markusse A.P., Kuster B.F.M., Marin G.B., Schouten J.C. **2000**. Catal. Today. 57: 146.

50) Koh C.A., Nooney R., Tahir S. **1997**. Catal. Lett. 47: 199.

51) Kokoh K. B. and Alonso-Vante N. **2006**. Electrocatalytic oxidation of lactose on gold nanoparticle modified carbon in carbonate buffer. J Applied Electroch. 36:147.

52) Landau M.V., Vradman L., Wolfson A., Madhusudhan R.P., Herskowitz M. **2005**. Dispersions of transition-metal-based phases in mesostructured silica matrixes: preparation of high-performance catalytic materials. C.R. Chimie. 8: 680.

53) Ludwig R., Ozga M., Zamocky M., Kulbe K. D., Haltrich D. **2003**. Formation of lactobionic acid by a novel biocatalytic process. Paper 342. Advances in Biocatalysis. In: Proc. 225th ACS National Meeting, New Orleans, LA.

54) Magnoux P., Lavaud N., Guisnet M. **2000**. Top. Catal. 13 : 291.

55) Mallat T., Baiker A. **1994**. Oxidation of Alcohols with Molecular Oxygen on Platinum Metal Catalysts in Aqueous Solutions. Catal. Today. 19: 247.

56) Martin D.J., Toce J.A., Anevski P.J., Tollefsen D. M., Abendschein D. R. **1999**. Anticoagulant and antithrombotic activity of maltodapoh, a novel sulfated tetrasaccharide. J. Pharmacol. Exp. Therapeut. 288: 516.

57) Mehnert C.P., Weaver D.W., Ying J.Y. **1998**. J. Am. Chem. Soc. 120: 12289.

58) Miyamoto Y, Ooi, T., Kinoshita S. **2000**. Production of Lactobionic Acid from Whey by *Pseudomonas sp. LS13-1*. Biotechnol. Lett. 22: 427.

59) Moulijn J.A., Makkee M. and van Diepen A.E. **2001**. Chemical Process Technology. New York: Wiley, pp 453.

60) Mulherin. B., Mullen T., Delaney R. A. M., Harper W. J. **1979.** Acid Catalyzed Hydrolysis of Lactose with Cation Exchange Resins. N Z. J Dairy Sci. Technol. 14: 127.

61) Nakayama M., Kimura A., Eguchi H., and Matsui T. **1982**. Eur. Pat. Appl. EP 48: 974; 97: 39, 31 le.

62) Nyqvist H., Niklasson M. **1985**. Flow Properties of Compressible Lactose-Containing Small Quantities of Drug Substances. Drug. Dev. Ind. Pharm. 11: 745.

63) Okada J., Morita S., Matsuda Y., and Takenawa T. **1967**. Yakugaku Zasshi. 87: 1326-1333.

64) Okado K., Ogas K., Tomita M. **1977**. Process for Preparing a Lactulose Containing Poweder for Feed. US patent. # 4, 142, 916.

65) Okitsu K., Mizukoshi. Y., Bandow H., Maeda Y., Yamamoto T., Nagata Y. **1996**. Formation of noble metal particles by ultrasonic irradiation. Ultrasonics Sonochemistry. 3: 249.

66) Önal Y., Schimpf S., Claus P. **2004**. Structure Sensitivity and Kinetics of D-Glucose Oxidation to D-Gluconic Acid over Carbon-Supported Gold Catalysts. J. Catal. 223: 122.

67) Peterbauer C.K., Galhaup C., Ludwig R, Kulbe K. D., Haltrich D. **2002**. Production of Lactobionic Acid by Enzyme Technology. Inter. Conf. "Biocatalysis in the Food and Drinks Industries", London UK, June 16-19.

68) Pritzwald-Stegmann B. F. **1986**. Lactose and some of its Derivatives. J Soc. Dairy Technol. 39: 91.

69) Raake W., Klauser R.J., Elling H., Meinetsberger E. **1989**. Anticoagulant and Antithrombotic Properties of Synthetic Sulfated bis-Lactobionic Acid Amides, Thromb. Res. 56: 719.

70) Roelfsema W.A., Kuster B.F.M. **2000**. Lactose and Derivatives, Ullman Encyclopedia of Industrial Chemistry, WileyVCH Verlag, A15: 10.

71) Roger L., Thapon J. L., Maubois J. L. **1977**. Continuous Lactose Hydrolysis in an Enzymatic Membrane Reactor. Nord. Mejeri-Tidsskr. 43: 38.

72) Ron van den Berg, Joop A. Peters, Herman van Bekkum. **1995**. Selective alkaline oxidative degradation of mono and di-saccharides by hydrogen peroxide using borate as catalyst and protecting group. Carbohydr. Res. 267: 65.

73) Saijonmaa T., Heikonen M., Kreula M., Linko P. **1978**. Preparation and Characterization of Milk Sugar Alcohol, Lactitol. Milchowissenschaft. 33: 733.

74) Satory M., Fuerlinger M., Haltrich D., Kulbe D.K., Pittner F., Nidetzky B. **1997**. Continuous Enzymatic Production of Lactobionic acid using Glucose-Fructose Oxidoreductase in an Ultrafiltration Membrane Reactor. Biotechnol. Lett. 19: 1205.

75) Schuurman Y., Kuster B.F.M., van der Wiele K., Marin G.B. in P. Ruiz, B. Delmon (Eds.). **1992**. New developments in selective oxidation by heterogeneous catalysis. Stud. Surf. Sci. Catal. 72: 43.

76) Shepherd R.E., Issacson Y., Chensny L., Zhang S., Kortes R., John K. **1993**. Lactobionic and Gluconic Acid Complexes of Fe II and Fe III; Control of Oxidation Pathways by an Organ Transplantation Preservant. J. Inorg. Biochem. 49: 23.

77) Smits P.C.C., Kuster B.F.M., van der Wiele K., van der Baan H.S. **1986**. Carbohydr. Res .153: 227.

78) Southard J.H., Belzer F.O. **1995**. Organ preservation. Annu Rev. Med. 46: 235.

79) Splechtna, B., Ptzelbauer I., Baminger U., Haltrich D., Kulbe D. K., Nidetzky B. **2001**. Production of Lactose-Free Galacto-Oligosaccharide Mixture by using Selective Enzymatic Oxidation of Lactose into Lactobionic Acid. Enzyme Microbial Technol. 29: 434.

80) Srivastava R. K., Nath N. and Singh M. P. **1967**. Kinetics and mecanism of oxidation of some disaccharides-melibiose, cellobiose, lactose and maltose - by hexacyano-ferrate (III) in alkaline medium. Tetrahedron. 23: 1189.

81) Stodola F .H, and Lockwood L.B. **1947**. The Oxidation Lactose and Maltose to Bionic Acids by Pseudomonas. J Bioi. Chem. 171: 213.

82) Sumitomo R., Kamada N. **1990**. Lactobionate as the most Important Component in UW Solution for Liver Preservation. Transplant. Proc. 22: 2198.

83) Tokarev A.V., Murzina E.V., Kuusisto J., Mikkola J.-P., Eränen K., Murzin D.Y. **2006**. Kinetic behaviour of electrochemical potential in three-phase heterogeneous catalytic oxidation reactions. J. Mol. Catal. A: Chemical 255: 205.

84) Vleeming J.H., Kuster B.F.M., Marin G.B., Oudet F., Courtine P. **1997.** J. Catal. 166: 148.

85) Webb B.H., Whittier E.O. **1970**. By-products from Milk 2nd ed. A VI Publishing Co., Westport, CT. 428p.

86) Wenkin M., Touillaux R., Ruiz P., Delmon B., Devillers M. **1996.** Influence of metallic precursors on the properties of carbon-supported bismuth-promoted palladium catalysts for the selective oxidation of glucose to gluconic acid. Appl. Catal. A.: Gen. 148: 181.

87) Wenkin M., Ruiz P., Delmon B., Devillers M. **2002.** The role of bismuth as promoter in Pd-Bi catalysts for the selective oxidation of glucose to gluconate. J Mol. Catal. A: Chem.180: 141.

88) Yang S.T., Silva E.M. **1995**. Novel Products and New Technologies for Use of a Familiar Carbohydrate, Milk Lactose. J Dairy Sci. 78: 2541.

89) Zadow J. G. **1984**. Lactose: Properties and Uses. J Dairy Sci. 67: 2654.

90) Zadow J. G. **1986**. The Use of Lactose in Food Products. In: Milk -The Vital Force. Proc. 22nd Int. Dairy Congress, Reidel, Dordrecht, pp. 737.

91) Zhao D., Feng J., Huo Q., Melosh N., Fredrickson G. H., Chmelka B. F., Stucky G. D. **1998**. Triblock Copolymer Syntheses of Mesoporous Silica with Periodic 50 to 300 Angstrom Pores. Science. 279: 548.

CHAPTER 3

HYPOTHESIS & OBJECTIVES

3.1. Hypothesis

The oxidation of lactose to LBA and glucose to gluconic acid with oxygen or air on the bimetallic supported catalysts has been performed. According to the oxidative-dehydrogenation mechanism, the support may improve the contact between the reactants and the Pd and Bi dispersion.

The catalyst conventional supports based on carbon reviewed in the literature does not maintain continuous dehydrogenation of sugars and the reaction stops at longer reaction time because the palladium surface is saturated with aldonic acid and hydrogen. In principle, the Bi redox cycle should have a greater capacity than the Pd redox cycle. The Bi:Pd ratio is seemed to be critical and bismuth adatoms should be fixed onto the surface of palladium.

Önal et al. [2004] have demonstrated that with an increasing in surface area or modifying the pore structure of the catalyst support, the initial reaction rate increased. Thus, the surface and pore characteristics of the support plays an important role to improve the access of the reactants to catalytic sites.

A structured support such as nanostructured siliceous materials [Zhao et al., 1998; Hamoudi and Belkacemi, 2004] will be able to improve the catalyst performance.

These statements allowed us to hypothesise that an improved catalyst system with a nanostructured silica support and an adequate loading and selective deposition of Pd and Bi nanoparticles would be able to maintain balanced and continuous redox reactions and enhance the activity, selectivity and stability of the catalyst. We also hypothesise that the optimization of process conditions with the improved catalyst system would further enhance the selective conversion of lactose to LBA.

3.2. Objectives

The **main objective** of this project is to selectively produce lactobionic acid via the partial oxidation of lactose over a bimetallic Pd-Bi catalyst supported on nanostructured silica materials.

The **specific objectives** are:

1. Formulation of the bimetallic Pd-Bi catalyst supported on nanostructured silica material;
2. Physico-chemical characterization of the formulated catalysts;
3. Optimization of the reaction conditions of lactose catalytic oxidation such as: metal loading on the nanostructured support, temperature, air flow, metal/lactose ratio, pH of the reaction medium, which lead to the highest selective conversion of lactose into LBA;
4. Performing the scale-up studies in the optimal conditions of lactose oxidation reaction;
5. Investigation of the catalyst stability.

CHAPTER 4

METHODOLOGY AND EXPERIMENTAL PROCEDURES

4.1. Project methodology

According to the specific objectives enounced earlier, the methodology of this project was developed and described in the scheme presented in Fig. 10.

4.1.1. Chemicals:

In this project, the following chemicals were employed:

- Pluronic acid P123 (BASF);
- TEOS (Sigma Aldrich);
- $Bi(NO_3)_2 \cdot 5H_2O$ (Aldrich);
- $Pd(NO_3)_2 \cdot xH_2O$ Aldrich);
- Lactose monohydrate (Sigma Aldrich);
- Lactobionic acid (Sigma Aldrich);
- NaOH solution, 50% (Fluka);
- Sodium acetate (Fluka);
- Bi standard for ICP (SCP Science, Quebec);
- Pd standard for ICP (SCP Science, Quebec).

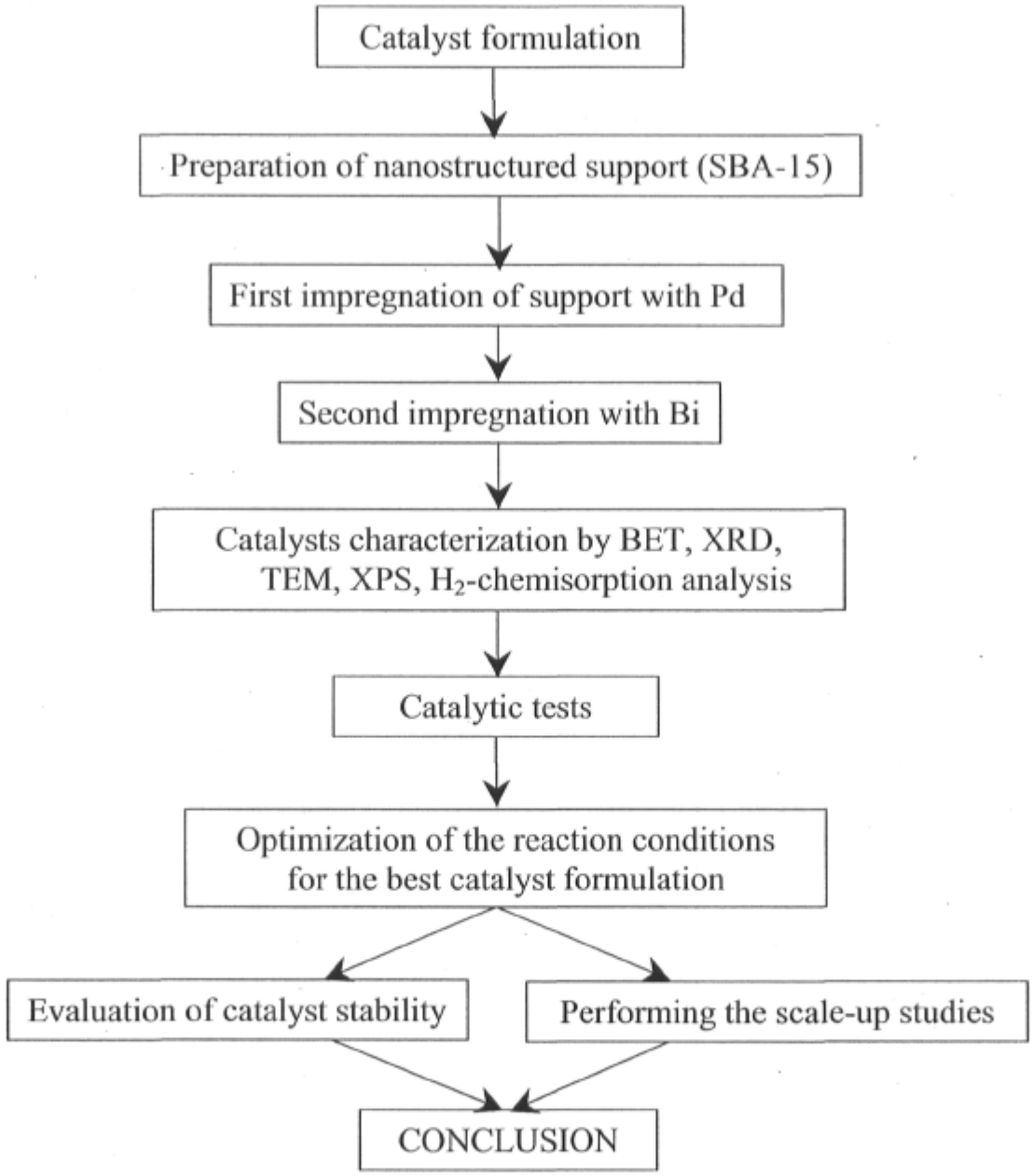

Fig. 10. The scheme including the principal steps of the research methodology

4.1.2. Equipment.

The equipments employed were:

- Ultrasonic bath TRANSSONIC T310, Germany;
- Magnetic hot-plate, Fisher;
- Two-pieces Jacketed reactor (1L), AceGlass, USA (Fig. 11);
- Water bath, PolyScience, Illinois, USA;
- Digital temperature controller, PolyScience, Illinois, USA;
- Disolved Oxygen probe, Cole-Parmer, Illinois, USA (Fig. 12);
- Benchtop dissolved oxygen meter, Cole Parmer, Illinois, USA;
- Pencil-thin pH electrode Acummet, Fisher Scientific;
- Titrator Mettler-Toledo, Switzerland (Fig. 13);
- Diffractometer with focusing beam monochromated Cu K_α radiation, Ultima III Rigaku, Japan (Fig. 14);
- Volumetric adsorption analyzer, Quantachrome Instruments, Boyton Beach, Florida (Fig. 15);
- HPLC ICS-2500 Dionex, USA (Fig. 16) equipped with:
  - Colonne CarboPac PA1, Dionex, USA;
  - Amperometric cell outfitted with gold electrodes and a Ag/AgCl reference electrode, Dionex, USA;
- Programmable furnace, Manfredi, Italy;
- Microscope JEOL JEM-1230, Japan;
- Spectrometer system Axis-Ultra, Kratos, U.K.

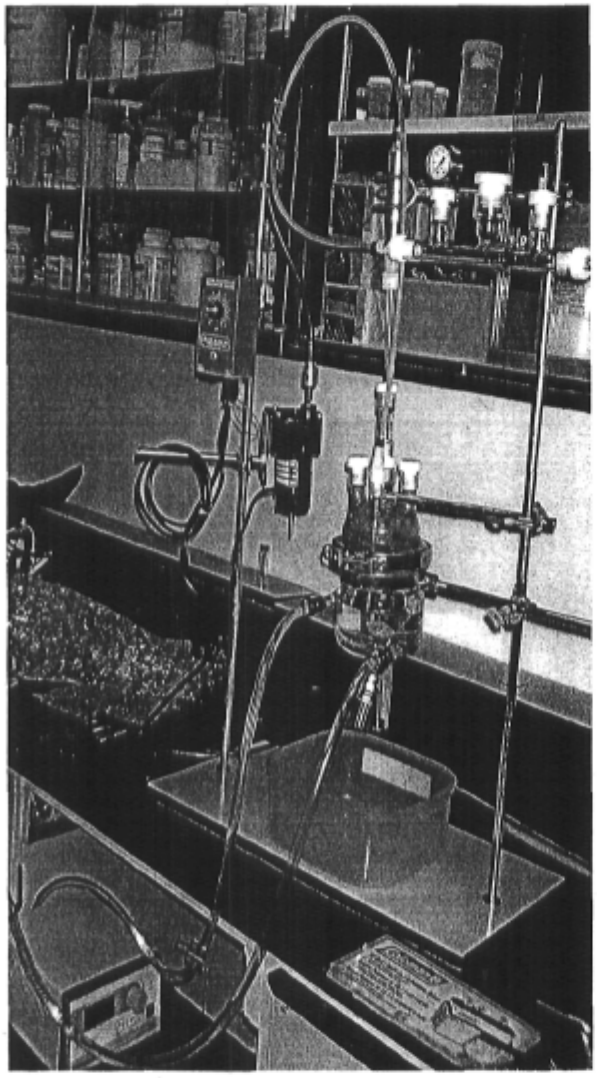

Fig. 11. Reactor, 1 L (AceGlass)

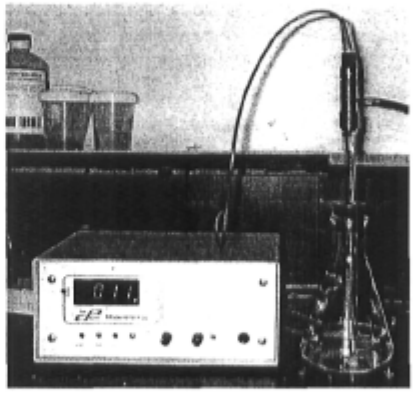

Fig. 12. Disolved oxigen probe and benchtop dissolved oxygen meter (Cole Parmer)

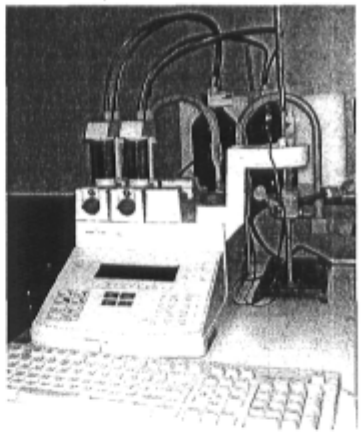

Fig. 13. Titrator (Mettler Toledo)

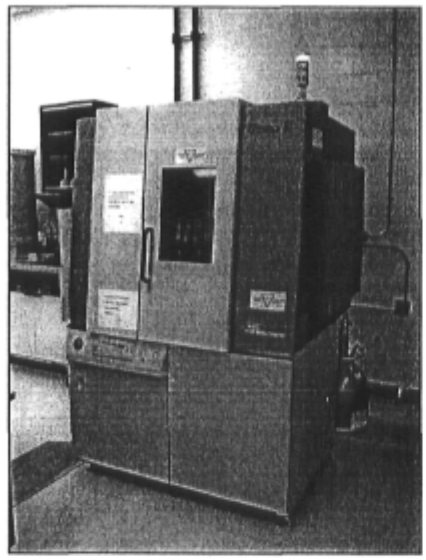

Fig. 14. Diffractometer (Ultima III Rigaku)

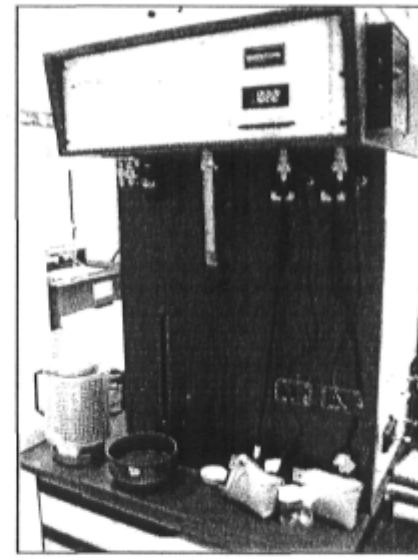

Fig. 15. Volumetric Physisorption/ Chemisorption station Analyzer (Quantachrome Instruments)

Fig. 16. HPLC (ICS-2500 Dionex)

4.2. Experimental procedures

4.2.1. Formulation of the Pd-Bi catalyst supported on nanostructured silica material

4.2.1.1. Synthesis of SBA-15

In accordance with the presented hypothesis, the SBA-15 material was chosen as nanostructured silica support. SBA-15 was synthesized in acidic medium *via* a synthetic route using poly(ethylene glycol)-poly(propylene glycol)-poly(ethylene glycol) triblock copolymer (Pluronic 123) as a templating agent, according to the two-step procedure [Zhao et. al; Choi et al. 2003]

Typically, 21.1 g triblock copolymer P123 (BASF) were dissolved in 658 g 2N HCl aqueous solution in a 1000 mL beaker while stirring at room temperature. The solution was heated to 40°C before adding drop wise 73 g tetraethylorthosilicate, TEOS (Aldrich). The mixture solution with the precipitated product was stirred for 23 h at 40°C, followed by aging step at 100°C for 24 h in a 1L Pyrex bottle. The precipitated product was filtered, washed with deionised water and dried at room temperature. Finally, calcination was carried out in a programmable furnace (Manfredi, Italy) at 540°C for 5 h with a heating rate of 3°C/min.

4.2.1.2. Impregnation of SBA-15 material with Pd

Pd/SBA-15 catalyst with a specified Pd loading was prepared in a 100 mL beaker by impregnation of 1 g SBA-15 silica material with aqueous solution of $Pd(NO_3)_2 \cdot xH_2O$ (Aldrich) which was used as Pd precursor [Plourde et al., 2004]. By dropwise addition, the surface of SBA-15 powder was uniformly covered by the solution of $Pd(NO_3)_2 \cdot xH_2O$ previously sonicated in a Transonic T310 ultrasonic bath. The sonication step was necessary for obtaining Pd particles [Chen et al. 2000].

The obtained slurry was kept stirred at room temperature for 24 h until dryness. The obtained solid powder was dried at 100°C for 24h. Finally, the calcination was performed in air at 540° C for 5h with a heating rate of 3°C/min. The reduction of the Pd/SBA-15 sample was performed in a glass cell especially designed, which was placed in the programmable furnace under hydrogen flow at 400°C for 3h [Plourde et al., 2004].

Bi-Pd/SBA15 catalysts with different Bi:Pd molar ratio and total metals charges were prepared by a second impregnation of Pd/SBA-15 with an aqueous solution of $Bi(NO_3)_2 \cdot 5H_2O$ (Aldrich) which was used as Bi precursor. Similar impregnation method was used. The solution of $Bi(NO_3)_2 \cdot 5H_2O$ was sonicated and added on the surface of catalyst powder Pd/SBA-15. The obtained slurry was kept under stirring for 24 h at room temperature and dried at 100°C for 24 h. Finally, the calcination was performed under air at 540°C for 5 h. The reduction of the Bi-Pd/SBA-15 sample was performed under hydrogen flow at 260°C for 2 h [Karski et al., 2002].

Using this procedure, 8 Pd-Bi catalysts (A, B, C, D, E, F, G, H) were prepared by varying the Pd and Bi loadings and tested for the oxidation of lactose. The results of these preliminary tests are summarized in Table 6.

4.2.2. Catalyst characterization

4.2.2.1. BET analysis

In the case of homogeneous catalytic reaction, the knowledge of the total surface area of the catalyst is required. This is obtained by the B.E.T. (Brunaeur-Emmet-Teller) method, in which the effect of total pressure of N_2 adsorbed on the solid at constant temperature is measured. This method assumed that the first layer of gas molecules is adsorbed more strongly than the subsequent layer, and that the heat of adsorption of subsequent layers is constant. They also assumed the absence of lateral interaction between adsorbed molecules [Brunauer et al., 1938].

The surface area was determined from the N_2 adsorption-desorption isotherms of the sample at 77 K using a volumetric adsorption analyzer (Model Autosorb-1, Quantachrome Instruments, Boyton Beach, FL).

First, the SBA-15 material was calcinated at 540 °C. The 1%Pd/SBA-15 sample was reduced to 400°C and the bimetallic catalyst was reduced to 260 °C. Prior to measurement, the catalysts samples (about 50.0 mg) were placed into the sample cell, heated to 200°C and degassed for 6 h until the pressure was less than 10^{-5} torr.

The samples were weighed and immersed in liquid N_2 to start the automatic procedure of the Modul Autosorb-1 controlled with an AS1Win 1.50 software.

For surface area of the samples, the multipoint method of BET equation was employed, which requires a linear plot of $1/[W(P_0/P)-1]$ vs P/P_0, using nitrogen as the adsorbate, in the P/P_0 range of 0.05 to 0.35.

BET equation:
$$\frac{1}{W\left(\left(P_0/P\right)-1\right)} = \frac{1}{W_m C} + \frac{C-1}{W_m C}\left(\frac{P}{P_0}\right)$$

in which W is the weight of gas adsorbed at a relative pressure, P/P_0, and W_m is the weight of adsorbate constituting a monolayer of surface coverage. The C constant of BET is related to the energy of adsorption in the first adsorbed layer and consequently its value is an indication of the magnitude of the adsorbent/adsorbate interactions.

The total pore volume was estimated from the volume of N_2 adsorbed at a relative pressure of 0.99. Pore size distributions were calculated by BJH method using the

desorption branch of the N_2 adsorption/desorption isotherms [Barrett et al. 1951]. By assuming cylindrical pore geometry, the mesopore size calculations are made using the Kelvin equation.

4.2.2.2. H_2 - Chemisorption analysis

The aim in chemisorption experiments is to determine the number of active sites present on a given sample. In practice, what is measured is the sample's chemisorption capacity at different adsorbate pressures. From this, the amount of adsorbate needed to form a monolayer of chemisorbed gas (V_m) is estimated.

H_2-chemisorption analysis was carried out in a gas chemisorption system (Model Autosorb-1C, Quantachrome Instruments, Boyton Beach, FL) at 313 K under atmospheric pressure. First, the reduced catalyst sample (216 mg) was pelletized. The sample was heated at 200°C under a flow of H_2 to assure the reduction state of the metal. Once sample preparation was completed, the sample was cooled down (generally under vacuum) to 40°C. The Chemosorb software conducted the entire analysis. Then, pre-selected doses of chemically adsorbing H_2 were sequentially added to the sample. Adsorbed volume (V) vs. equilibrium pressure (P) isotherms was generated. The first isotherm collected after sample preparation represents the combined contributions of chemisorption (on strong sites) and physical adsorption (if any) on the sample. V_m was estimated by extrapolation to $P = 0$ of combined isotherm.

The Pd surface area, crystallite size and the catalyst dispersion were calculated assuming that two hydrogen atoms are adsorbed per surface Pd metal atom using the Chemisorb program (Quantachrome Instruments).

4.2.2.3. XRD analysis

X-Ray Diffraction (XRD) identifies the crystal structure of the crystalline and polycrystalline material. The periodic nature of crystal lattices creates specific rules for the amount of x-rays leaving a sample being bombarded with monochromatic X-rays.

X-ray diffraction analyses were performed to investigate the crystallinity of the metal catalysts incorporated into the framework of the mesostructured silica SBA-15 and to estimate the average particle sizes.

XRD patterns were obtained using a Rigaku Ultima III (Japan) diffractometer with focusing beam monochromated Cu K_α radiation. The measurements were made at 40 kV and 44 mA.

The values of the crystal size were estimated from the broadening of a single well-resolved peak of catalysts using Scherrer formula [Klug and Alexander, 1974]:

$L = \frac{k\lambda}{\beta \cos\theta}$, where k=0.94, λ=0.1542 nm the Cu K_α radiation wavelength, β is the full width at half maximum of the peak in radians and θ is the Bragg angle.

The powder catalyst samples were uniformly dispersed in thin layers on a glass slide.

4.2.2.4. TEM analysis

Transmission Electron Microscopy (TEM) images the structure of thin solid films by forcing monoenergetic electrons through the thin film, while detecting the transmitted electrons intensity. TEM specimens must be 200 nm thick or thinner to allow sufficient electron transmission. Imaging the diffraction pattern of the transmitted electrons allows identification of crystal structure and lattice defects in the materials.

The investigation of uniform structure of the nanostructured support and the particle size distribution in the mesoporous framework is possible with the transmission electron

microscopy. As pointed out by Flynn et al. [1974], the measurement of a reliable particle size distribution from electron image is based on the three following implicit assumptions:

1. The size measured on the image is equal to the true size of the particle (multiplied by magnification);
2. All particle have the same probability of being observed on the image, whatever their size;
3. Contrast arising from the support cannot be confused with contrast arising from the particles.

TEM images were obtained with a JEOL JEM-1230 (Tokyo, Japan) microscope with 80 kV acceleration speed. The samples were prepared in ethanol solution then dried and disposed in uniformly thin layer on a glass support. TEM analyses were performed for SBA-15 and the formulation D of the catalyst. The images were acquired automatically by computer software.

4.2.2.5. XPS analysis

X-Ray photoelectron spectroscopy (XPS), also referred to as Electron Spectroscopy for Chemical Analysis (ESCA), identifies elements by analyzing energies of photoelectrons ejected by monochromatic X-rays bombardment. The energy of each photoelectron is directly related to the atom from which it was removed; therefore identifying elements on a sample surface is possible. A high-resolution spectrometer sums the number of ejected photoelectrons at specific levels of energy, and these accumulates are converted into elemental compositions. The valence state(s) or chemical bonding environment(s) are also identifiable from these accumulates.

The surface of catalyst with formulation D was studied by XPS analyse. The instrument was an Axis-Ultra system spectrometer from Kratos (U.K.) equipped with an electrostatic analyzer of large ray, a system of detection of 8 channels, a source of double X-rays Al-Mg without a monochromator and an Al source with a monochromator. The system also has an electron gun of very low energy for the effective neutralization of the important electrostatic load, which appears on the samples electrically insulating at the time

of their exposure to the monochromatic beam of X-rays. This spectrometer is installed in a system with vacuum whose basic pressure is of 5 X 10^{-10} mbar. The room of ESCA analysis is connected to a room of multi-purpose transport/ preparation connected itself to the introduction gate for a fast introduction of the samples in analysis position.

The necessary quantity of catalyst powder was introduced in a cup of copper. The pressure in the ESCA room was about 5 X 10^{-8} torr during the analyses.

All the spectra were recorded with the Al monochromatic source with a power of 300 Watts, with the gun of neutralization under operation. The flyover spectrum used to determine the elementary composition was recorded with pass energy in the analyzer of 160eV and a step of energy of 1eV, lenses in hybrid mode, which maximizes the sensitivity. The detailed spectra with high resolution were recorded with the pass energy of 40 or 20 eV, and a step of energy of 50 or 100 meV (lenses in hybrid mode); the spectra with high resolution are used for the chemical analysis [Moulder et al., 1992]. The electron beam of neutralization was oriented perpendicular to the bottom of the bowl, the photoelectrons were analyzed in the normal direction with the bowl and the beam of X-ray was incidental with 30 degrees compared to the bottom of the bowl. The computer analyzed the recording peaks. The adjustment of the envelope calculated with the experimental spectrum was carried out in an automatic way by CasaWPS software (Kratos, UK).

4.2.3. Catalytic oxidation of lactose to LBA

4.2.3.1. Preliminary tests

The first experiments of the oxidation of lactose were carried out in 20 mM aqueous solutions of (α) -D (+) lactose (Aldrich) (0.7206 g lactose in 100 mL water). As a batch reactor was employed an Erlenmeyer of 300 ml, which was placed on a hotplate (Fisher Scientific). A bath with water is used to monitor the temperature, which was verified with a digital thermometer. On top of the beaker a pencil-thin pH electrode (Accumet Single-jonction Model) coupled with a titrator (Mettler Toledo, Switzerland), an oxygen probe coupled on a benchtop dissolved oxygen meter (Cole Parmer, Illinois, USA) and a syringe pump tube for NaOH addition were placed into the slurry.

First, lactose solution was purged with nitrogen for 30 minutes to limit oxygen presence in the system until air is introduced for the reaction. The stirring rate was kept at 300 rpm. After the temperature was increased at desired temperature, the catalyst powder is added to lactose solution and air bubbling was started. The reactions were started with reduced catalysts. The stirring rate was 1000 rpm. The LBA formed during the reaction was neutralized by drop wise addition of 1M NaOH solution to maintain a constant pH in the reaction medium under microaerial conditions. The scheme of the apparatus is shown in Fig. 17.

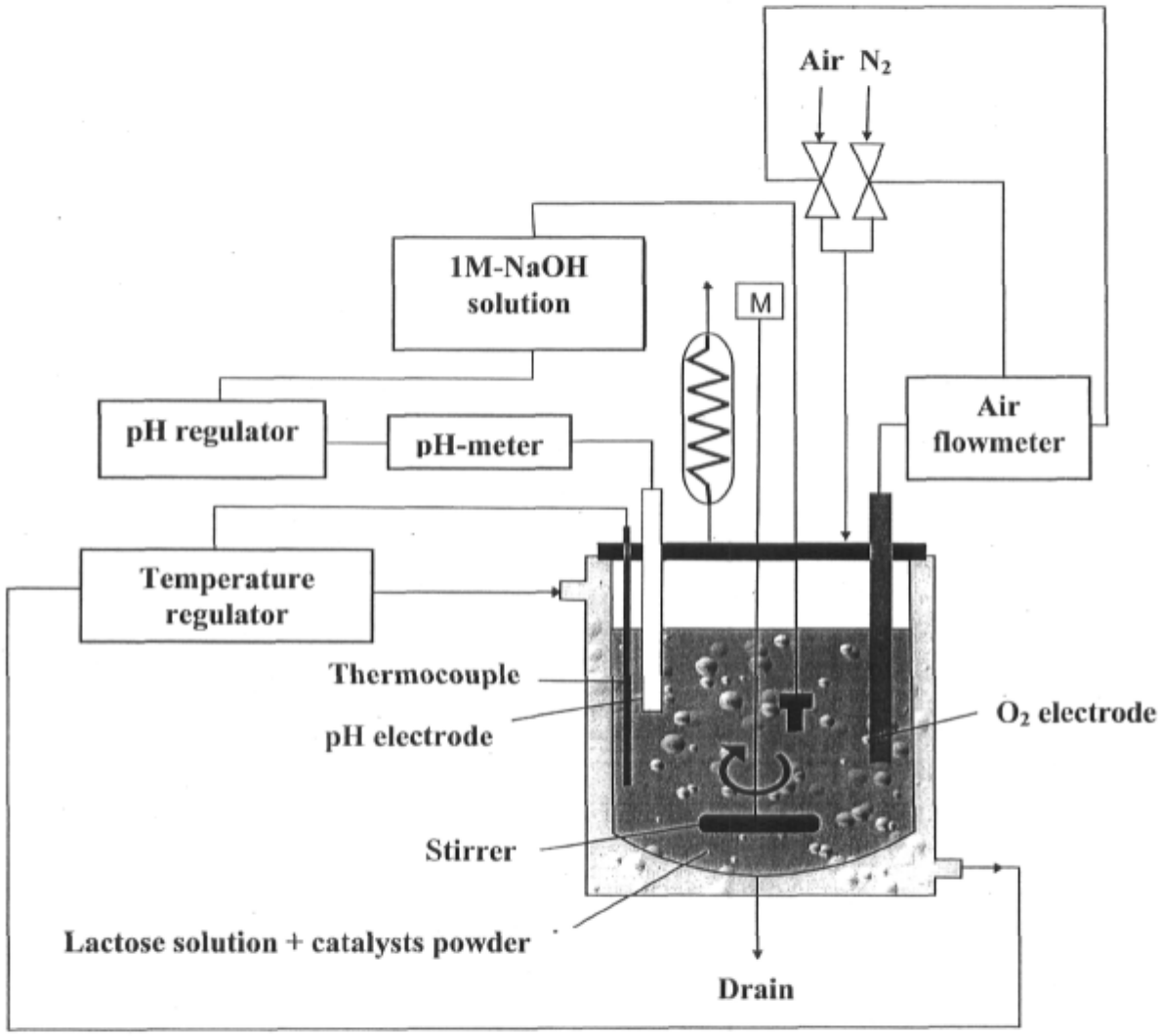

Fig. 17. Scheme for catalytic oxidation reaction of lactose

Three reaction procedures were developed and tested to assess microaerial conditions:

1. Bubbling of nitrogen through 100 mL lactose solution during 30 min to strip the dissolved oxygen, than 5 min exposure of the solution to atmospheric air; heating until the desired temperature was attained and starting the reaction by introducing the reduced catalyst powder and stirring at 1000 rpm.

2. The same conditions as procedure 1 where air was bubbled at 20 mL/min for 3 hours.

3. The same conditions as procedure 1, in addition, consecutive air and nitrogen were periodically introduced for best controlling the dissolved oxygen during the reaction. For the first hour 10 minutes of air bubbling was alternated with 5 min N_2 and for the last 2 hours 10 minute of air bubbling was alternated with 10 minutes of N_2. The airflow rate was 20 mL/min. The oxygen probe was plunged in the reaction mixture to verify the dissolved oxygen.

Aliquots of 0.1 mL of reaction media were periodically withdrawn for HPLC analysis.

4.2.3.2. Optimization of oxidation reaction conditions

The experiments were performed with procedure no. 3 for various conditions:

- Keeping constant the pH level at 9 and studying the effect of temperature at 38, 50, 65 and 80°C on the lactose conversion and catalyst selectivity;
- Keeping the temperature at 65°C and studying the effect of pH level in reaction medium at 7, 8 and 9;
- Keeping the temperature at 65°C and constant pH=9 for studying the effect of total metals charges of the catalyst on the catalyst performance;
- Keeping the temperature at 65°C and constant pH=9 and studying the promoter effect of Bi on the catalyst performance by verifying different Bi:Pd ratios;
- Keeping the temperature at 65°C and constant pH=9 for studying the effect of different catalyst/lactose ratios.

4.2.3.3. Scale-up studies for catalytic oxidation of lactose

The best catalyst found in the first tests which exhibited the highest activity and selectivity towards LBA was used for the scale-up studies. Two Erlenmeyer of 500 mL, 1000 mL and a glass reactor of 1000 mL were employed.

The two-piece pressure reactor 1 L (AceGlass, USA) equipped with a jacket was coupled to a water bath controlled by a digital temperature controller (PolyScience, Illinois, USA). On top of the reactor a pencil-thin pH electrode (Accumet Single-jonction Model) coupled with a titrator (Mettler Toledo, Switzerland), an oxygen probe coupled on a benchtop dissolved oxygen meter (Cole Parmer, Illinois, USA) and a syringe pump tube for NaOH addition were placed into the slurry. Also, air and N_2 entries were previewed. The stirrer shaft was equipped with a blade.

400 mL of 20 mM aqueous solution of (α) -D (+) lactose (Aldrich) was initially purged with nitrogen for 30 minutes to limit oxygen presence in the system until air is introduced for the reaction. The digital temperature controller was set at 67.5°C. At the desired temperature 0.6 g catalyst (0.15 g catalyst/100 mL lactose solution) was added in the reactor. Procedure no. 3 was started.

Aliquots of 0.1 mL of reaction mixture were periodically withdrawn for HPLC analysis.

4.2.3.4. HPLC analysis

The samples of reaction mixture were analysed using a chromatographic system DX- ICS 2500 (Dionex, USA) equipped with gradient pump GP50 and an electrochemical detector ED50 with a thin-layer type amperometric cell outfitted with gold electrodes and a Ag/AgCl reference electrode. The chromatographic separation of lactose and LBA was performed on a CarboPac PA1 analytical column (4mm×250 mm i.d. Dionex) and a CarboPac PA1 guard column (4mm×50mm i.d. Dionex) at a flow-rate of 1 mL/min.

A gradient controller was used to adjust the required solvent gradient in order to quickly detect, clean and reactivate the electrode surface. NaOH solution 50% (Fluka) and

anhydrous NaOAc (Fluka) were used to prepare the eluents in deionized water. All solvents were stored in closed, pressurized bottles with helium splashing.

Compositions of three solutions A, B and C were as follows: solution A= 0.1M NaOH, solution B=0.5M NaOAc, solution C=0.2M NaOH. The flow rate of mobile phase was 1 mL/min. The gradient used for the analysis was as follows: 100% eluent A was used for 10 min followed by a linear gradient to reach the eluent composition at 60% A and 40% B. This composition was maintained for 10 min, and then the eluent was returned to 100% A in 10 min following a linear gradient.

The detector pulse duration settings were T1=200 ms, T2=200 ms and T3=400 ms and the detector applied potentials were E1=0.05 V, E2=0.75 V, E3=-0.15V.

Prior to analysis, the samples of 0.1 mL of reaction mixture were diluted in 100 ml water. α-lactose monohydrate (Sigma Aldrich) and lactobionic acid (Sigma Aldrich) were used as standards to calibrate the HPLC analysis procedure.

The volume of aliquot sample injected was 25 μL. The Chromeleon software (Dionex inc., USA) was used to perform the calibration curve and integrated all chromatographic data.

4.2.3.5. ICP analysis

The detection of Pd and Bi in the samples of reaction mixture was performed with an Inductively Coupled Plasma Optical Emission Spectrometer (Perkin-Elmer Optima 3000, Massachusetts, USA).

First, the samples were acidified with concentrated HNO_3 above pH=2. The ICP system was flushed with the solution sample for 45 sec. About 2 mL of sample was pumped with 1.5 ml/min in the nebulizer which transforms the aqueous solution into an aerosol. The computer interface WinLab 32 (Perkin-Elmer, Massachusetts, USA) has identified and quantified the metals in the sample by taking into acount the wavelenght for Bi of 223.061 nm and for Pd of 340.458 nm.

4.3. References

1) Barrett E.P., Joyner L.G., Halenda P.P. **1951**. The determination of Pore Volume and Area Distributions in Porous Substances. I. Computations from Nitrogen Isotherms. J. Am. Chem. Soc. 73: 548.
2) Brunauer S., Emmett P.H. and Teller E.. **1938**.
3) Flynn P.C., Wanke S.E. and Turner P.S. **1974**. J. Catal. 33: 233.
4) Hamoudi and Belkacemi. **2004**. Cubic Mesoporous Silica with Tailored Large Pores. J. Porous. Mat. 11: 47.
5) Klug, H. P. and Alexander L. **1974**. X-ray Diffraction Procedure. John Wiley & Sons: New-York.
6) Moulder J.F. et al. **1992**. Handbook of X-ray photoelectron spectroscopy. Perkin-Elmer Corp.
7) Plourde M., Belkacemi K., Arul J. **2004**. Hydrogenation of Sunflower Oil with Novel Pd Catalysts Supported on Structured Silica. Ind. Eng. Chem. Res. 43: 2382.

CHAPTER 5

RESULTS AND DISCUSSION

5.1. Catalysts characterization

5.1.1. BET analysis

The N_2 adsorption-desorption isotherms at 77K were performed for SBA-15, Pd/SBA-15 and Pd-Bi/SBA-15 materials.

The surface area for the samples was calculated with the multipoint BET method. The average diameter of mesopores was obtained from the maximum of a pore size distribution calculated using the BJH method.

All the data regarding textural and surface characteristics of the support and the prepared catalysts are presented in Table 3.

Table 3. Textural and surface characteristics of the catalysts

Formulation of catalyst	Description	BET surface area (m^2/g)	Pore Diameter (nm)	Total Pore Volume (cm^3/g)
Support	SBA15	901.9	6.8	1.31
A	1%Pd/SBA15	836.9	6.2	1.20
D	1.02%Pd/0.64%Bi/SBA15	807.4	6.2	1.22
B	5%Pd/5%Bi/SBA15	606.1	5.2	0.87

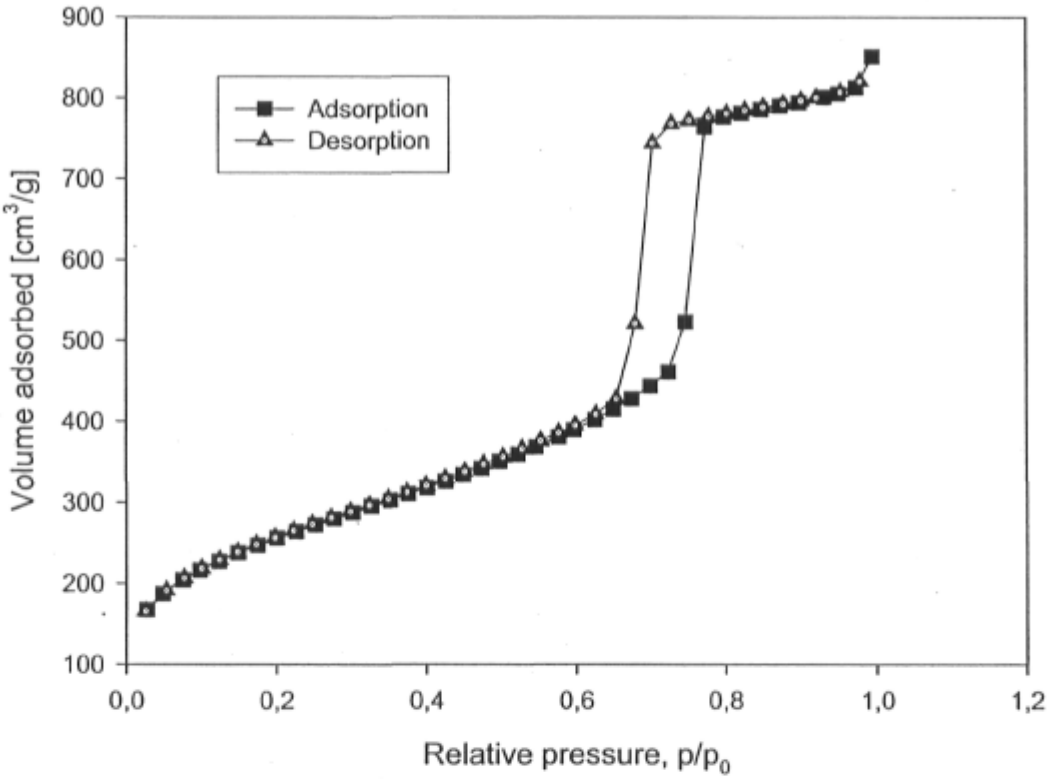

Fig. 18 . N_2 Adsoption-desorption isotherms for SBA-15 material calcinated at 540 °C.

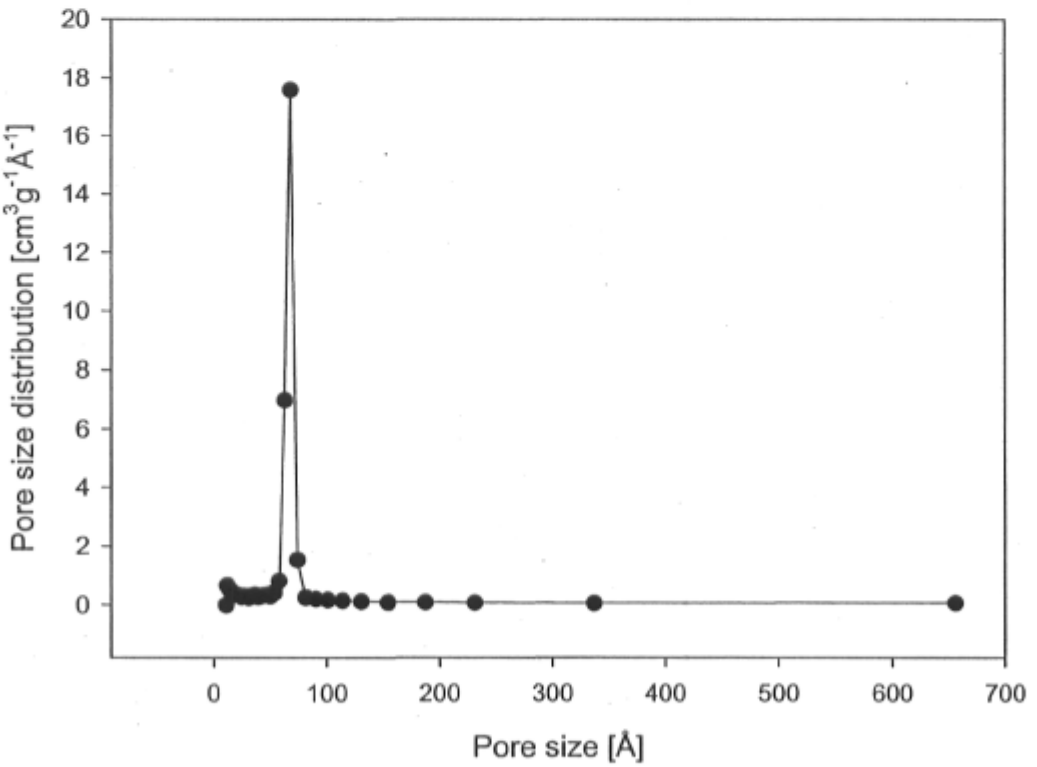

Fig. 19. BJH pore size distribuion for SBA-15 material calcinated at 540 °C.

In Fig. 18, the calcined SBA-15 material presents a characteristic type IV isotherm for mesoporous materials with a pronounced hysteresis loop with two parallels as defined by IUPAC [Sing et al., 1985]. The presence of the hysteresis loop indicates high pore size uniformity and facile pore connectivity [Krug and Jaroniec, 2003]. The amount adsorbed is always greater at any given relative pressure along the desorption branch than along the adsorption branch. The capillary condensation of the SBA-15 sample that takes place in mesopores with the increase in the adsorbed amount begins at relative pressure (P/P_0) at 0.65 and finishes rapidly arround 0.8. For ordered mesoporous solids, those higher-pressure parts of the plots can be used to calculate the primary mesopore volume and the external surface area (the surface area of the other pores present in these materials) [Kruk and Jaroniec, 2003].

It was found that BET surface area and total pore volume of SBA-15 are 901.9 m^2/g and 1.31 cm^3/g, respectively, which are similar to those of conventional SBA-15. The pore size distribution was estimated by BJH method (Fig. 19).

It has been recognized that SBA-15 materials contain both meso and microporosity [Lukens Jr. et al, 1999; Van der Voort et al., 2002; Kruk et al., 2003]. The presence of microporosity within the pore walls endows the 2D hexagonal channels with a 3D pore connectivity [Ryoo et al., 2001], promoting molecular transport in catalysis and adsorption.

In conclusion, the SBA-15 prepared is a mesoporous material with large pores (>6 nm), high specific surface and pore volume.

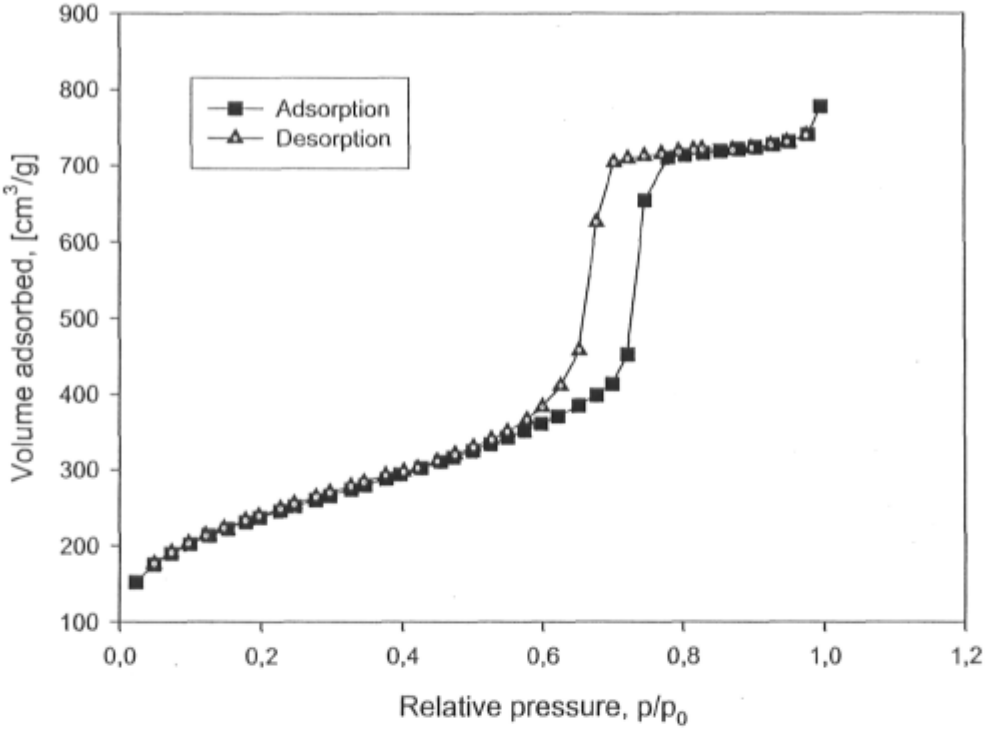

Fig.20. N_2 Adsoption-desorption isotherms for 1% Pd/SBA-15 sample.

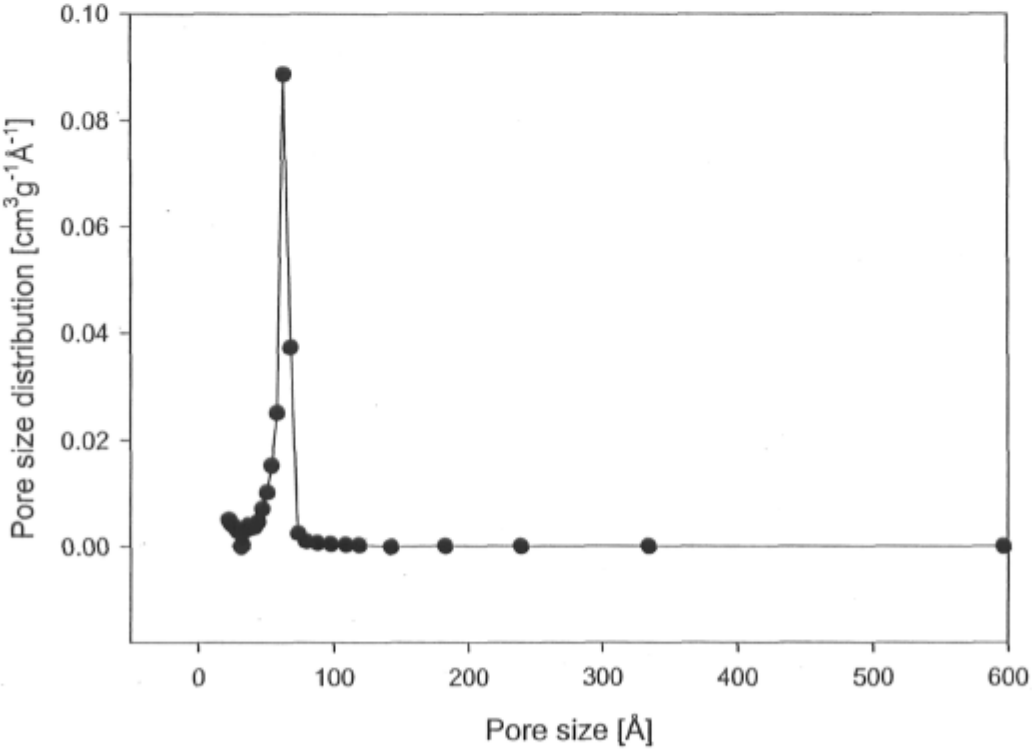

Fig. 21. BJH pore size distribution for 1%/SBA-15 sample.

In Fig. 20, the calcined 1%Pd/SBA-15 material also presents a typical isotherm of the type IV characteristic for mesoporous materials with a pronounced hysteresis loop. The capillary condensation of the 1%Pd /SBA-15 sample, begins at relative pressure (P/P_0) at near 0.60, which indicates smaller pore size of the sample. It was found that BET surface area and total pore volume of 1%Pd/SBA-15 are 836.9 m^2/g and 1.20 cm^3/g, respectively. The pore size distribution was estimated by BJH method (Fig. 21).

The impregnation of SBA-15 material with 1% (wt.) Pd led to mesoporous material with a high specific surface and pore volume. However, these textural properties were lower than those obtained for unmodified SBA-15 materials. The average pore size of the materials was found to remain practically unchanged. This result suggests that the formation of Pd particles within the mesoporous silicas did not lead to the destruction or blocking of the mesoporous framework channels. Thus, the mesoporous framework of SBA-15 was preserved.

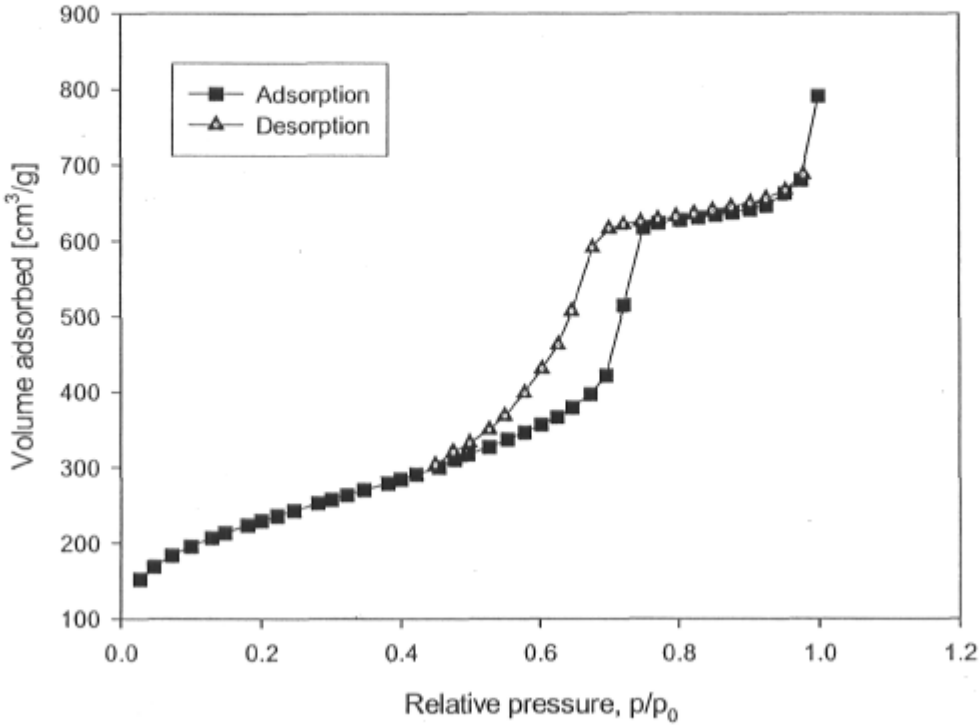

Fig. 22. N_2 Adsoption-desorption isotherms for 1.02% Pd 0.64%Bi/SBA-15 catalyst.

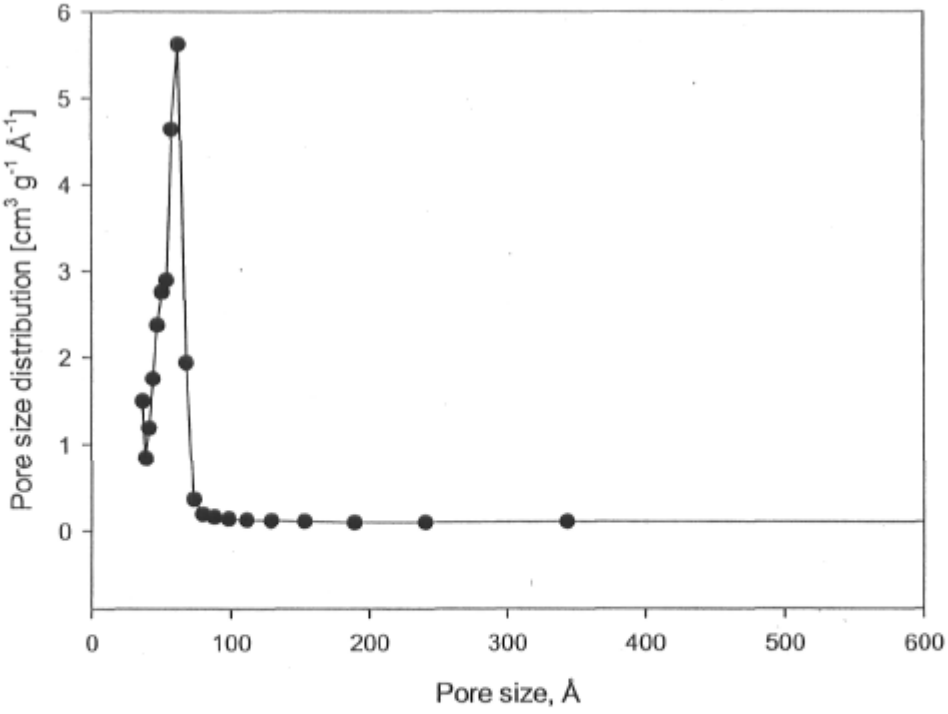

Fig. 23. BJH pore size distribution for 1.02% Pd 0.64%Bi/SBA-15 catalyst.

In Fig. 22, the calcined 1.02% Pd 0.64%Bi/SBA-15 catalyst also presents a type IV isotherm characteristic for mesoporous materials with a pronounced hysteresis loop. The second impregnation with Bi of SBA-15 material with 1% (wt.) Pd led to a mesoporous material with still high specific surface and pore volume. The average pore size of the materials (Fig. 23) and specific surface were found to remain practically unchanged. Accordingly, these results suggest that the impregnation with Bi do not lead to the destruction or blocking of the mesoporous framework channels.

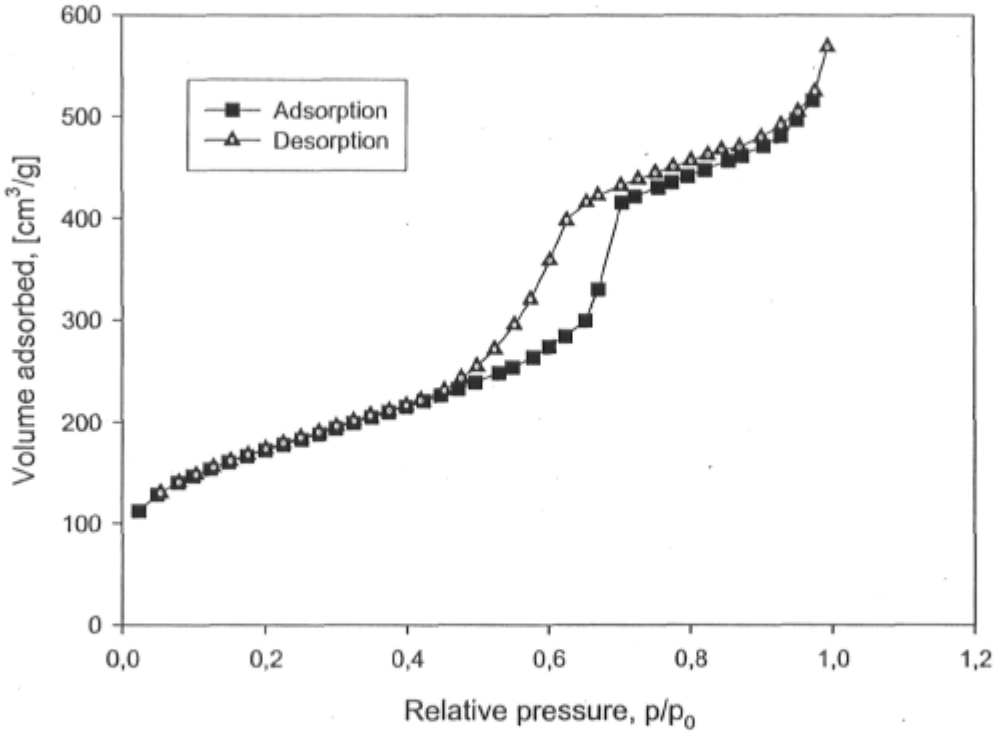

Fig . 24. N_2 Adsoption-desorption isotherms for 5% Pd 5%Bi/SBA-15 catalyst.

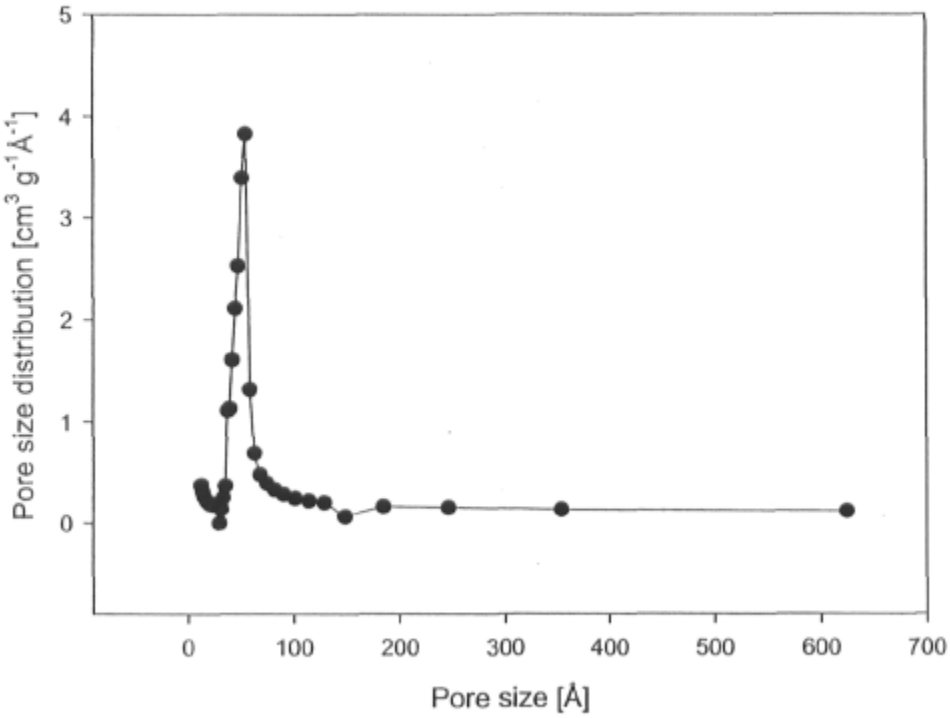

Fig. 25. BJH pore size distribution for 5%Pd 5% Bi%/SBA-15 catalyst.

In the case of a 5%Pd 5%Bi/SBA-15 material with a much greater loading in metals (10%) of SBA-15, the N_2- adsorption-desorption isotherms are also typical for mesoporous materials with a hysteresis loop (Fig. 24). However, the capillary condensation of the sample, beginning at relative pressure (P/P_0) near 0.5, indicates smaller pore sizes for the sample.

It was found that BET surface area and total pore volume of 5%Pd 5%Bi/SBA-15 was 606.1 m^2/g and 0.87 cm^3/g, respectively. The pore size distribution was estimated by BJH method (Fig. 25).

5.1.2. H_2 - Chemisorption analysis

In Fig. 23, the plot of volume of H_2 uptake (V) by the sample versus equilibrium hydrogen pressure (P/P_0) isotherms was presented and V_m was estimated by extrapolation to P = 0 of combined isotherm (C).

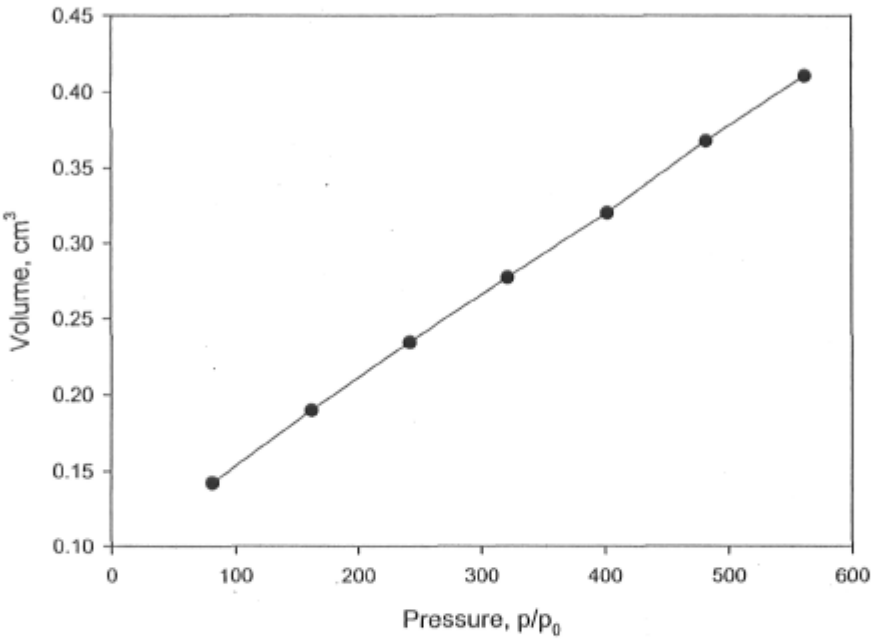

Fig. 26. The combined isotherm (C) of the H_2-chemisorption for 1%Pd/SBA-15.

Table 4. Data obtained by H_2-chemisorption analysis.

Sample weight, g	H_2 uptake, cm^3	H_2 uptake/g sample, cm^3/g	Monolayer H_2 uptake µmol /g sample	Percent metal dispersion, %	Active metal surface area, m^2/g sample	Average crystallite size, nm
0.216	0.0986	0.4575	20.3636	43.36	1.932	2.6

The data presented in Table 4 were calculated assuming:

- the adsorbtion stoechiometry Pd/H= 2;
- Pd density of 12.02 $g \cdot cm^{-3}$;
- metal surface area of 7.874 A^2/atom;
- Pd shape = 6 (sphere).

Metal dispersion, namely the ratio between surface and total metal atoms, is a critical factor for several catalytic reactions and generally it has to be as high as possible. The 1%Pd/SBA-15, which was directly reduced after Pd deposition on the calcined SBA-15 demonstrated 43.36% metal dispersion and it was found that the Pd nanoparticles has attained 2.6 nm in the mesoporous silica frameworks (Table 5). It is obvious that the average Pd particle diameter did not exceed the mesopore diameter of SBA-15, suggesting that the Pd clusters were formed within the confined mesopore space, and their maximum size was controlled by the pore diameter [Yuranov et al, 2003]. Pd clusters were found to be resistant against sintering during calcination (540 °C, 5 h).

Also, a high active metal surface area of 193.2 m^2/g Pd proved a high activity of the 1%Pd/SBA-15 sample.

5.1.3. XRD patterns

As shown in Fig. 27, the XRD results for the calcined SBA-15, prepared using $EO_{20}PO_{70}EO_{20}$ (Pluronic 123) as a templating agent, confirmed that the ordered hexagonal structure was formed. Figure 27 demonstrates three well-resolved diffraction peaks, which can be ascribed to the (1 0 0), (1 1 0) and (2 0 0) reflections associated with hexagonal symmetry [Zhao et al., 1998].

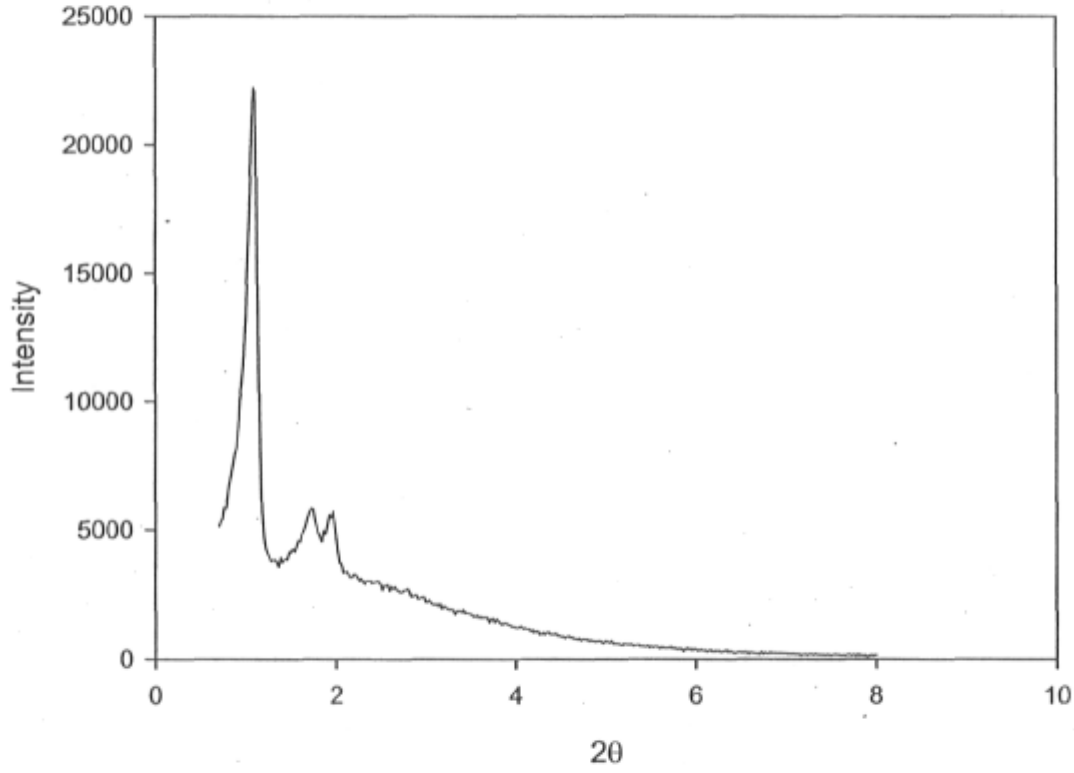

Fig. 27. Small angle XRD patterns of SBA-15 silica material

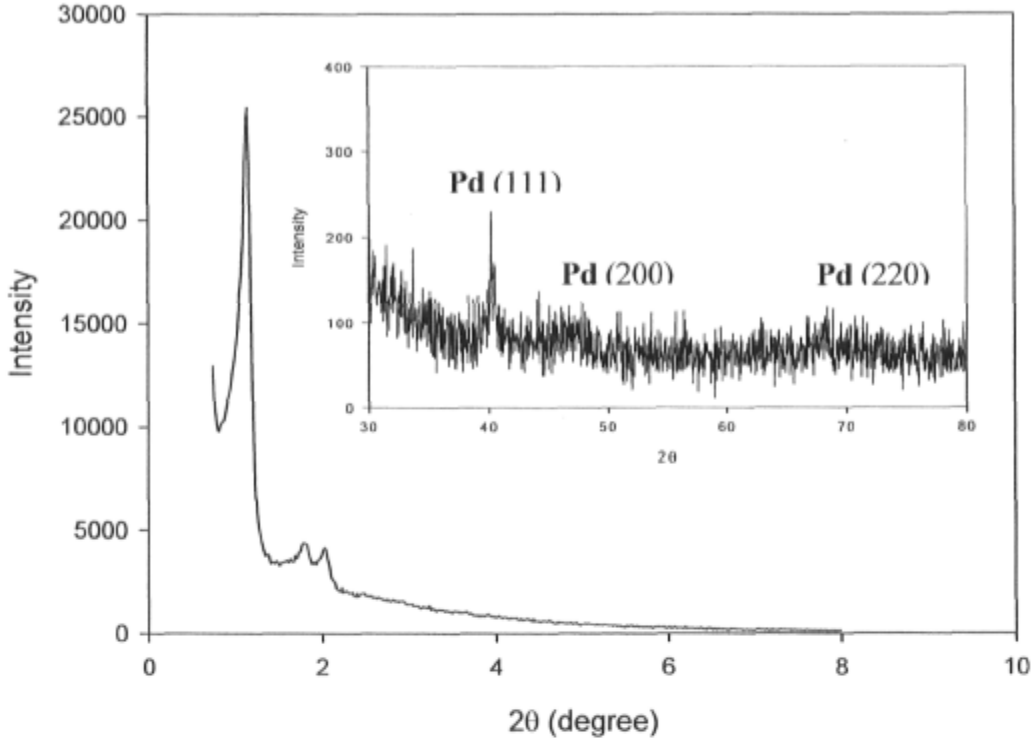

Fig. 28. Small and wide angle XRD patterns of 1% Pd SBA-15

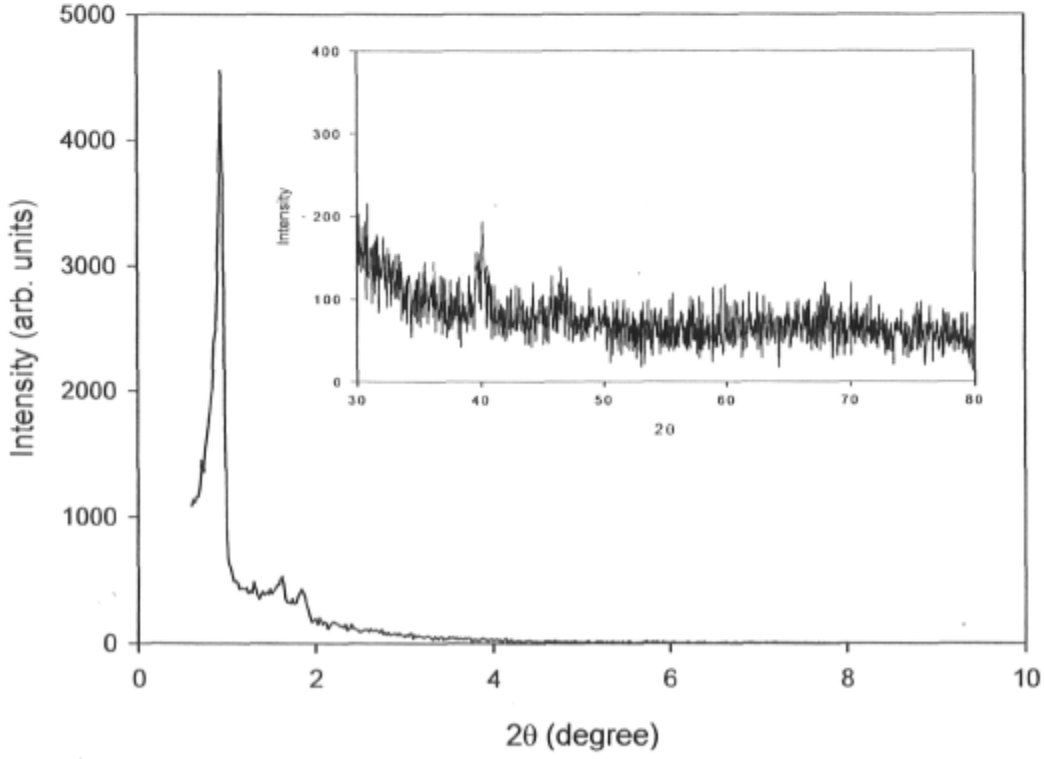

Fig. 29. Small and wide angle XRD patterns of 1.02% Pd 0.64%Bi/SBA-15 (formulation D)

Prior to XRD analyses the powder samples of 1%Pd/SBA-15 were reduced in H_2 at 400°C. The small angle XRD patterns for the 1%Pd/SBA-15 (Fig. 28) showed three peaks intensity and resolutions were diminished gradually as the metals loading increased. However, the ordered hexagonal structure of SBA-15 support is preserved.

The possibility of the formation of Pd metal during loading process was confirmed by wide angle XRD patterns for the 1%Pd/SBA-15. The characteristic reflections from the (1 1 1), (2 0 0) and (2 2 0) Pd crystal planes are presented.

The small angle XRD pattern for the 1.02%Pd 0.64%Bi/SBA-15, which was reduced in H_2 at 260°C, also presents the three well-resolved diffraction peaks (Fig. 29) associated with hexagonal symmetry. The wide-angle XRD patterns have shown a smaller intensity for the first characteristic peak and a bigger intensity for the second. This pattern may be ascribed to Pd–Bi alloy formation.

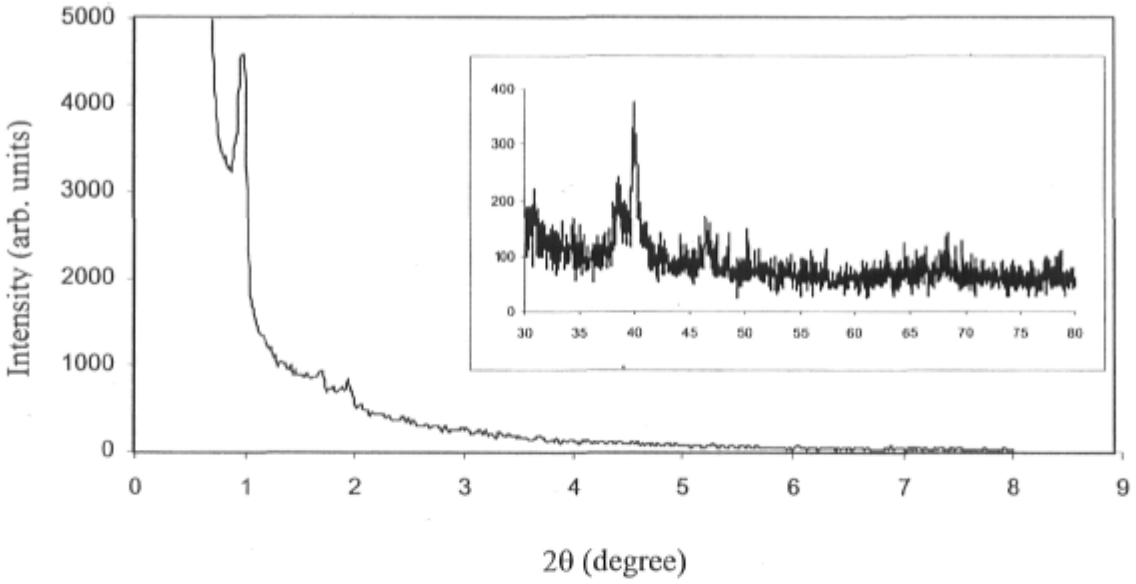

Fig. 30. Small and wide angle XRD patterns of 5% Pd 5%Bi/SBA-15 (formulation B)

The small angle pattern of 5%Pd 5%Bi/SBA-15 catalyst also present a hexagonal ordered structure (Fig 30). The wide angle XRD pattern showed an important alteration of the first peak characteristic to Pd crystal plan, corresponding to the apparition of intermetallic Bi-Pd compounds.

The crystallites' size was found to be around 10 nm for PdBi alloy and around 11 nm for Pd.

For the 5%Pd/SBA-15 catalyst, the crystallites' size of Pd was calculated at about 25 nm employing the Scherrer equation (Annexe A, Fig. 54).

Similary, for the 5%Pd 5%Bi/SiO_2, after reducing in hydrogen at 533K, Karski, [2006] identified the crystalline phase of BiPd and Bi_2Pd compounds by references to the ASTM data files. In this case, the probability of formation of BiPd and Bi_2Pd compounds in 5%Pd 5%Bi/SBA-15 is very high.

5.1.4. TEM images

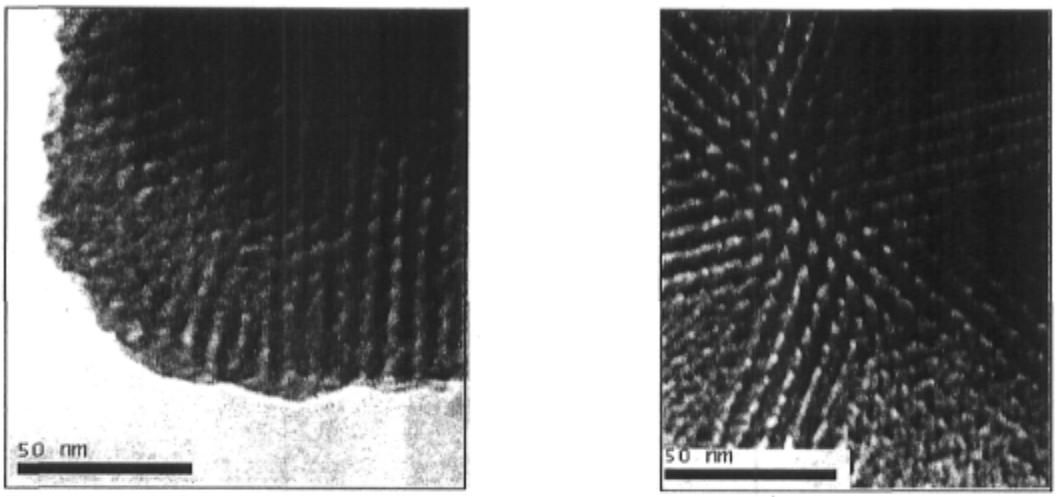

Fig. 31. TEM images of the SBA-15 material

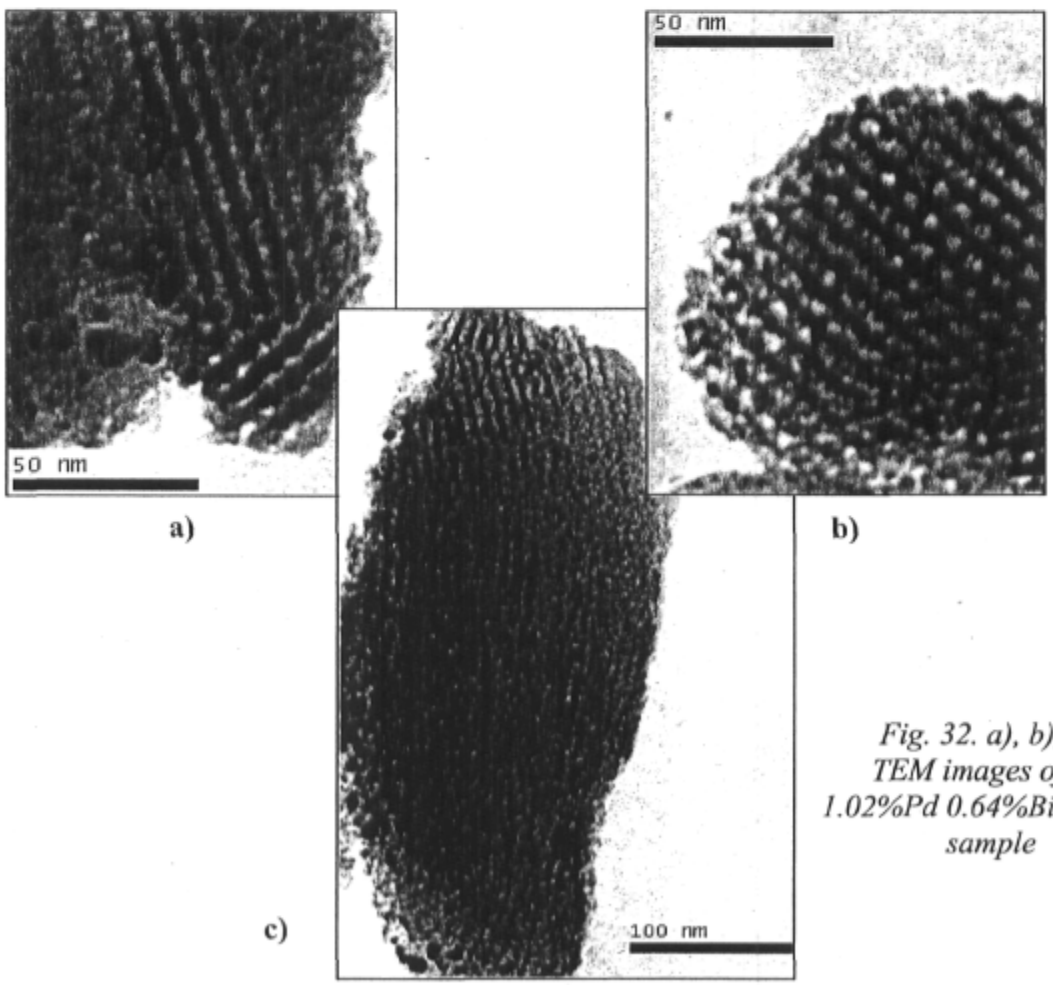

Fig. 32. a), b), c). TEM images of the 1.02%Pd 0.64%Bi/SBA-15 sample

The prismatic array of pores with hexagonal symmetry of the SBA-15 sample is detected by TEM (Fig. 31). The X-ray diffraction and nitrogen adsorption results were consistent with the hexagonal ordered structure observed in the TEM images.

The TEM images of the 1.02%Pd 0.64%Bi/SBA-15 (Fig. 32) provide further information on the Pd and Bi nanoparticles within the mesoporous silica framework channels. Fig. 32.a) shows the straight mesoporous channels parallel to the long axis, and metal nanoparticles are observed both in the mesoporous channels and on the external surface of the silica support. The black dots smaller than 6 nm and larger than 8 nm correspond to the metal particles located in the channels and on the surface, respectively (Fig. 32 b). It should be noted that metal particles even on the external surface are relatively well dispersed and the growth of particle is not significant (Fig. 32 c).

The particle size was about 2–8 nm and this coincides with that obtained by H_2-chemisorption and XRD analysis. The metal crystallites composed of both Pd and Bi seem to be uniformly distributed.

5.1.5. XPS analysis

The two metal elements, Pd and Bi, were detected (Fig. 33) and the apparent concentrations of the elements were given in atomic % in the Table 5.

Pd was found in the form of Pd^0. The chemical state of Bi was evaluated with the peak Bi 4d 5/2 (Fig. 34).

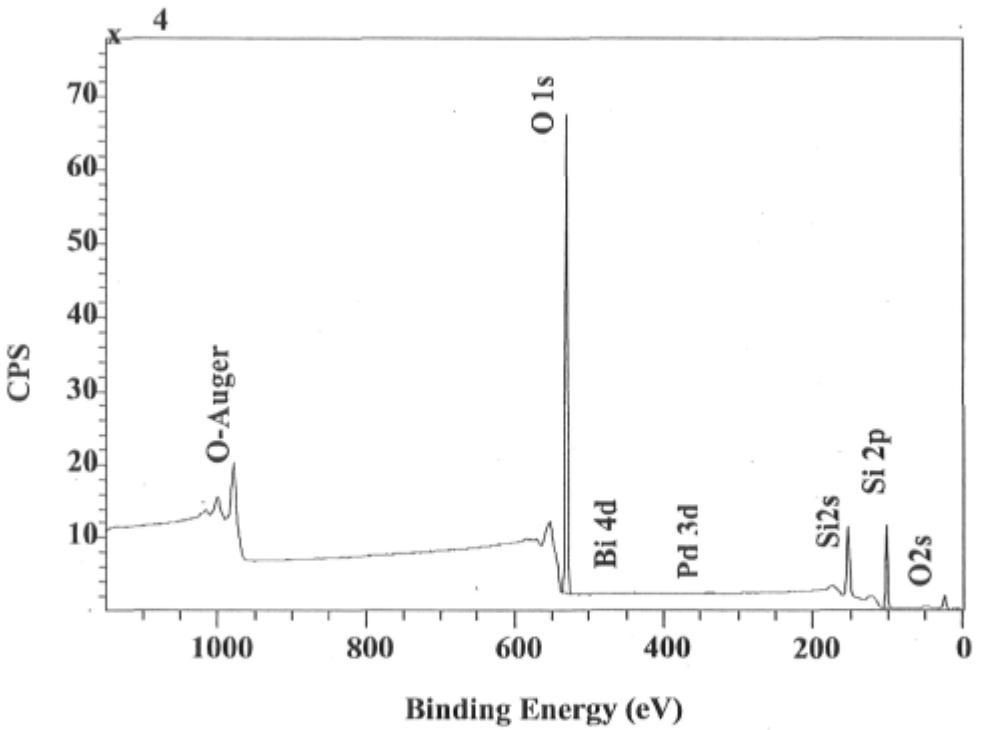

Fig. 33. XPS spectra for 1.02%Pd 0,64%Bi/SBA-15 sample

Table 5. The surface concentration of the elements by XPS analysis

Peaks name	Position (eV)	FWH	Area	At%
O 1s	530.89	2.943	115995.6	69.395
Bi 4d	439.89	5.874	1146.4	0.121
Pd 3d	332.89	3.387	795.6	0.069
Si 2p	101.89	3.036	21378.6	30.415

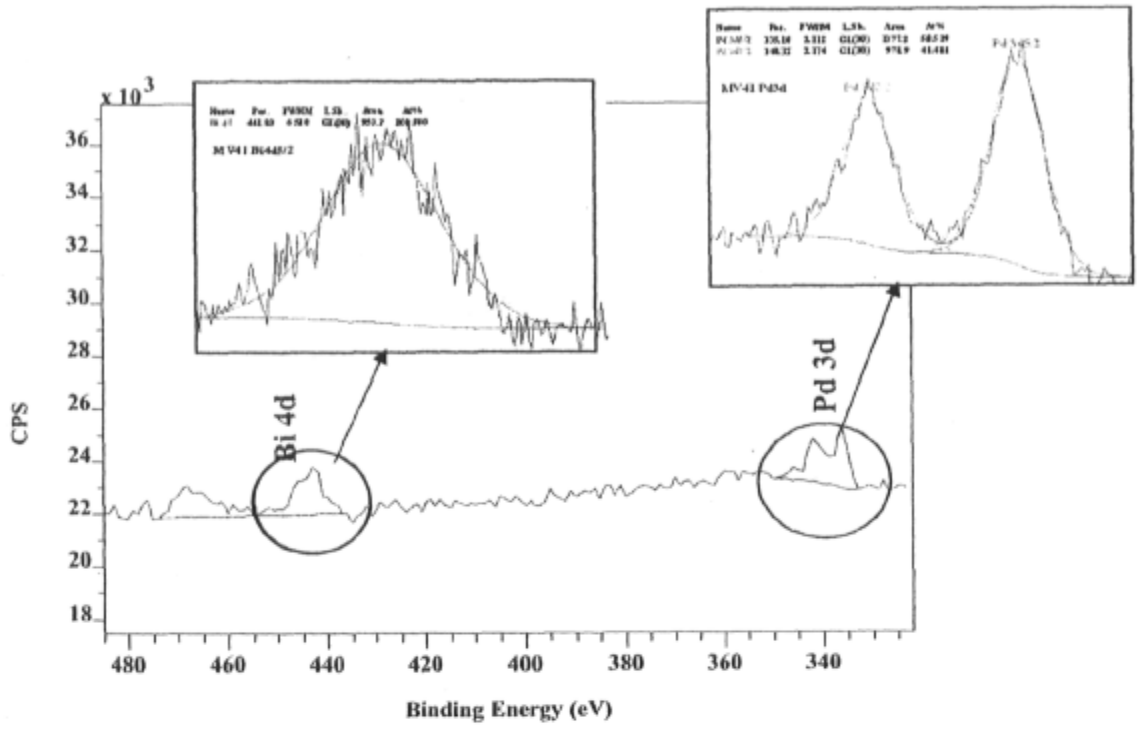

Fig. 34. Enlarging spectra for Bi4d and Pd3d

Usually, the chemical state of Bi is evaluated with the peaks 4f, but in this case it seems to be impossible. The other peaks, not very intense, are drowned in the tail of the loss of energy of Si2s, as shown in Fig. 35, where the positions awaited for Bi4f are between 156.8 and 162.3 eV. Therefore, the peak Bi4d5/2 was studied in accordance with the NIST XPS Database, [2000].

A recording of the peak Si2p (Fig. 35) was carried out, in order to correct and update energy for all the other spectra. The value imposed for Si2p silica was 103.6 eV and the corrected binding energies are presented in Table 6.

Table 6. Corrected binding energies in XPS analysis

Peaks name	Corrected binding energy, eV
O 1s	532.8
Bi 4d	441.8
Pd 3d 5/2	335.1
Pd 3d 3/2	340.32
Si 2p	103.6

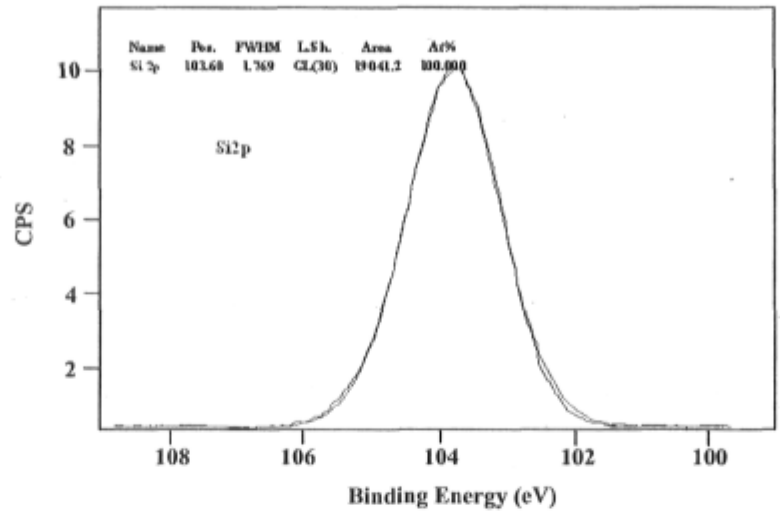

Fig. 35. XPS spectra for Si2p.

The binding energy corrected at 532,8 eV for the peak O 1s corresponds to what is expected for silica, according to Moulder et al., [1992].

The binding energy for Pd3d 2/5 corresponds to Pd^0 (metallic Pd).

The data available for Bi4d 5/2 deviates notably from the values ascribable to metallic Bi (440.0-440.4eV). The binding energy of 441.8 eV, mainly the same when one considers the Bi-Se compounds, seems to confirm that Bi is in a chemical state, which is not the pure metal state. These explanations can be reflected by the presence of intermetallic alloy Pd-Bi, whose stoichiometry of surface would be roughly $Bi_{1.75}Pd$.

5.2. Catalytic oxidation of lactose

The catalytic results are expressed as conversion of lactose (X, %) and the selectivity of lactose into lactobionic acid (S, %).

Those parameters were defined as:

$$X(\%) = \left[1 - \frac{[LAC]}{[LAC]_0}\right] \times 100$$

$$S(\%) = \left[\frac{[LBA]}{[LAC]_0 - [LAC]}\right] \times 100$$

Where $[LAC]_0$ = the initial concentration of lactose

[LAC]= the concentrations of lactose at time t

[LBA] = the concentrations of sodium lactobionate

These concentrations are obtained by HPLC analyses of the samples prelevated during the oxidation reaction.

Examples of HPLC chromatograms are shown in the fig. 36.

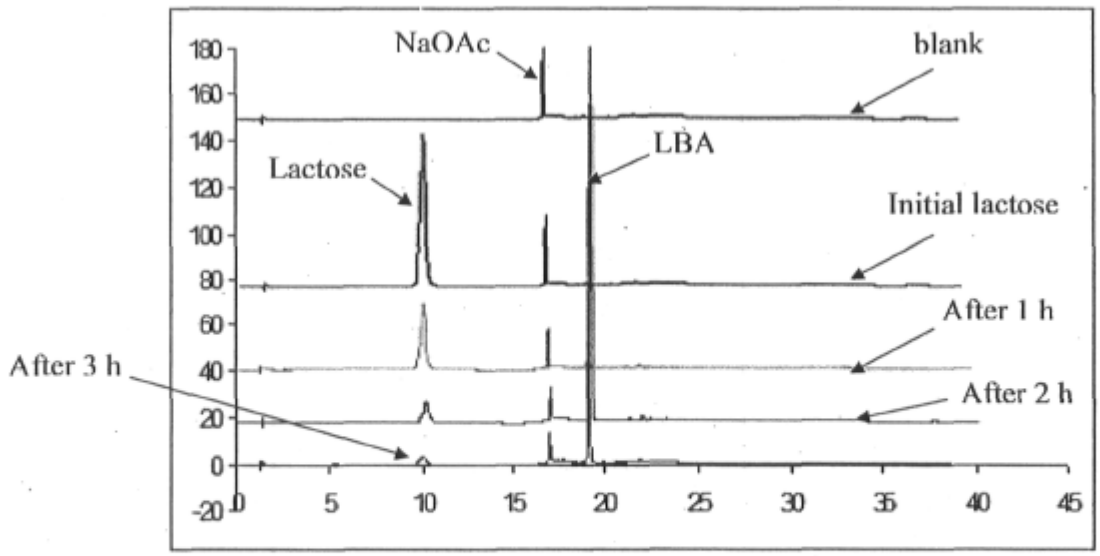

Fig. 36. Chromatograms obtained by HPLC analysis for the reaction mixture during 3 hours.

5.2.1. Preliminary tests of lactose oxidation

The experiments were performed at 65°C and pH=9 under microaerial conditions (20 mL/min airflow). All three procedures explained in the previous chapter were employed. The preliminary data of lactose conversion under different reaction conditions were presented in Table 7. The maximum reaction time was 3 hours.

The maximum of lactose conversion was observed in experiment no. 9 in the case of 1.02%Pd 0.64%Bi/SBA-15 catalyst (Bi:Pd=0.3 molar ratio) with 0.21 g catalyst/g lactose ratio using procedure 3. A very good lactose conversion was also reached by the 0.81%Pd 0.44%Bi/SBA-15 (Bi:Pd=0.3 molar ratio) but in the conditions of a greater catalyst/lactose ratio (0.28). Contrarily, the 0.5%Pd 0.5%Bi/SBA-15 catalyst did not perform because it provided the lowest lactose conversion. As is shown in the literature [Karski et. al., 2005, 2006; Hendriks et al. 1990] only the bimetallic catalysts with (1-5)%Bi and 5%Pd supported by SiO_2 or C were employed. In this study, testing the 5%Pd 5%Bi/SBA-15 did not demonstrate a good lactose conversion. This situation is probably due to the large Pd nanoparticle obtained which is not confined in the mesoporous channels of SBA-15 and conducted at a lower Pd dispersion then the catalyst with 1%Pd loading and the difference in the textural and chemical properties of the two supports.

Table 7. Performance of different formulated Bi-Pd/SBA-15 catalysts for partial oxidation of 20 mM lactose solutions (0.7206 g lactose in 100 mL water) to lactobionic acid under varied aeration conditions and catalyst/ lactose ratios.

No. exp./ Type of the catalyst	Pd loading, % wt.	Bi loading, % wt.	Total metal loading, % wt.	Bi:Pd, molar ratio	g catalyst/ g lactose ratio	Reaction procedure	1 hour		2 hours		3 hours	
							Lactose conversion, % wt	LBA, g/l	Lactose conversion, % wt	LBA, g/l	Lactose conversion, % wt	LBA, g/l
1/A	1.00	0.00	1.00	-	0.14	1	26.77	1.29	33.33	1.99	36.14	2.52
2/B	5.00	5.00	10.00	0.50	0.14	1	11.49	0.75	34.48	2.54	46.84	3.09
3/C	1.07	1.08	2.15	0.50	0.14	1	32.58	2.16	48.42	3.42	60.48	3.67
4/D	1.02	0.64	1.66	0.30	0.14	1	33.54	1.91	51.58	3.67	67.88	4.41
5/D	1.02	0.64	1.66	0.30	0.14	2	48.11	3.84	72.67	5.75	77.62	5.88
6/D	1.02	0.64	1.66	0.30	0.14	3	45.33	4.04	69.68	5.02	82.54	5.23
7/D	1.02	0.64	1.66	0.30	0.21	2	72.82	4.82	82.12	5.92	83.58	5.89
8/D	1.02	0.64	1.66	0.30	0.28	2	62.95	4.12	85.24	5.17	89.64	5.9
9/D	1.02	0.64	1.66	0.30	0.21	3	57.57	4.05	93.00	6.56	96.14	6.8
10/E	1.01	0.22	1.23	0.10	0.14	3	47.94	3.09	55.46	3.99	66.24	5.22
11/F	0.81	0.44	1.25	0.30	0.14	1	28.59	1.43	45.89	3.63	62.20	4.49
12/F	0.81	0.44	1.25	0.30	0.28	2	50.93	3.91	87.06	6.13	95.01	6.68
13/G	0.83	0.82	1.65	0.50	0.14	1	15.32	1.09	38.71	2.82	53.35	3.78
14/H	0.50	0.50	1.00	0.50	0.14	1	10.21	0.71	17.38	1.01	18.45	1.28

5.2.2. The dissolved oxygen

The first tests of the oxidation of lactose were carried out in order to find the best aeriation conditions for the three-phase reaction medium. The oxygen flow was found optimum for 20 mL/min and provided a good aeration rate at 65°C with a stirring rate of 100 rpm. The consumption of oxygen is most rapid at the starting of the reaction and the oxygen level is almost constant between 1-2%, for about 30 min. Subsequently, the dissolved oxygen increased drastically and the saturated concentration values were attained (18-24%). At this point, the rate of consumption of lactose was decreased dramatically and the reaction stopped. The third procedure developed, which employed the N_2 for stripping the oxygen, is the best way of keeping the oxygen level constant. Therefore, the excellent conversions of lactose (see Table 7) were obtained when the oxygen concentration was kept at about 1% of the equilibrium concentration of the dissolved oxygen during reaction, as has already been mentioned in the literature [Hendriks et al., 1990]. In this way, catalyst deactivation by overoxydation is avoided and the oxidation reaction of lactose is performed continuously.

5.2.3. The influence of catalyst/lactose ratio

The experiments for the optimization of catalyst/lactose ratio were performed with procedure 2 at 65°C, airflow of 20 mL/min, 1000 rpm and pH=9.

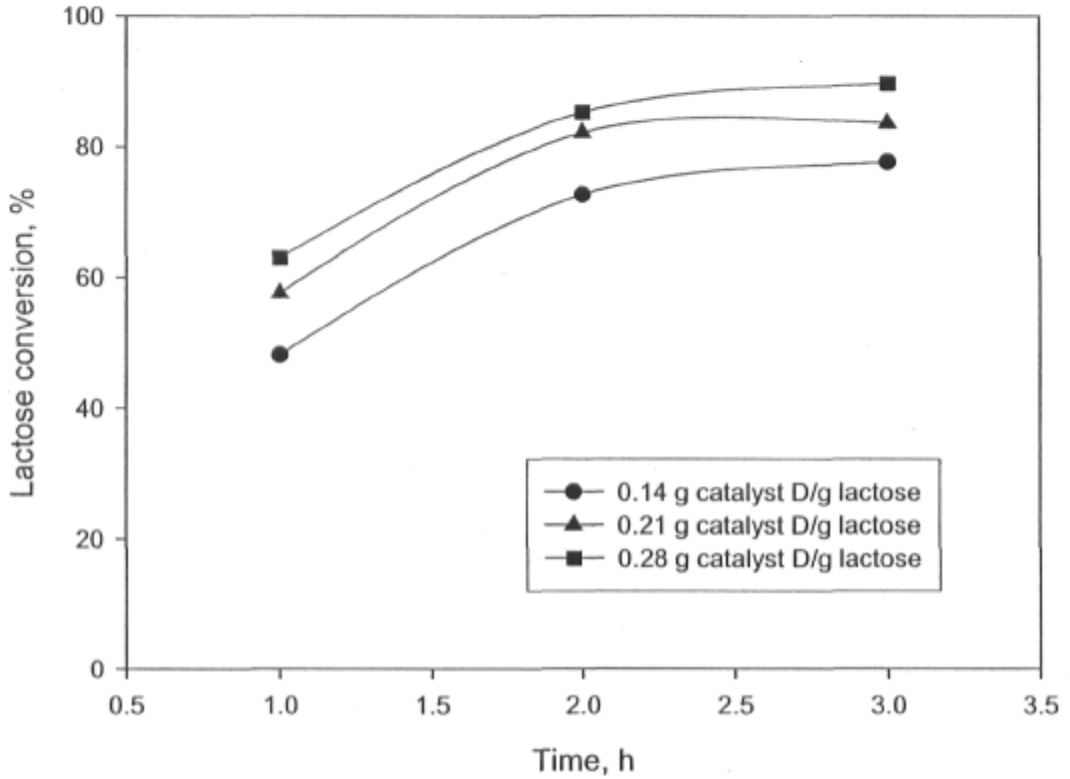

*Fig. 37. The effect of catalyst/lactose ratio on the conversion of lactose in the reactions performed with catalyst D (*1.02%Pd 0.64%Bi/SBA-15)

Figure 37 shows the effect of the catalyst/ lactose ratio on lactose conversion for 3 reactions using 1.02%Pd 0.64%Bi/SBA-15 catalyst. The greatest lactose conversion was obtained for the 0.28 g catalyst/g lactose. Using 0.21 g catalyst/g lactose resulted in a conversion of lactose after 3 hours a little beat smaller than the conversion in the case of 0.28 g catalyst/g lactose ratio. In the respect of the ultimate goal of any catalyst to provide a very good performance in smallest quantity, it seems to be reasonable to consider an optimum catalyst/lactose ratio of 0.21. This ratio is comparable with those reported by Abbadi et al. [1997].

5.2.4. The optimization of Bi:Pd molar ratio of the bimetallic catalyst

The experiments for the optimization of Bi:Pd ratio were performed at 65°C, 20 mL/min airflow, 1000 rpm and pH=9.

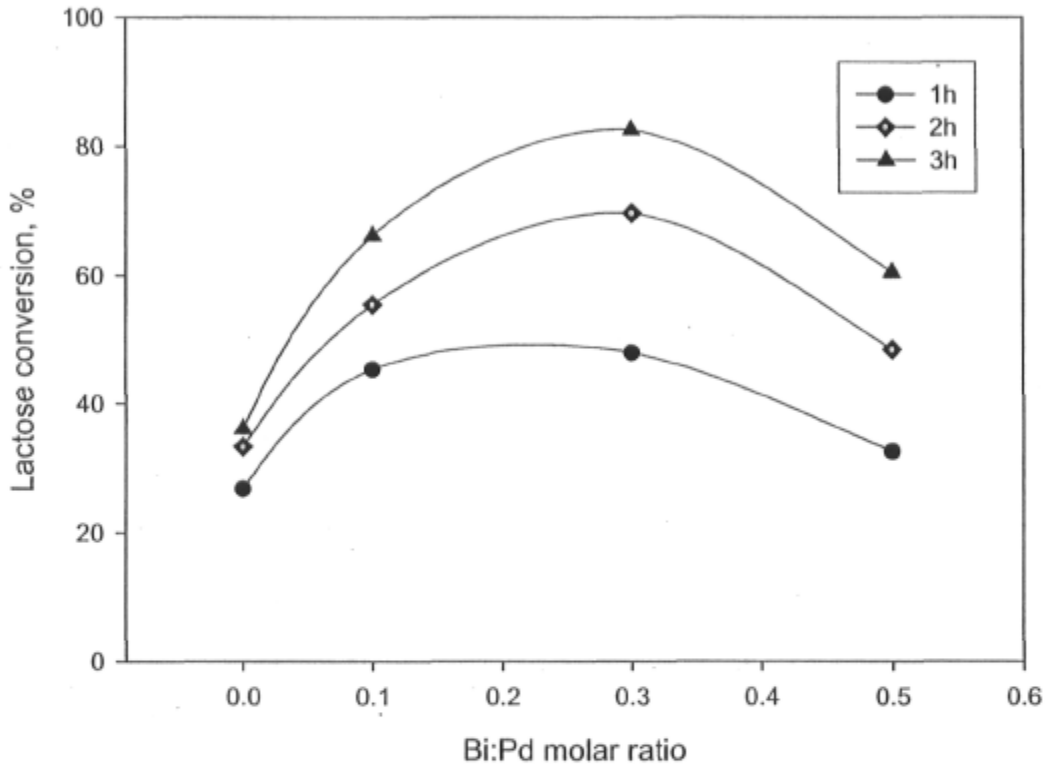

Fig. 38. The promoter effect of Bi on the lactose conversion.

In the absence of bismuth, the activity of Pd/SBA-15 is much lower because catalysts deactivate rapidly during oxidation reaction. As shown in Fig. 38, the addition of bismuth drastically improves the catalytic activity of the Pd/SBA-15 catalyst in the oxidation of lactose to LBA. The Bi:Pd molar ratio equal to 0.1, 0.3 and 0.5 were used in studying the promoting effect of bismuth. According to Wenkin et al. [2002], the promoting role of bismuth appears more evidently in the range 0.33<Bi/Pd<1.0 and the maximum conversion of lactose observed was for the catalyst with Bi:Pd=0.5 – 0.67 [Hendriks et al., 1990]. In this study the maximum of lactose conversion was observed for the promoted catalyst with Bi:Pd molar ratio of 0.3.

5.3. Kinetics of lactose oxidation.

5.3.1. Effect of temperature on the kinetics of lactose oxidation.

The experiments performed for studying the effect of temperature in the range 38°C – 80°C on the kinetics of reaction have involved the catalyst with formulation D (1.02%Pd 0.64%Bi/SBA-15) and the procedure 3. The pH has been kept constant at 9 and the ratio catalyst/lactose used was 0.21.

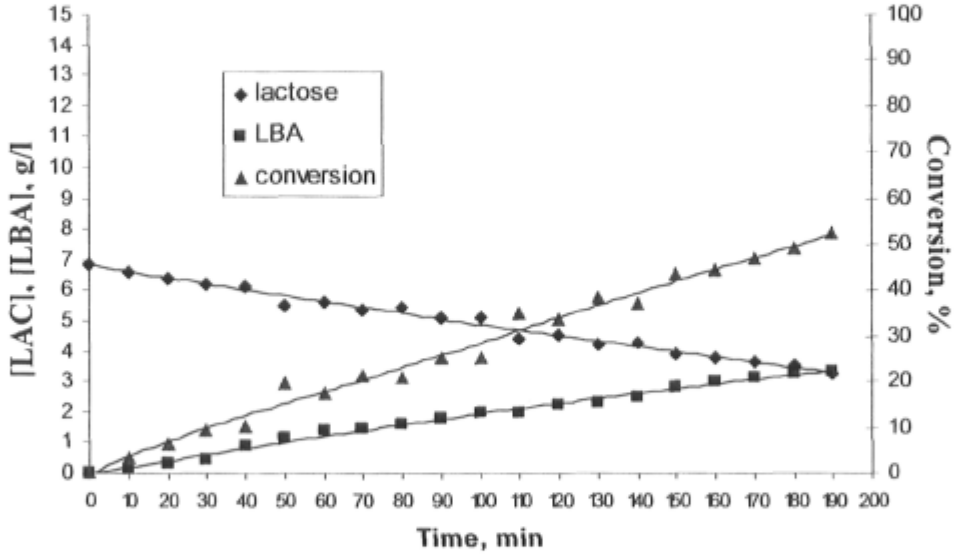

Fig. 39. The kinetics of lactose oxidation at 38 °C and pH=9 in presence of 1.02%Pd 0.64%Bi/SBA-15 catalyst.

In Fig. 39, the kinetics of lactose oxidation performed at 38°C and pH=9 presents a slow rate of lactose consumption. The reaction reached a maximum conversion of 49.05% after 3 hours. The selectivity of lactose conversion into LBA was found 100% during reaction. At 38°C, it was very difficult to maintain an optimum amount of dissolved oxygen in reaction medium because the solution reached the saturated concentration in dissolved oxygen very fast. Therefore, the catalyst deactivated by overoxidation and modest lactose conversions was obtained.

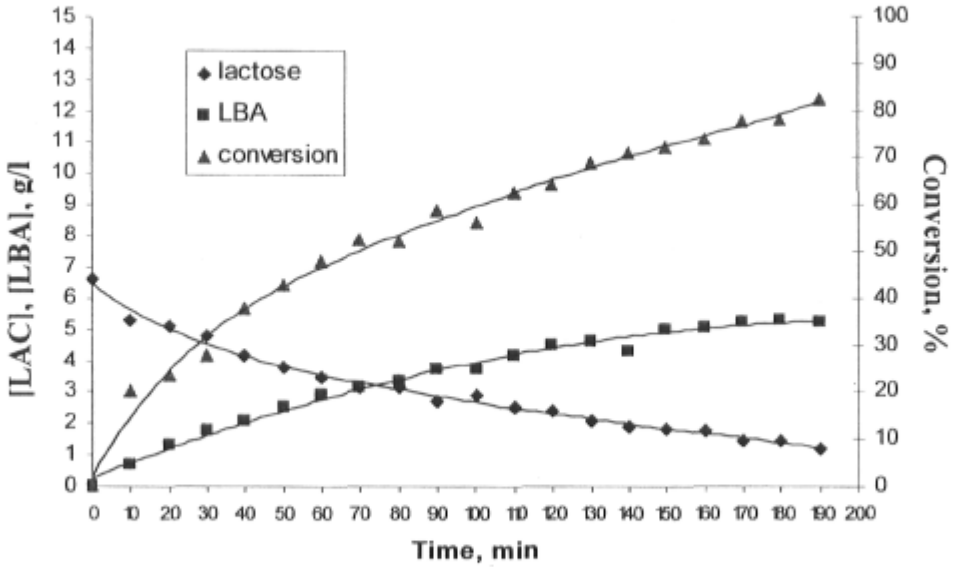

Fig. 40. The kinetics of lactose oxidation at 50 °C and pH=9 in presence of 1.02%Pd 0.64%Bi/SBA-15 catalyst.

The kinetics at 50°C (Fig. 40) exhibited a more pronounced consumption rate of lactose, where the conversion reached 78 % after 3 hours with the tendency to continue lactose oxidation. The catalyst was still active after 3 hours of reaction, but the lactose conversion reached moderate values. No other products were detected in the reaction mixture during reaction.

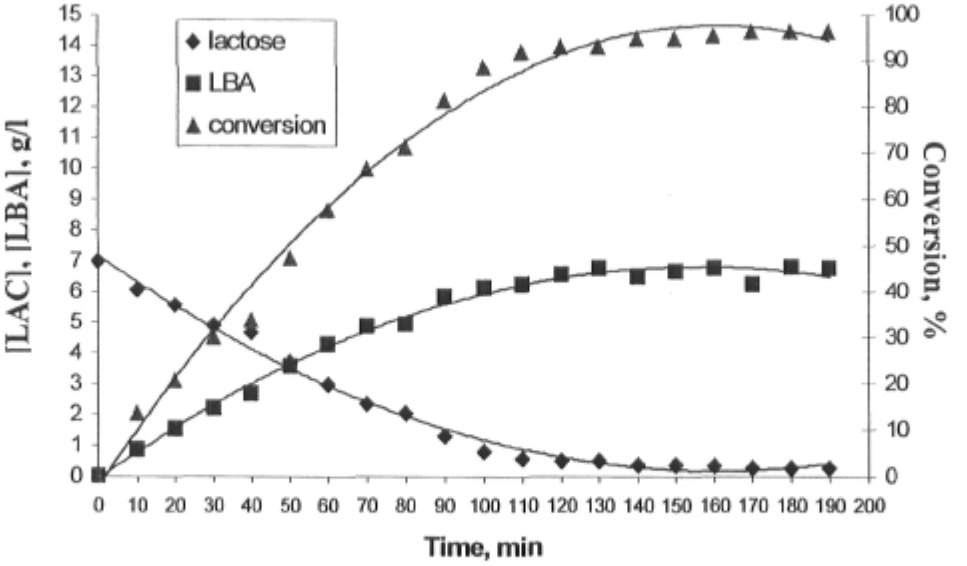

Fig. 41. The kinetics of lactose oxidation at 65 °C and pH=9 in presence of 1.02%Pd 0.64%Bi/SBA-15 catalyst

In Fig. 41, the kinetics of lactose oxidation performed at 65°C and pH=9 showed during the first 2 hours of reaction a high rate of consumption of lactose, reaching a conversion of 93%. After 3 hours, the maximum of lactose conversion was 96%. The selectivity of the catalyst during the reaction of lactose oxidation into LBA was found always 100%.

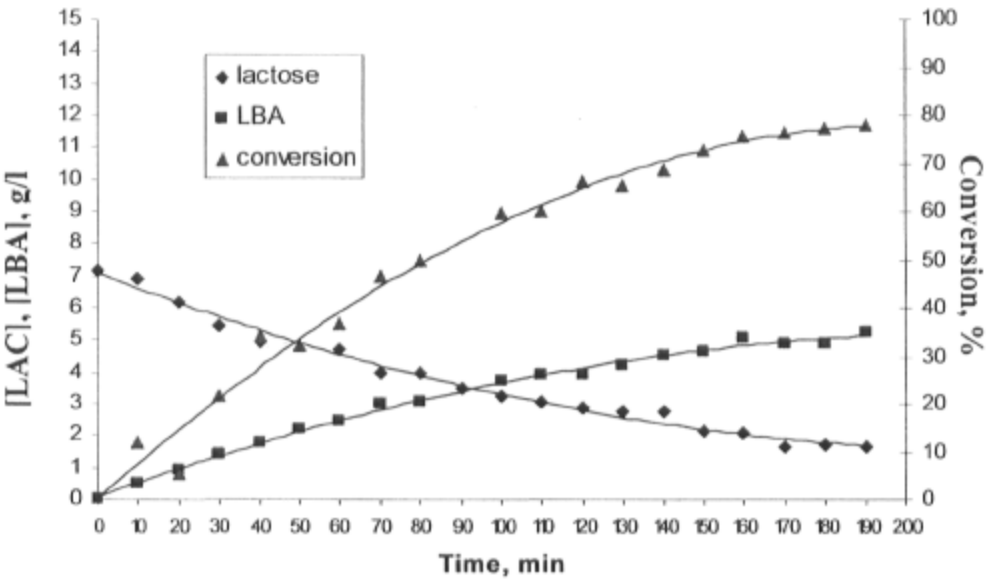

Fig. 42. The kinetics of lactose oxidation at 80 °C and pH=9 in presence of 1.02%Pd 0.64%Bi/SBA-15 catalyst

In Fig. 42, the kinetics of lactose oxidation performed at 80°C and pH=9 exhibited an acceptable consumption rate of lactose, reaching a conversion of 77% after 3 hours. At relatively higher temperature (80°C), the oxygen solubility decreased readily, thus the available O_2 concentration was too low to sustain and maintain the oxidation activity, which could explain the decrease in the lactose conversions value.

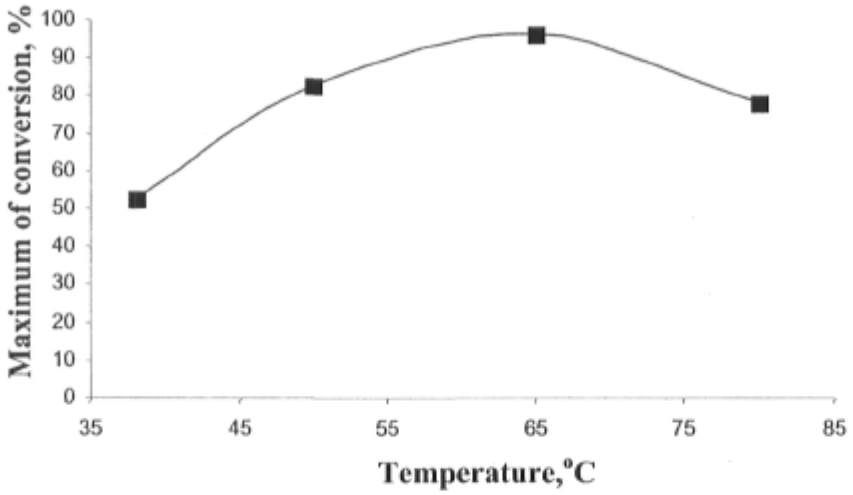

Fig. 43. The effect of temperature on the maximum of lactose conversion

Fig. 43 shows the optimal temperature of 65°C in the oxidation reaction of lactose where the maximum conversion of lactose was obtained. Moreover, while the solubility of oxygen in water decreases with increasing temperature, the concentration of oxygen in the aqueous phase should limit the overall reaction rate of lactose oxidation at higher reaction temperature. As shown in Fig. 39 and Fig. 40, at lower temperatures the reaction is limited by kinetics. However, the temperature has not affected the catalyst selectivity in LBA, which was 100% in all cases.

5.3.2. Effect of the pH on the kinetics of lactose oxidation

The experiments performed to study the effect of the pH of reaction mixture on the kinetics of reaction involved the catalysts with formulation D (1.02%Pd 0.64%Bi/SBA-15) and F (0.81%Pd 0.44%Bi/SBA-15) and procedure 3. In both cases the temperature was maintained at 65°C and the catalyst/lactose ratio was 0.21.

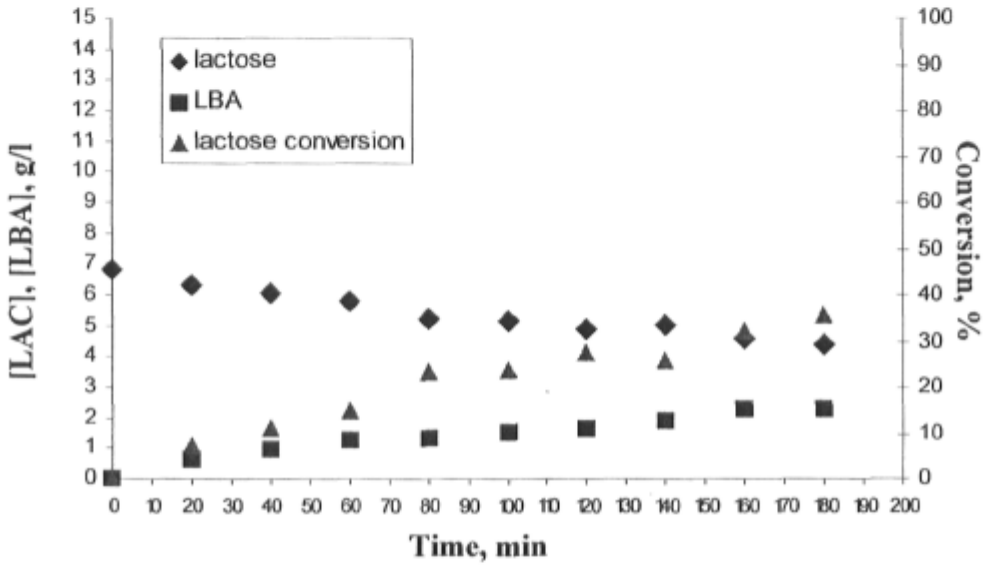

Fig. 44. The kinetics of the oxidation of lactose at 65 °C and pH=7 in presence of 1.02%Pd 0.64%Bi/SBA-15 catalyst

In the experiments performed at pH=7, the kinetics of the oxidation of lactose shows a slow reaction rate in Fig. 44 and the maximum of lactose conversion after 3 h hardly reached 36%. At this pH, the catalyst was deactivated by self-poisoning with acidic product LBA by blocking the active centres on the catalyst surface. Therefore, it was hard to carry out the oxidation reaction, which halted quickly.

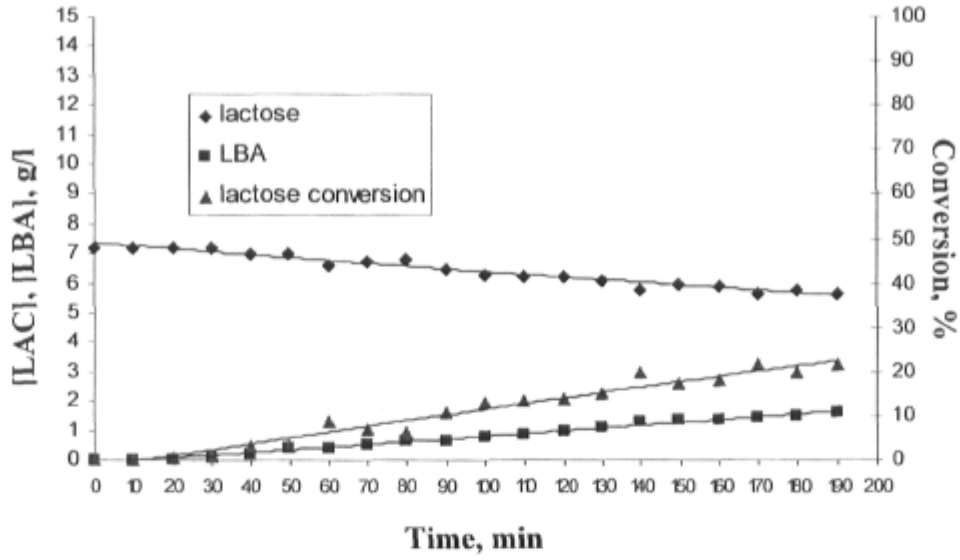

Fig. 45. The kinetics of the oxidation of lactose at 65 °C and pH=7 in presence of 0.81%Pd 0.44%Bi/SBA-15 catalyst

The same phenomenon is observed for the oxidation reaction, which involved de catalyst with formulation F. The lactose conversion after 3 hours had hardly reached 20 %.

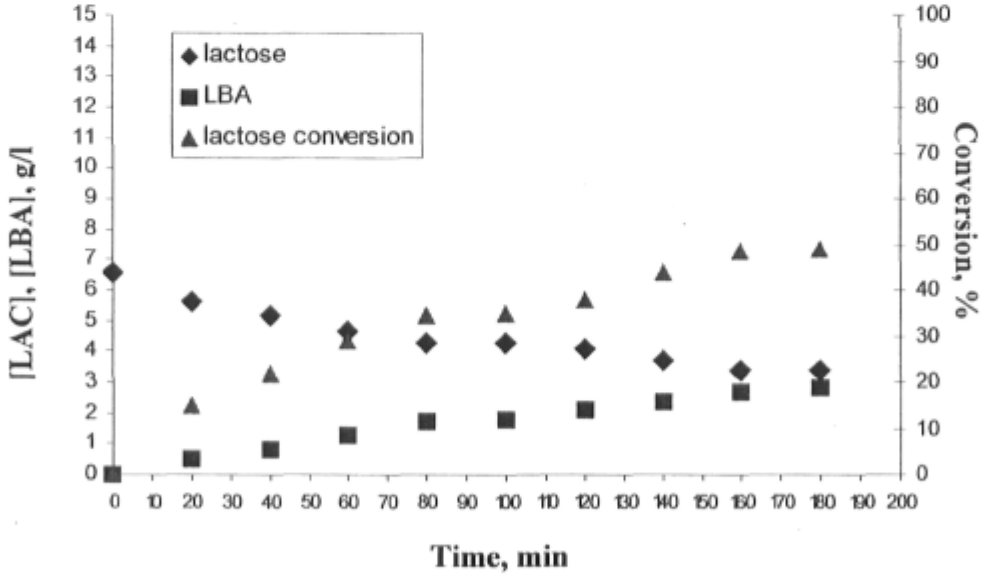

Fig. 46. The kinetics of the oxidation of lactose at 65 °C and pH=8 in presence of 1.02%Pd 0.64%Bi/SBA-15 catalyst

The kinetics of oxidation reaction of lactose carried out at pH=8 shows a maximum of lactose conversion of 49% (Fig. 46). Obviously, the reaction rate was greater than in the reaction performed at pH 7.

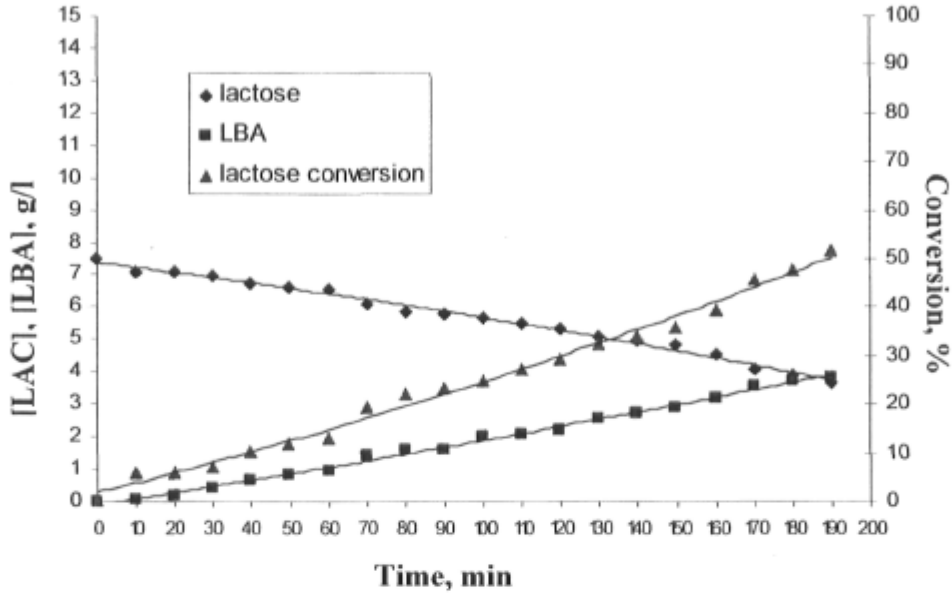

Fig. 47. The kinetics of lactose oxidation at 65 °C and pH=8 in presence of 0.81%Pd 0.44%Bi/SBA-15 catalyst

The reaction performed with formulation F of catalyst has reached a maximum of lactose conversion of 48% almost at the same level found for formulation D. Clearly, the kinetics of the reaction was improved by increasing the pH.

As shown Fig. 41 and Fig. 48, the kinetics at pH=9 demonstrates that the reaction rate was accelerated and the lactose conversion reached 85% after 3 hours for the reaction performed with formulation F of catalyst and 96% in the case of formulation D, indicating again that increasing pH has a beneficial effect in improving the kinetics of the reaction.

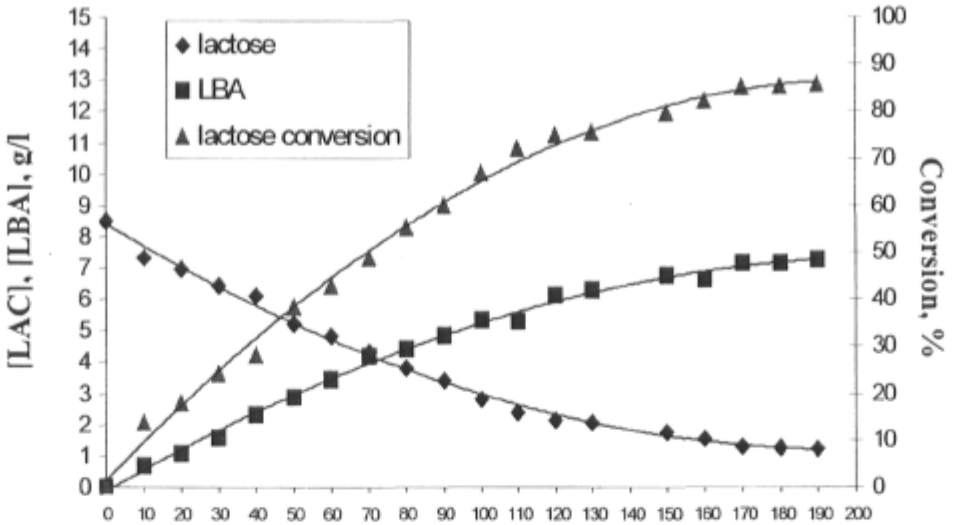

Fig. 48. The kinetics of the oxidation of lactose at 65 °C and pH=9 in presence of 0.81%Pd 0.44%Bi/SBA-15 catalyst

Consequently, the reaction rate clearly accelerates with increasing pH value (Fig. 49). A possible explanation for this phenomenon can be due to the negligible effect of catalyst deactivation by self-poisoning in alkaline solution, as LBA is deprotonated and, thus no longer capable of blocking active centers on the catalyst surface [Besson and Gallezot, 2001; Besson and Gallezot, 2003]. The catalyst selectivity in the oxidation reaction of lactose into LBA was 100% for the pH=7 –9.

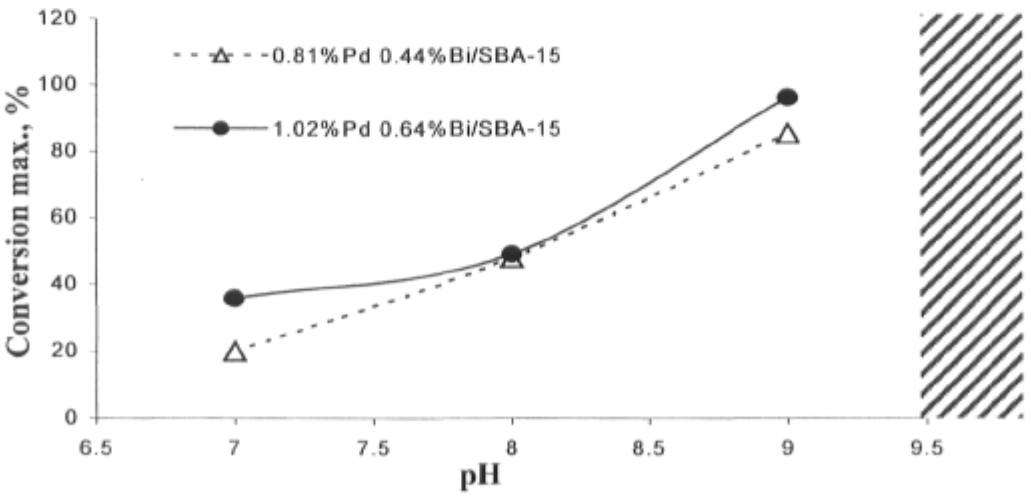

Fig. 49. Influence of pH on the kinetics of the lactose oxidation

The activity of the bimetallic Pd-Bi/SBA-15 catalyst is greater in an alkaline reaction condition. The selectivity to LBA decreased dramatically at higher pH values (>9.5) as a result of by-product formation catalyzed in strong alkaline solution and the partial consummation of the catalyst. Dissolution of the silica support with decoloration of the reaction medium was observed.

In conclusion, pH=9 was the optimal value proposed for the oxidation of lactose in the condition of high selectivity and activity of the bimetallic catalyst.

5.3.4. The stability of the catalyst

The ICP analysis of a reaction mixture was performed in the case of reaction of the oxidation of lactose where the conditions were found optimal and in presence of 1.02%Pd 0.64%Bi/SBA-15 catalyst. The leaching of the Bi and Pd in the reaction mixture was found to be 1.2 mg/L and 0.2 mg/L for Bi and Pd, respectively. The catalyst demonstrated that it is very stable and further batches of the lactose may be oxidized with the same charge of catalyst. Further studies are required to provide the recycling capability of the used catalyst.

5.3.5. Scale-up studies of the oxidation of lactose

In view to demonstrate that the kinetics of the oxidation of lactose can be scaled-up, the studies were performed at 65°C, pH=9 and catalyst/lactose ratio=0.21, with bigger reaction volumes. The highest performing catalyst (1.02%Pd 0.64%Bi/SBA-15) was involved. For the scale-up studies various reaction volumes (V_r) and reactor volumes (V_R) were employed.

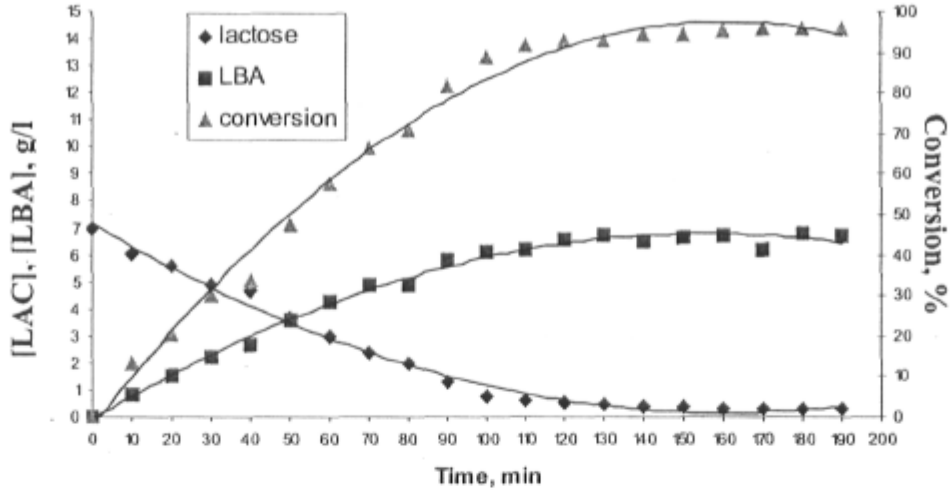

Fig. 50. The kinetics of the experiment performed in an Erlenmeyer (V_R=300 mL, V_r=100 mL).

The airflow was maintained at 20 mL/min and the stirring rate was 1000 rpm. When a small reaction volume is employed (100 ml) and V_r/V_R=0.33, the reaction rate is fast and high lactose conversions where reached (Fig. 50). Also, the performance of the catalyst regarding its activity and selectivity is very high. This may be ascribed to a very good oxygen transfer on the surface of the catalyst in the reaction mixture, which maintains a high rate of lactose consumption.

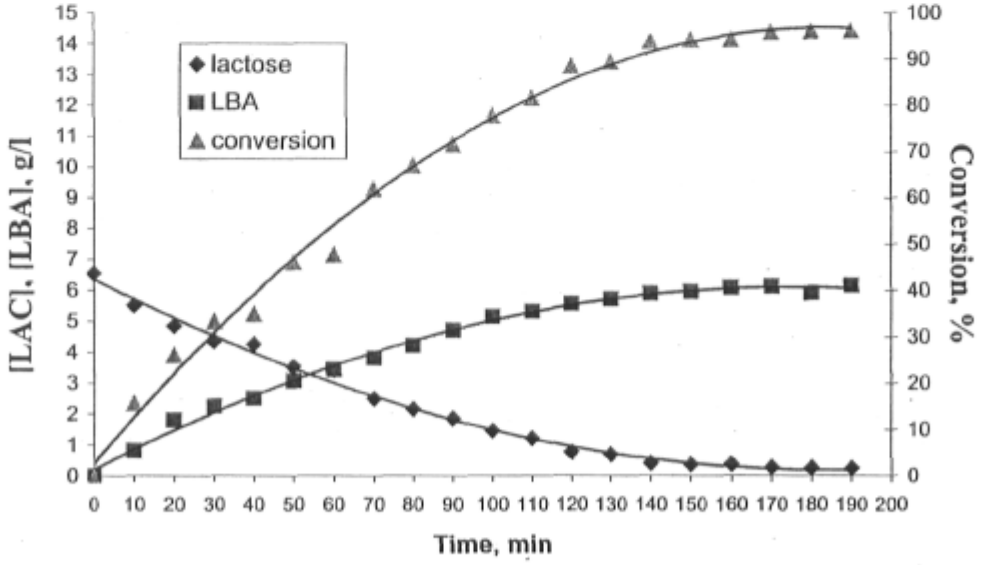

Fig. 51. The kinetics of the experiment performed in an Erlenmeyer (V_R=1000 mL, V_r=500 mL).

When the reaction volume was 500 mL and V_r/V_R=0.5 without changing the reactor shape, the reaction rate was comparable with those carried out in a smaller reaction volume and the lactose conversion was 96%, practically the same (Fig. 51). The stirring rate was always kept at 1000 rpm, but the airflow was maintained at 100 mL/min.

According to the results obtained, the scale-up studies were very encouraging and following studies were carried out in a reactor (AceGlass, USA) with V_R=1000 mL. The kinetics is presented in Fig. 52.

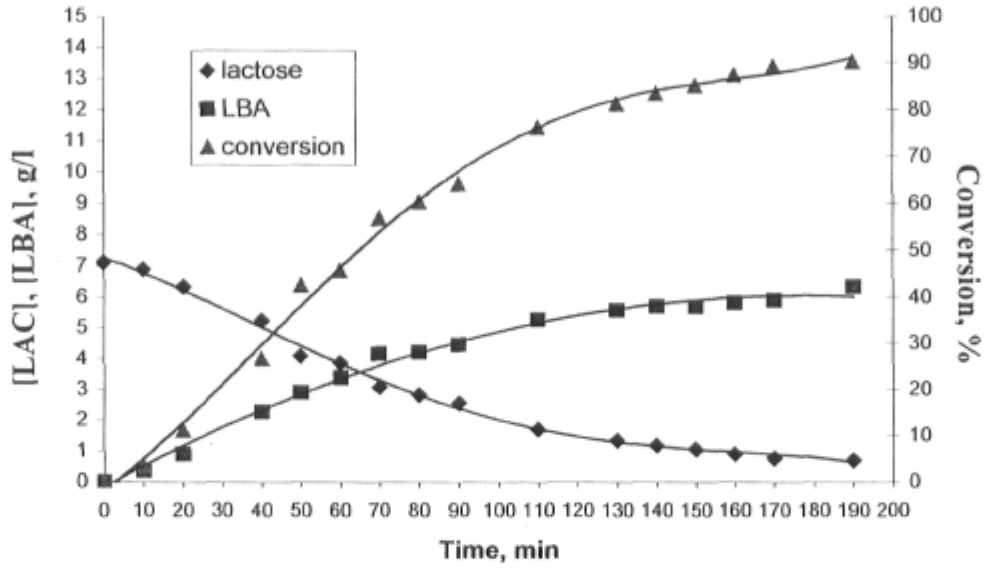

Fig. 52. The kinetics of the experiment performed in AceGlass reactor (V_R=1000 mL, V_r=400 mL).

In this experiment, the stirring rate was kept at 1000 rpm, and the airflow was maintained at 80-100 mL/min. The lactose conversion was 90%, slightly lower than that obtained in previous studies. Otherwise, the results remain good, but improvement of mass transfer in reaction mixture is necessary. Thus, increasing the stirring rate or changing the shape of the agitator may result in a better mass transfer and thus increase the reaction rate for the oxidation of lactose performed in 1L AceGlass reactor. Further studies are required to optimize the design of the reactor for this reaction.

5.4. Discussion

A typical SBA-15 material with a specific surface of 901.1 m^2/g and pore size of 6.8 nm was synthesized. The N_2 adsorption-desorption isotherm at 77K of SBA-15 materials prepared showed an isotherm of the type IV characteristic for mesoporous materials with hysteresis loop. After successive impregnation with Pd and Bi, the N_2 adsorption-desorption isotherms also presented the hysteresis loop, which demonstrated that the mesoporous framework of SBA-15 was preserved. For 1%Pd loading of SBA-15 support it was observed that the surface area had not significantly diminished (Table 3). The bimetallic 1.02%Pd 0.64%Bi/SBA15 also preserved the mesoporous structure with a large specific surface.

The powder XRD patterns also showed that the hexagonal mesostructure of SBA-15 was preserved after consecutive impregnation with Pd and Bi (Fig. 23 and Fig. 24). The impregnation with Pd was successfully made because Pd was highly dispersed on the SBA-15 support (43%). The nanoparticles of Pd with 2.6 nm were found by H_2-chemisorption in the 1%Pd/SBA-15 sample. Clearly, with increasing metal loading of the catalyst, the growth of crystallites size of Pd and PdBi alloy was shown by XRD analysis.

TEM images confirmed the ordered hexagonal framework of SBA-15 and the layout of the Pd and bimetallic nanoparticles into the pores of SBA-15. In the case of the highest performing catalyst 1.02%Pd 0.64%Bi/SBA-15, the Pd and PdBi nanoparticles were found in the range of 3–8 nm with a very good dispersion on the SBA-15 support.

The XPS analysis of the 1.02%Pd 0.64%Bi/SBA-15 revealed that the activation of bimetallic 1.02%Pd 0.64%Bi/SBA-15 in hydrogen at temperature 533K leads to the formation of a Bi-Pd alloy with a stoechiometric formula $Bi_{1.75}Pd$. Bismuth was not found as separate particles on the support. The Pd was found in the metallic state on the catalyst surface. Keresszegi et al [2004], analyzing Pd-Bi/Al_2O_3 catalyst, they supposed that when the Pd 3d peak intensity decreased, the Bi covered a considerable fraction of Pd. In our case the Pd 3d peak intensity remained constant and Bi 4f shifted, which explained the formation of the Bi-Pd particles on the catalyst surface. This $Bi_{1.75}Pd$ alloy may have a

positive influence on the catalytic properties of the bimetallic system in the oxidation of lactose. Karski, [2006] demonstrated that Pd-Bi/SiO_2 systems showed the presence of intermetallic compounds of BiPd and Bi_2Pd type, while Wenkin et al. [1996] reported the occurrence of BiPd, Bi_2Pd_5 and $BiPd_3$ in the active phase of carbon-supported Bi-Pd catalysts. The differences result from surface chemical reactivity of the supports (C, SiO_2), the textural characteristics (SiO_2, SBA-15) as well as activation conditions.

The first tests of the oxidation of lactose revealed the important role of dissolved oxygen in the reaction mixture. Three procedures were developed and carried out for different types of Bi-Pd/SBA-15 catalysts. Oxidation of lactose in the presence of Bi-Pd/SBA-15 catalysts was carried out with procedure no. 3, which controlled the amount of dissolved oxygen in the reaction mixture. The microaerial conditions represented the best way to conduct the oxidation of lactose to the highest conversion and selectivity towards LBA formation. Therefore, all the experiments were performed with a strict control of dissolved oxygen by the consecutive bubbling of air and N_2. The reaction mixture must be not saturated with oxygen because the catalyst is very sensitive to over oxidation and the reaction stops. By bubbling the N_2, the dissolved oxygen was decreased to a level below 1% of the equilibrium concentration. After 3 hours, the oxidation of lactose was stopped because the yield in LBA remains practically the same. This situation is due to the catalyst deactivation mostly by overoxidation. The reaction mixture becomes supersaturated in oxygen and the catalyst became inefficient.

The start-up procedure of reaction involves the degassing of lactose solution at 0% dissolved oxygen, increasing the temperature and the addition of the freshly reduced catalyst while increasing the stirring rate to 1000 rpm. Most of the experiments were performed in stirred slurry reactors, which are most suitable for screening new catalysts to laboratory scale.

It was observed that the highest conversion of lactose (96%) was obtained for the formulation D of the catalyst (1.02%Pd 0.64%Bi/SBA-15) where the reaction performed with procedure 3 and catalyst/ lactose ratio = 0.21.

Also for the catalyst with formulation F (0.81%Pd 0.44%Bi/SBA-15) a lactose conversion of 95 % was obtained after 3 hours of reaction, but with a greater catalyst/lactose ratio of 0.28. The catalyst with formulation B (5%Pd 5%Bi/SBA-15)

showed a low lactose conversion probably due to the large crystallite size of the metals, which did not fit in the mesoporous structure of SBA-15. XRD proved the formation of a bimetallic Bi-Pd compound. Other catalysts with different metal compositions were prepared and employed in the oxidation reaction after the activation by reduction in H_2 at 533K.

Finally, the optimum metal loading of catalysts was obtained with 1.02%Pd and 0.64%Bi. Hendriks et al. [1990] showed that the reaction rate is strongly dependent on the amount of promoter used. The understanding of the influence of the addition of the second metal to palladium catalysts on their performance involves good knowledge of the chemical state of both Pd and co-metal and the degree of an intimate interaction between those two components [Karski, 2006].

The experiments for the optimization of Bi:Pd molar ratio have shown that the Bi acts as a promoter for Pd in the catalytic oxidation of lactose. No influence of the Bi:Pd molar ratio was detected on the catalyst selectivity for LBA. The unpromoted catalyst A (1%Pd/SBA-15) led to the lowest lactose conversion compared with the maximum of lactose conversion for the bimetallic catalysts with the same Pd loading. An optimum ratio Bi:Pd =0.3 for the catalyst with formulation D was found. The beneficial effect of bismuth was clearly demonstrated. The deactivation of the catalyst by self-poisoning, overoxidation or corrosion of the noble metal was avoided when the Bi-Pd catalyst was involved in oxidation reaction of lactose in optimized process conditions.

The highest conversion of lactose was obtained for the reaction which involves the catalyst/lactose ratio=0.28. Although, in the case of catalyst/lactose ratio=0.21, the conversion of lactose was slightly lower and was considered as the optimum catalyst/lactose ratio. It is important to notice that during the HPLC analysis the presence of another product other than LBA was not detected. The selectivity of catalyst was 100%.

The leaching of the Bi in the solution mixture was found to be 1.2 mg/L and for Pd was found to be 0.2 mg/L. Besson et al. [1995] did not notice any Bi dissolution from Bi-Pd catalyst in which the promoter element was selectively deposited in the noble metal at a low Bi loading (Bi/Pd=0.1). It has also been proved that the Bi dissolution increased when the Bi:Pd ratio increased [Karski, 2006]. Wenkin et al. [2002] suggested that bismuth involved in the active phase of the catalyst tends to dissolve until the catalyst surface is

characterized by a particular composition, corresponding to two Pd atoms for one Bi atom. In this case the Bi loss from the catalysts in the solution mixture is small and it proves that $Bi_{1.75}Pd$ found by XPS analysis stands for the stability of the catalyst.

The kinetics of the reaction of the oxidation of lactose has shown a strong dependence of the lactose conversion with the pH and the temperature. At 65°C, the concentration of dissolved oxygen in the reaction medium provides a better oxygen mass transfer and diffusion onto the surface of the catalyst. This behaviour may be due to the solubility of oxygen in water, which decreases with increasing temperature.

The pH value of the reaction mixture has a crucial effect on the reaction rate of LBA formation. The reaction rate clearly accelerates with increasing pH value. The maximum conversion was observed for the pH=9. In the experiments performed at higher pH values ($\geq$ 9.5) dissolution of mesoporous silica support was observed with the formation of by-products, which cause a decrease in catalyst selectivity and activity.

The oxidation of lactose with air in the aqueous phase over Bi-Pd/SBA-15 catalysts occurs via an oxidative-dehydrogenation mechanism specific for the heterogeneous aldose oxidation on the bimetallic Bi-M (M=Pd, Pt) catalyst, which also explains the promoter role of the Bi, as previously reported in the literature.

For an easy understanding of kinetic data and oxygen mass transfer, the mechanism of the oxidation of lactose proposed, is similar to the mechanism explained by Tokarev et al. [2006]. The mechanism involves the adsorption of lactose on the catalyst surface with a hydride transfer to a free metallic site, simultaneously with the dehydrogenation of the substrate. So, the lactobionic acid is formed in one step by simultaneous deprotonation and hydride transfer and the rate of this step is likely to increase at higher pH. This step is immediately followed by desorption of H^+ and OH^- from surface to form water and hydrogen. The LBA desorption in alkaline medium is faster than the surface reaction therefore the oxidative-dehydrogenation mechanism is performed continuously. When the reaction is not performed in an alkaline medium, the catalyst is deactivated by self-poisoning due to a strongly adsorption of LBA on the catalyst surface.

The scale-up studies were carried out in microerial conditions at 65°C and pH=9 with 100, 250 and 400 mL of 20 mM lactose solution in presence of 1.02%Pd 0.64%Bi/SBA-15 catalyst. The results obtained for much bigger volumes were similar to

those obtained in 100 mL solution. In the 1000 mL AceGlass reactor, by employing 400 mL lactose solution, the maximum conversion of lactose reached 90%, with a selectivity of 100% into LBA. In conclusion, the scale-up studies showed promising results for the production of LBA by the oxidation of lactose at large scale.

5.5. References

1) Abbadi A., Gotlied K.F., Meiberg J.B.M., van Bekkum H. **1997**. Appl. Catal. A: General. 156: 105.
2) Besson M., Lahmer F., Gallezot P., Fuertes P., Fleche G. **1995**. Catalysts. J Catal. 152: 116.
3) Besson M. and Gallezot P. **2000**. Catal. Today. 57: 127–141.
4) Besson M. and Gallezot P., in: R.A. Sheldon, H. van Bekkum (Eds.), Fine Chemicals through Heterogeneous Catalysis, Chap. 9.3.Wiley–VCH, **2001**, pp. 509–510.
5) Besson M., Gallezot P. **2003.** Catal.. Today. 81: 547–559.
6) Sing K.S.W., Everett D.G., Haul W.A.W., Moscow L., Pierotti R.A., Rouquerol J. and Siemieniewska T. **1985**. Pure Appl. Chem. 57: 603.
7) Hendriks H. E.J., Kuster B. F.M., Marin G. B. **1990**. Carbohydr. Res. 204:121.
8) Karski S., Witonska I., Goluchowska J. **2005**. J Mol.Catal. A: Chemical 245: 225.
9) Karski S. **2006**. J. Mol. Catal. A: Chemical 253: 149.
10) Kerresszegi C., Grunwaldt J.-D., Mallat T. and Baiker A. **2004.** J. Mol. Catal. 222: 273.
11) Kruk M., Jaroniec M., Joo S.H., Ryoo R., **2003**. J. Phys. Chem. B. 107: 2205.
12) Lukens Jr. W.W., Schmidt-Winkel P., Zhao D., Feng J., Stucky G.D.. **1999**. Langmuir 15: 5403.
13) Moulder J. F. et al. Handbook of X-ray photoelectron spectroscopy 1992. Perkin-Elmer Corp.
14) NIST XPS Database, NIST Standard Reference Database 20, Version 3.3 (Web Version), **2000**.
15) Ryoo R., Ko C. H., Kruk M., Antochshuk V., Jaroniec M. **2000**. J. Phys. Chem. 104: 11465.
16) Tokarev A.V., Murzina E.V., Kuusisto J., Mikkola J.-P., Eränen K., Murzin D.Y. **2006**. J. Mol. Catal. A: Chemical 255: 205-206.

17) Van Der Voort P., Ravikovitch P.I., De Jong K.P., Benjelloun M., Van Bavel E., Janssen A.H., Neimark A.V., Weckhuysen B.M., Vansant E.F. **2002**. J. Phys. Chem. B 106: 5873.

18) Wenkin M., Ruiz P., Delmon B., Devillers M. **2002**. J Mol. Catal. A: Chem.180: 145.

19) Wenkin M., Touillaux R., Ruiz P., Delmon B., Devillers M. **1996**. Appl. Catal. A.: Gen. 148: 181.

20) Yuranov I., Moeckli P., Suvorova E., Buffat P., Kiwi-Minsker L., Renken A. **2003.** J. Mol. Catal. A: Chemical 192: 239.

21) Zhao D., Huo Q., Feng J., Chmelka B. F., Stucky G. D. **1998**. J. Am. Chem. Soc 120: 6024.

CHAPTER 6

CONCLUSIONS

The catalytic oxidation of lactose was successfully accomplished in microaerial conditions and alkaline medium in the presence of a novel bimetallic catalyst Pd-Bi supported on a mesostructured silica support.

Uniform deposition of metal nanoparticles with controlled particle size onto mesoporous silica support with subsequent activation leads to an active bimetallic catalyst. Nonetheless, bimetallic Bi-Pd catalysts offer performance due to the two active metals that somehow cooperate to enhance the activity and selectivity of the catalyst. Due to its higher affinity for oxygen, bismuth acts as a co-catalyst preventing the deactivation of the catalyst by overoxidation.

The highest conversion of lactose (96%) was obtained for the reaction, which involves the formulation D of the catalyst (1.02%Pd 0.64%Bi/SBA-15). Using the new catalytic method lactose was selectively oxidized at 65°C and pH=9 in 3 hours with 100% selectivity to LBA.

The microaerial condition provided the continuous oxidation of lactose by avoiding the catalyst over oxidation. Therefore, the best way to obtain the highest conversion of lactose was to control the amount of dissolved oxygen in the reaction medium. In view to protect the catalyst from over oxidation, an oxidation procedure was developed.

It was found that the optimum Bi:Pd molar ratio of 0.3 of the catalyst D (1.02%Pd 0.64%Bi/SBA-15) was conducted with the formation of a Bi-Pd alloy with stoechiometric formula $Bi_{1.75}Pd$. By far this compound seems to be responsible for the activity and

selectivity of the bimetallic catalyst. Also, the catalyst has shown its stability after 3 hours of reaction because the metal leaching in the aqueous solution was very small.

Compared with other catalysts in the field of oxidation of aldoses, the novel bimetallic catalyst supported by mesoporous silica proved its efficiency with a much smaller loading in metals. The nanostructured support SBA-15 demonstrated its important role in assuring a high dispersion of metal nanoparticles.

The reaction conditions for the oxidation of lactose were optimized. These conditions were also tested in a larger volume of reaction.

Future studies of the kinetics of the oxidation of lactose would allow a detailed explanation of the mechanism oxidation of lactose, which is useful for reactor design.

In conclusion, LBA can be produced at industrial scale by a novel catalytic method, which employed a new nanostructured catalytic material that achieves the ultimate goal of "green chemistry": chemical manufacturing optimized to minimize energy use and waste generation.

CONTRIBUTIONS

The results of this project have been presented at the following conferences:

- The 19th Canadian Symposium on Catalysis in Saskatoon, May 2006;
- The 56th Canadian Chemical Engineering Conference in Sherbrooke, October 2006;
- Mini-Symposium of Department of Chemical Engineering, Université Laval, Quebec, December 2006.

SUGGESTIONS FOR FURTHER WORK

Considering the existing results accomplished in this work, the future studies in catalytic oxidation of lactose will require:

- More detailed and reliable kinetic investigations for providing the kinetic model of catalytic oxidation of lactose;
- From the experimental standpoint, the recording of oxygen uptake during reaction is very important for the kinetic model. Also improving the stirring rate and the agitator type of the reactor may be essential for enhancing reaction rate and lactose conversion in LBA in less than 3 hours;
- Continuous research efforts must be focused to study the issues related to catalyst deactivation. An investigation of the catalyst regeneration has to be studied systematically to assess any commercial viability of the catalytic oxidation of lactose based on the bimetallic Pd-Bi/SBA-15 catalyst.

ANNEXE A

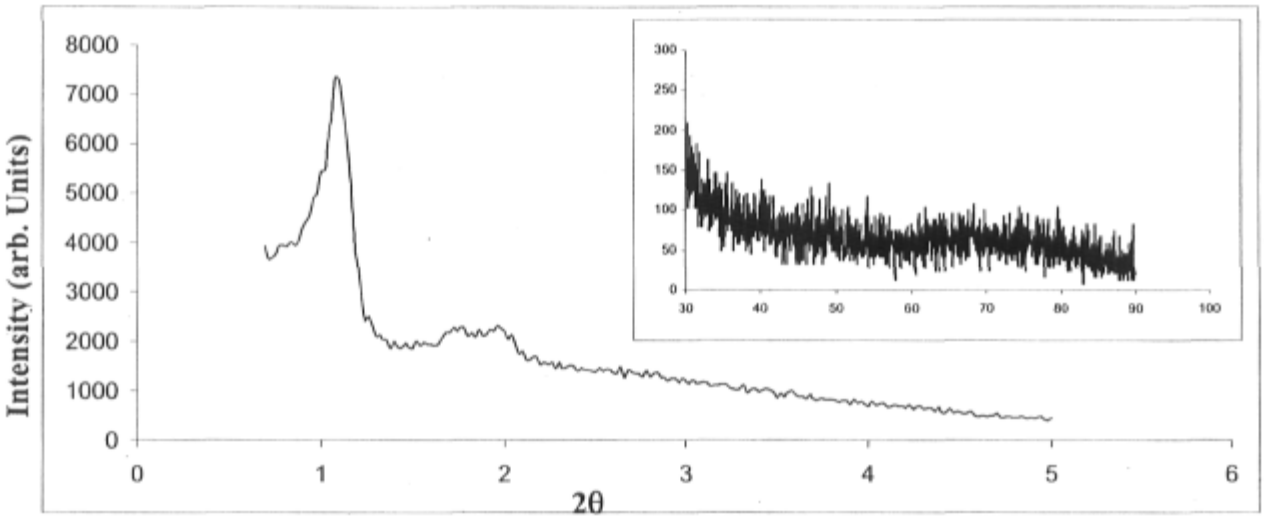

Fig. 53. Small and wide angle XRD patterns of 0.81%Pd 0.44%Bi /SBA-15 catalyst

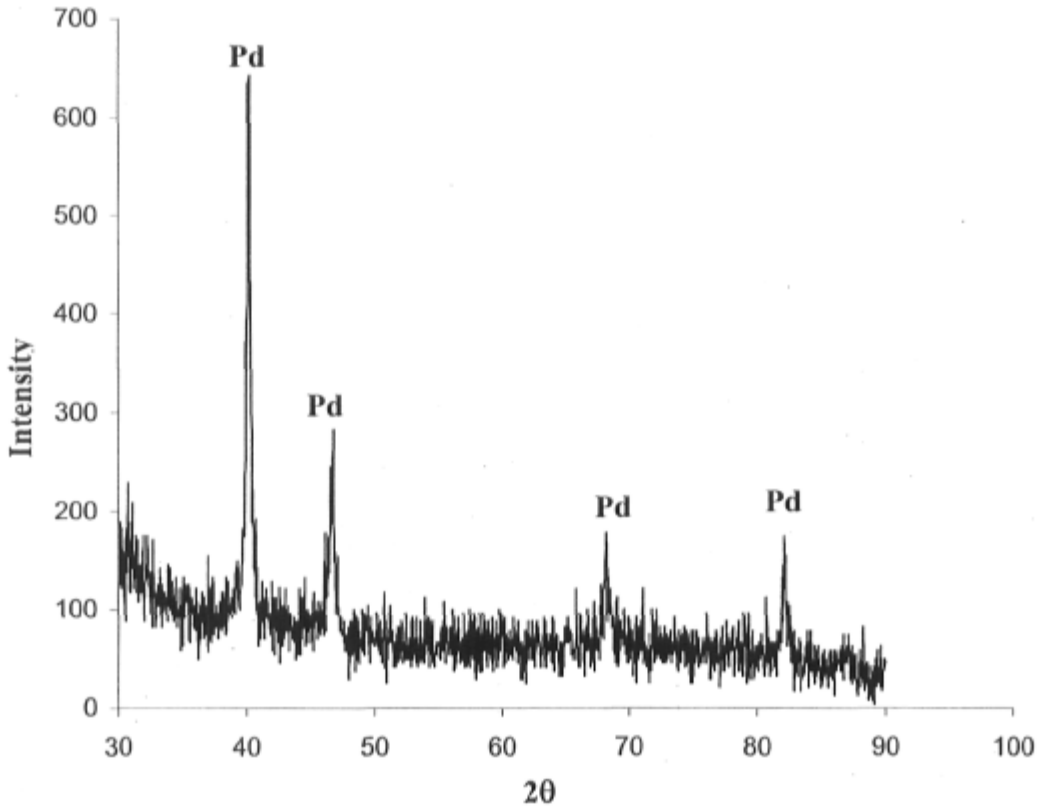

Fig. 54. Wide angle XRD patterns of 5%Pd /SBA-15

ANNEXE B

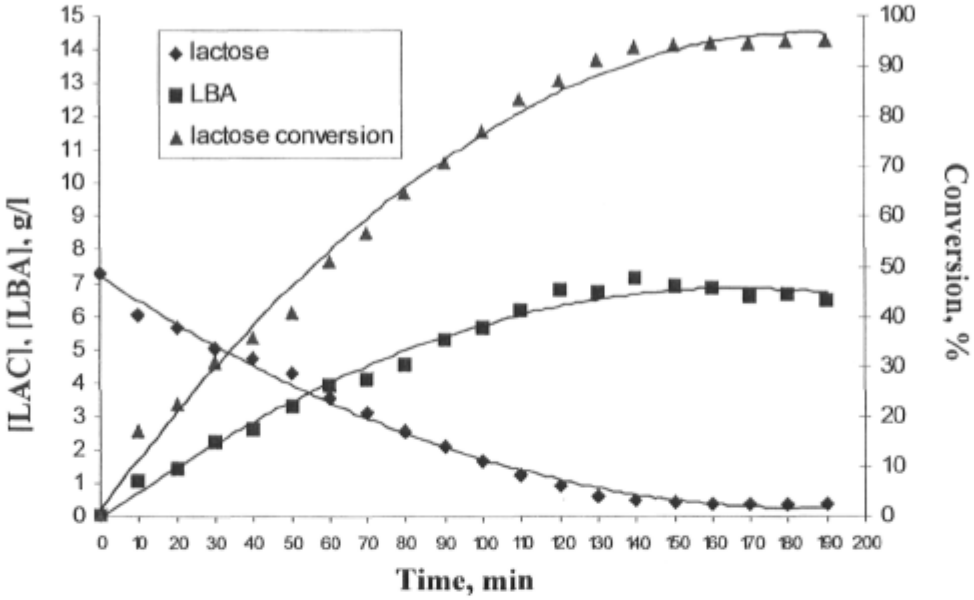

Fig. 55. The kinetics of oxidation reaction of 100 mL lactose solution (20 mM) at 65°C and pH=9 in presence of 0.28 g 0.81%Pd 0.44%Bi/SBA 15 catalyst /g lactose.

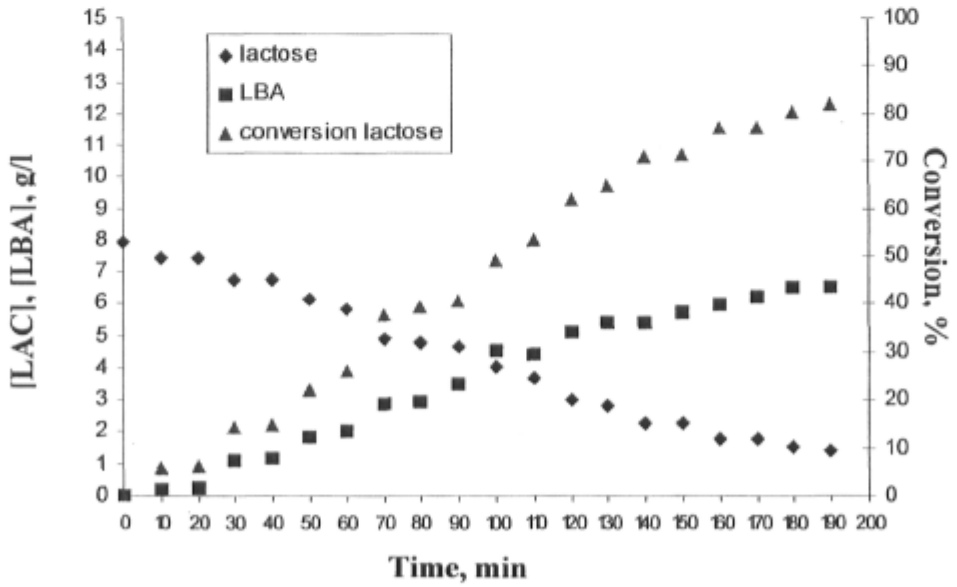

Fig. 56. The kinetics of oxidation reaction of 100 mL lactose solution (20 mM) at 50°C and pH=9 in presence of 0.21 g 0.81%Pd 0.44%Bi/SBA 15 catalyst /g lactose.

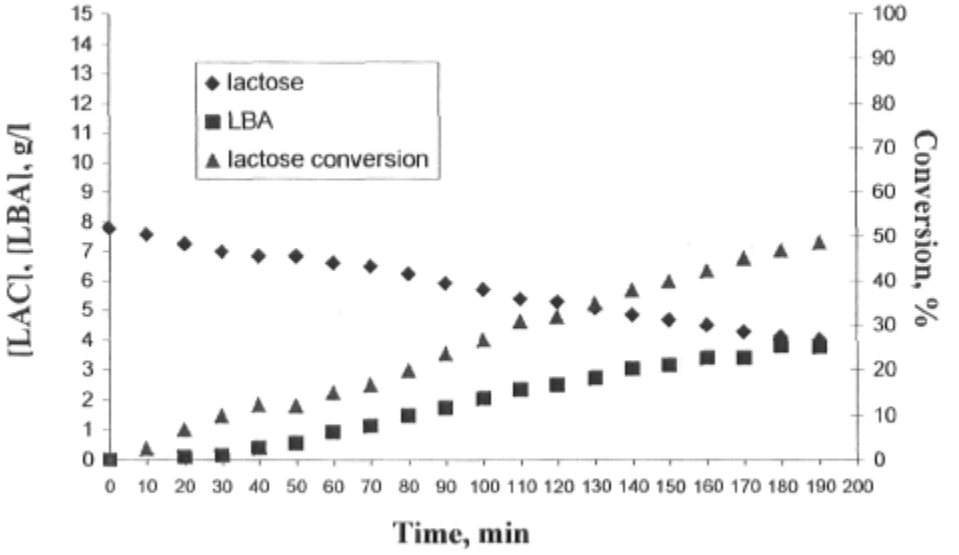

Fig. 57. The kinetics of oxidation reaction of 100 mL lactose solution (20 mM) at 38°C and pH=9 in presence of 0.21 g 0.81%Pd 0.44%Bi/SBA 15 catalyst /g lactose.

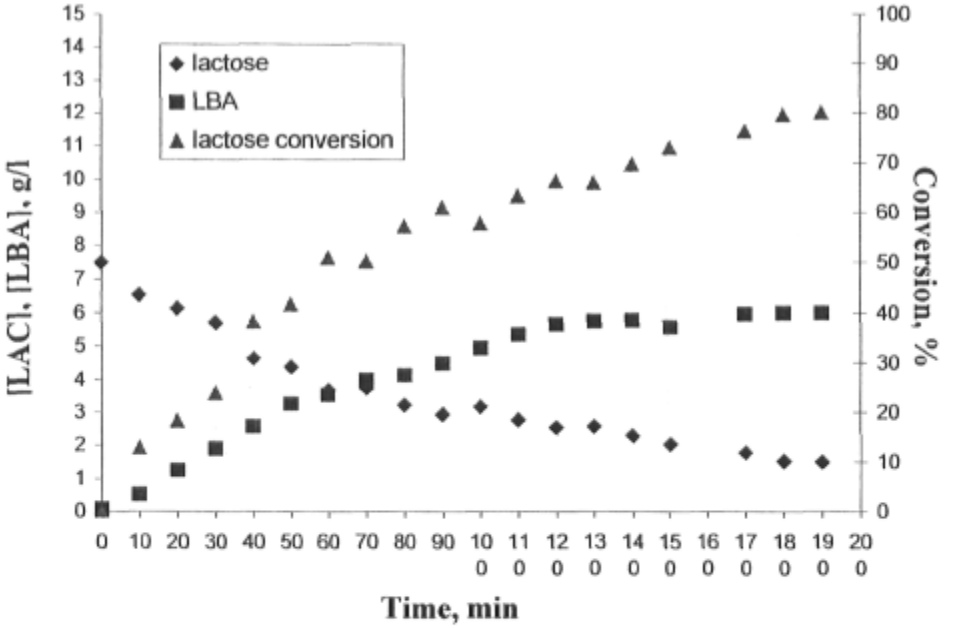

Fig. 58. The kinetics of lactose oxidation of 100 mL lactose solution (20 mM) at 75-80°C and pH=9 in presence of 0.81%Pd 0.44%Bi/SBA 15 catalyst with a charge of 0.21 g catalyst/g lactose.

ANNEXE C

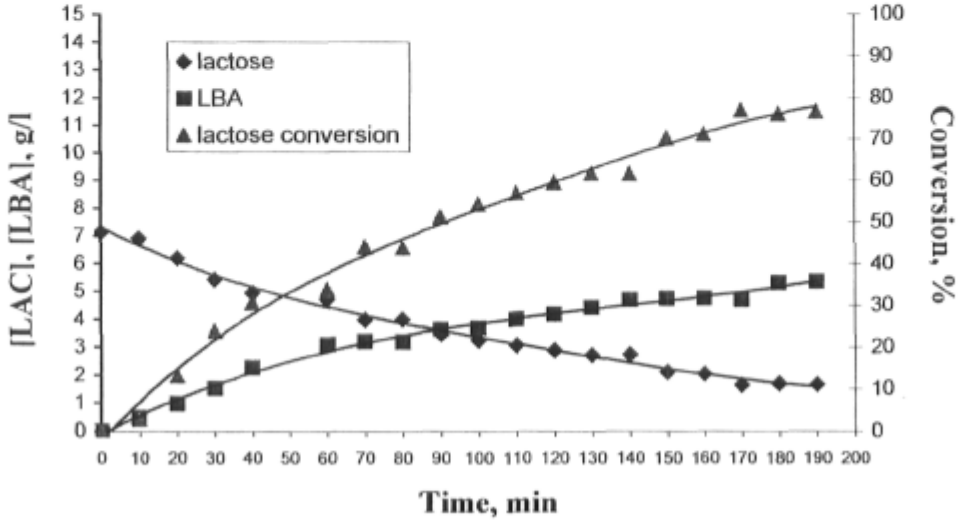

Fig. 59. The kinetics of lactose oxidation for the reaction performed in 400 mL lactose solution 20 mM in 1L AceGlass reactor at 50°C and pH=9 in presence of 0.21g 1.02%Pd 0.64%Bi/SBA 15 catalyst /g lactose.

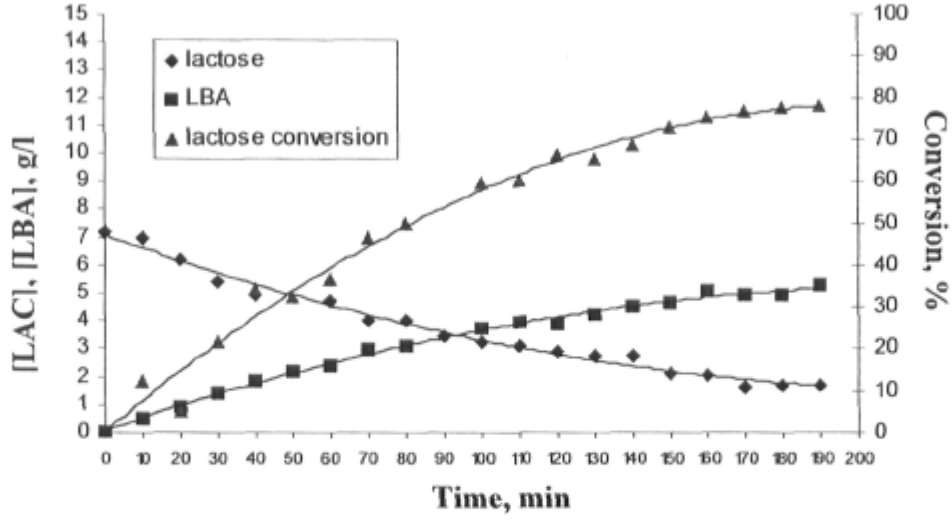

Fig. 60. The kinetics of lactose oxidation for the reaction performed in 400 mL lactose solution 20 mM in 1L AceGlass reactor at 80°C and pH=9 in presence of 0.21g 1.02%Pd 0.64%Bi/SBA 15 catalyst /g lactose.